DETAILED STUDY OF THE 22 AUGUST 2005 LANDSLIDE AND DISTRESS ON THE NATURAL HILLSIDE AT KWUN YAM SHAN, BELOW TATE'S RIDGE

GEO REPORT No. 239

Maunsell Geotechnical Services Limited

GEOTECHNICAL ENGINEERING OFFICE
CIVIL ENGINEERING AND DEVELOPMENT DEPARTMENT
THE GOVERNMENT OF THE HONG KONG
SPECIAL ADMINISTRATIVE REGION

DETAILED STUDY OF THE 22 AUGUST 2005 LANDSLIDE AND DISTRESS ON THE NATURAL HILLSIDE AT KWUN YAM SHAN, BELOW TATE'S RIDGE

GEO REPORT No. 239

Maunsell Geotechnical Services Limited

This report is largely based on GEO Landslide Study Report No. LSR 5/2007 produced in July 2007

Table of Contents
Table of Contents
Table of Contents
Table of Contents

© The Government of the Hong Kong Special Administrative Region

First published, November 2008

Prepared by:

Geotechnical Engineering Office,
Civil Engineering and Development Department,
Civil Engineering and Development Building,
101 Princess Margaret Road,
Homantin, Kowloon,
Hong Kong.

Table of Contents
Table of Contents
Table of Contents
Table of Contents

PREFACE

In keeping with our policy of releasing information which may be of general interest to the geotechnical profession and the public, we make available selected internal reports in a series of publications termed the GEO Report series. The GEO Reports can be downloaded from the website of the Civil Engineering and Development Department (http://www.cedd.gov.hk) on the Internet. Printed copies are also available for some GEO Reports. For printed copies, a charge is made to cover the cost of printing.

The Geotechnical Engineering Office also produces documents specifically for publication. These include guidance documents and results of comprehensive reviews. These publications and the printed GEO Reports may be obtained from the Government's Information Services Department. Information on how to purchase these documents is given on the second last page of this report.

R.K.S. Chan
Head, Geotechnical Engineering Office
November 2008

Table of Contents
Table of Contents
Table of Contents
Table of Contents

FOREWORD

This report presents the findings of a detailed study of a landslide incident (Incident No. 2005/08/0422) that occurred on a natural hillside at Kwun Yam Shan, below Tate's Ridge. The landslide was reported in the early morning of 22 August 2005 following heavy rainfall on 19 and 20 August 2005. The landslide involved a total displaced volume of about 2,350 m³, much of which remained in the source area. About 1,000 m³ of material detached from the source and developed into a debris flow, which travelled a total distance of about 330 m down a drainage line, finally coming to rest within the drainage line. An approximately 10 m section of the MacLehose Trail was severed. No casualties were reported as a result of the landslide.

Significant signs of distress were subsequently identified on the hillside above the source area of the August 2005 landslide. Extensive tension cracks defined an area of distressed hillside within which relatively smaller scale tension cracks, collapse features and erosion gullies are present.

The key objectives of the study were to document the facts about the landslide and the distressed hillside, present relevant background information and establish the probable causes of the landslide and the observed distress. The scope of the study comprised desk study, site reconnaissance, detailed field mapping, engineering geological mapping, ground investigation and laboratory testing, together with theoretical analyses. Recommendations for follow-up actions are presented separately.

The report was prepared as part of the Landslide Investigation Consultancy for landslides occurring in Kowloon and the New Territories in 2006, for the Geotechnical Engineering Office, Civil Engineering and Development Department, under Agreement No. CE 50/2005 (GE). This is one of a series of reports produced during the consultancy by Maunsell Geotechnical Services Limited.

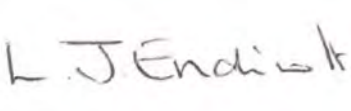

Dr. L.J. Endicott
Project Director
Maunsell Geotechnical Services Limited

Agreement No. CE 50/2005 (GE)
Study of Landslides Occurring in Kowloon and the New Territories in 2006 - Feasibility Study

Table of Contents
Table of Contents
Table of Contents
Table of Contents

CONTENTS

		Page No.
	Title Page	1
	PREFACE	3
	FOREWORD	4
	CONTENTS	5
1.	INTRODUCTION	8
2.	THE SITE	9
	2.1 Site Description	9
	2.2 Water-carrying Services and Other Utilities	10
	2.3 Maintenance Responsibilities and Land Status	10
	2.4 Regional Geology	10
	2.5 Geotechnical Area Studies Programme (GASP)	11
3.	SITE HISTORY AND PAST INSTABILITIES	11
	3.1 Site History	11
	3.2 Past Instabilities	12
	3.2.1 Natural Terrain Landslide Inventory (NTLI), Enhanced Natural Terrain Landslide Inventory (ENTLI) and Large Landslide Database	12
	3.2.2 Aerial Photograph Interpretation	13
	3.2.3 GEO's Landslide Database	13
4.	THE AUGUST 2005 LANDSLIDE AND POST-FAILURE OBSERVATIONS	14
	4.1 General	14
	4.2 Source Area	15
	4.3 Debris Trail	16
	4.3.1 Source Area to MacLehose Trail (CH35 to CH65)	16
	4.3.2 Upper Debris Trail (CH65 to CH188)	16
	4.3.3 Lower Debris Trail (CH188 to CH330)	17
	4.4 Distressed Hillside Adjacent to the August 2005 Landslide	18

		Page No.
4.5	Emergency Remedial Works on the August 2005 Landslide and the Distressed Hillside and Field Observations	20
5.	GEOLOGY, GEOMORPHOLOGY AND GROUND INVESTIGATION	21
5.1	General	21
5.2	Ground Investigation	21
5.3	Superficial Deposits	22
5.3.1	Young Colluvium	22
5.3.2	Old Colluvium	23
5.4	Solid Geology	23
5.4.1	Clay Bands	25
5.5	Laboratory Testing, Permeability Testing and Soil Properties	26
5.6	Geomorphology	27
6.	GEOLOGICAL AND GEOMORPHOLOGICAL MODEL	28
6.1	Landslide Susceptibility	29
7.	HYDROGEOLOGY	29
7.1	General	29
7.2	Groundwater Conditions	30
7.3	Underground Streams and Cavities	30
8.	ANALYSIS OF RAINFALL RECORDS	31
9.	THEORETICAL STABILITY ANALYSES	32
9.1	The August 2005 Landslide	32
9.2	The Distressed Hillside	33
10.	DIAGNOSIS OF THE PROBABLE CAUSES OF THE AUGUST 2005 LANDSLIDE AND THE DISTRESS ON THE HILLSIDE	34
10.1	The August 2005 Landslide	34
10.2	The Distress on the Hillside	35
11.	DISCUSSION	36
12.	CONCLUSIONS	39
13.	REFERENCES	39

Page No.

LIST OF TABLES 42

LIST OF FIGURES 44

LIST OF PLATES 69

APPENDIX A: AERIAL PHOTOGRAPH INTERPRETATION 102

APPENDIX B: CROSS-SECTIONS ALONG DEBRIS TRAIL 117

APPENDIX C: GROUND INVESTIGATION INFORMATION 128

LIST OF DRAWINGS 138

1. INTRODUCTION

In the early morning of 22 August 2005, following heavy rainfall on 19 and 20 August 2005, a landslide (Incident No. 2005/08/0422) was reported to have occurred on a natural hillside at Kwun Yam Shan, below Tate's Ridge (Figure 1 and Plates 1 and 2). The landslide involved a total displaced volume (terminology after Cruden & Varnes, 1996) of about 2,350 m^3 from the source area (about 1,000 m^3 of material detached from the source and about 1,350 m^3 of material remained in the source area below a series of tension cracks). The detached material entered an ephemeral drainage line, where it developed into a channelised debris flow. The landslide debris travelled a total distance of about 330 m down the drainage line (Drawing No. 1). An approximately 10 m section of the MacLehose Trail was severed. No casualties were reported as a result of the landslide.

Significant signs of distress, in the form of an extensive system of tension cracks with local maximum down throws of more than 1 m (refer to Drawing No. 2), were subsequently identified on the hillside about 50 m uphill of the source area of the August 2005 landslide (Figure 2). These tension cracks defined an area of distressed hillside where relatively smaller scale tension cracks, collapse features and erosion gullies were located.

Following the incident, Maunsell Geotechnical Services Limited (MGSL), the 2006 Landslide Investigation Consultant for Kowloon and the New Territories, carried out a detailed study for the Geotechnical Engineering Office (GEO), Civil Engineering and Development Department (CEDD), under Agreement No. CE 50/2005 (GE).

The key objectives of the study were to document the facts about the landslide and adjacent distressed hillside, present relevant background information and establish the probable causes of the landslide and the observed distress. Recommendations for follow-up actions are reported separately.

This report presents the findings of the detailed study, which comprised the following key tasks:

(a) review of all relevant documents relating to the study area,

(b) aerial photograph interpretation (API),

(c) topographical surveys, engineering geological mapping and detailed field observations and measurements,

(d) ground investigation and laboratory testing,

(e) analysis of rainfall records,

(f) theoretical stability analysis, and

(g) diagnosis of the probable causes of the landslide and the extensive tension cracks.

Table of Contents
Table of Contents
Table of Contents
Table of Contents

2. THE SITE

2.1 Site Description

The August 2005 landslide and the distress are located on a north-northeast facing hillside, about 200 m to the north of Tate's Ridge and about 500 m south of Kwun Ping Road, Kwun Yam Shan (Figure 1). The site is within, and adjacent to, a densely vegetated, linear topographical depression (about 60 m wide by 100 m in length) between two rounded spurlines and at the head of an ephemeral drainage line. The MacLehose Trail is about 30 m to the north of the toe of the August 2005 landslide source area (Figure 2).

The August 2005 landslide is located to the west side of the mouth of the topographical depression and above a convex break-in-slope (Figure 2). The crown of the landslide source area is located at an elevation of about 448 mPD with the toe located at about 430 mPD. Based on the post-landslide topographical survey of the flank of the August 2005 landslide carried out by the Survey Division of the CEDD, the hillside is inclined at an angle of between 25° and 28° above the break, steepening to between 30° and 35° below the break-in-slope attaining a maximum of 40° along the debris trail (Figure 3).

The distressed hillside is situated immediately to the southeast of the August 2005 landslide, which is located within the above mentioned topographical depression. The elevation of the uppermost (southern), recent tension crack within the distressed hillside is about 50 m to the south, and about 18 m uphill, of the landslide, at an elevation of about 464 mPD (Figure 2 and Plate 3). The possible toe of the distressed hillside lies at an elevation between 430 mPD and 440 mPD. The inclination of the hillside within the topographical depression varies from about 35° at the sides of the depression to about 10° to 12° within the central portion of the depression (Figure 2). The average inclination through the distressed hillside, which is bounded by extensive tension cracks (see Section 4), is about 20° to 25° (Figure 4). Numerous colluvial boulders, some several metres across, are scattered across the natural hillside and possible rock exposures as well as colluvial boulders are present along the rounded spurlines.

The plan area of the topographical depression is about 5,500 m², with an upslope catchment of approximately 20,000 m².

There is much anthropogenic disturbance particularly evidence of past military activities on the hillside, which includes abandoned military structures along Tate's Ridge and an extensive network of military tracks, trenches, pits and tunnels (see Section 3.1). Two man-made excavations on the hillside, possible wartime tunnels/caves, are in close proximity of the distressed hillside, about 5 m to 10 m uphill of the southernmost tension crack (Figure 2 and Plate 4). The tunnel is about 0.7 m wide by 1 m high near the portal and is connected to a wider space inside (the size and conditions of the inner part of the tunnel are not certain as difficulty was encountered in exploring it using closed-circuit television (CCTV)). Another open pit, about 4 m by 5 m in size, is located to the east of the tunnel. About 10 m to the south of these tunnels is a series of chevron shaped trenches on the hillside. These trenches, possibly wartime relics, are generally about 1 m to 1.2 m wide by 1 m deep (Figure 2 and Plate 5). These likely wartime relics (which were formed about 70 years ago and probably disused after end of World War II in 1945, see Section 3.1) are generally overgrown with vegetation and are in a dilapidated condition.

Table of Contents
Table of Contents
Table of Contents
Table of Contents

The hillside above the distressed hillside is vegetated and is inclined at about 30° gradually reducing to about 15° near Tate's Ridge located about 100 m to the south. The hillside below the study area is densely vegetated and is inclined at about 30° to 40° that gradually reduces to 10° to 20° along the streamcourse (Figure 3). The nearest facility below the study area is Kwun Ping Road, which is about 500 m to the north of the August 2005 landslide (Plate 2). A few registered squatter structures are located in the vicinity of the streamcourse below Kwun Ping Road, and some single-storey to 3-storey village houses at Kwun Yam Shan and Tso Tui Ha (Kwun Yam Fa Yuen) are located further downstream (Plate 2).

2.2 Water-carrying Services and Other Utilities

According to the information provided by the Water Supplies Department (WSD) and the Drainage Services Department (DSD), apart from a DSD sewage tunnel about 70 m to the northeast of the August 2005 landslide (at an invert of about 24 mPD, i.e. about 370 m below rockhead level), there are no records of other water-carrying services in the vicinity of the landslide site and the distressed hillside. A plastic pipe (ranging from 30 mm to 50 mm in diameter) was observed to be running along the hillside below the toe of the August 2005 landslide source area at about 426 mPD. The pipe was leaking during the initial inspection in August 2005 and was subsequently repaired (see Figure 2).

2.3 Maintenance Responsibilities and Land Status

There are no registered slopes in the vicinity of the study area. Based on the information obtained from Lands Department (Lands D), the August 2005 landslide and the adjacent distressed hillside are situated on unleased and unallocated government land within the Ma On Shan Country Park.

2.4 Regional Geology

According to the Hong Kong Geological Survey (HKGS) 1:20 000 scale Solid and Superficial Geology Map Sheet No. 7 (GCO, 1986), the site is underlain by crystal and lithic tuff, coarse ash tuff, tuff-breccia, tuffite with local feldsparphyric rhyolite (Figure 5).

The geological setting is described by Addison (1986) and was updated by Sewell *et al* (2000). The recent updating of the Solid and Superficial Geology Map Sheet No. 7, using borehole and field mapping information (Fugro Scott Wilson (FSW), 1999, Campbell *et al*, 2000), has led to a re-assignment of the coarse ash crystal tuffs and sedimentary rocks at the site, to the Cretaceous Mount Davis Formation from the Shing Mun Formation. These rocks are reported as being thermally altered (hornfels) where they are close to the adjacent granitic intrusion (GCO, 1986). Addison (1986) described the outcrops at Tate's Cairn and Tate's Ridge as "complexly faulted and intruded" and "generally comprising dark, bluish grey ash crystal tuffs". He also noted common, thin (up to 0.5 m) and discontinuous units of laminated dark grey mudstones. Campbell *et al* (2000) reported more detail of the geology at Tate's Ridge and indicated that interbedding of the mudstone and the significant local variations in weathering degree relate to contact metamorphism.

Table of Contents
Table of Contents
Table of Contents
Table of Contents

A feldsparphyric rhyolite dyke, trending approximately east-west in the vicinity of the MacLehose Trail, is shown on the 1:20 000 geological map at about the location of the August 2005 landslide. The rhyolite dyke ends at a photolineament along the linear topographical depression (Figure 5).

Major intrusive rocks are reported about 200 m to the north of the August 2005 landslide near the end of the 2005 landslide debris trail (Figure 5). The rocks occur in complex outcrops, including "numerous sheets of fine-grained granite, screens of tuff and coarse-grained granite, and sheets of quartz monzonite" (Addison, 1986). The dominant material is poorly exposed fine-grained granite that appears "to be mainly equigranular with shattered megacrysts". The granite on Tate's Cairn is very pale grey and strongly recrystalised, indicating that the granite was very close to the roof of the intrusion.

2.5 Geotechnical Area Studies Programme (GASP)

Geotechnical data relating to the study area were compiled as part of the Geotechnical Control Office's (GCO, renamed GEO in 1991) Geotechnical Area Studies Programme (GASP) Report No. II, Central New Territories (GCO, 1987a). The data are shown on 1:20, 000 scale maps, which are to be used for regional appraisal and strategic planning purposes. It should be noted that these maps are not intended for the assessment of local areas, such as the subject hillside, because of the limited resolution of the maps.

The Engineering Geology Map indicates that the hillside on which the August 2005 landslide occurred comprises predominantly pyroclastic rocks with colluvium downhill. The Geotechnical Land Use Map (GLUM) designates the terrain as generally GLUM Class IV (i.e. with extreme geotechnical limitation). The Physical Constraints Map shows the terrain affected by the landslide to be a zone of instability associated with colluvial terrain, with colluvium indicated downhill of the landslide site. Part of the area, in which the tension cracks and disturbed ground are located, is indicated to be a zone of instability associated with insitu terrain.

3. SITE HISTORY AND PAST INSTABILITIES

The history of the study area has been determined from an interpretation of the available aerial photographs, together with a review of relevant documentary information (Figure 6). Detailed observations from the aerial photograph interpretation (API) are summarised in Appendix A.

3.1 Site History

Based on the earliest available aerial photograph taken in 1956, the study area comprises natural terrain and is located within a linear topographical depression between rounded spurlines (Figure 6 and Appendix A). Two ephemeral drainage lines are observed along the western side of the topographical depression and a possible third ephemeral drainage line runs approximately through the centre of the topographical depression (Figure A3).

Table of Contents
Table of Contents
Table of Contents
Table of Contents

There is much evidence of anthropogenic disturbance across the hillside. Military structures are present along the ridgeline and there is a number of chevron shaped wartime trenches. One such trench can be seen to extend into the upper eastern side of the depression (Figure 6), and other related excavations (possibly Japanese tunnels/caves) are present on the natural hillside above the depression. These military structures were originally part of the Gin Drinker's Line, which was constructed by the British military authorities between 1936 and 1938, before the outbreak of World War II. Some caves were built during the Japanese occupation period (AFCD, 2005). Several footpaths cross the site, notably the MacLehose Trail which crosses the hillside to the north of the study area, two footpaths, FP1 and FP2 (Figures A1 and A5), that cross the central portion of the distressed hillside, and a third footpath, FP3 (Figure A1 and A5), that crosses above the linear depression. These footpaths (FP1, FP2 and FP3) are probably wartime tracks that are no longer in use.

Apart from a landslide that occurred between 1956 and 1963 (see Figure 7 and Section 3.2), there are no observable changes to the subject hillside between the time of the pre-1963 landslide and the present day, except for a general increase in the density of the vegetation.

3.2 Past instabilities

3.2.1 Natural Terrain Landslide Inventory (NTLI), Enhanced Natural Terrain Landslide Inventory (ENTLI) and Large Landslide Database

In 1995, GEO compiled the Natural Terrain Landslide Inventory (NTLI), from the interpretation of high-level (10,000 ft to 20,000 ft) aerial photographs dating from 1945 to 1994 (Evans *et al*, 1997; King, 1999). According to the NTLI, three landslides with tag Nos. 07SEC0166, 07SEC0167 and 07SEC0168 are indicated on the hillside affected by the August 2005 landslide (Figure 7). Landslide tag No. 07SEC0166 is a recent landslide which coincides with the pre-1963 landslide identified from API and from site inspection. Landslide tags Nos. 07SEC0167 and 07SEC0168 are relict landslides located on the hillside affected by the August 2005 landslide. Landslide tag No. 07SEC0168 is more distinct and has approximate dimensions of 8 m by 5 m by 1.5 m depth while landslide tag No. 07SEC0167 is less distinct and has approximate dimensions of 5 m by 3 m by 1 m depth. Both landslides can be seen in the 1956 aerial photographs (Section 3.2.2). A further five landslides are recorded in the NTLI in the catchment to the west of the August 2005 landslide, with tag Nos. 07SEC0161 to 07SEC0165 (Figure 7).

In 2004, GEO commenced a project to update the NTLI using low altitude (8,000 ft and below) aerial photographs and produced an Enhanced Natural Terrain Landslide Inventory (ENTLI). The ENTLI records the three NTLI features identified near the August 2005 landslide as tag Nos. 07SE01324E, 07SE0135E and 07SE0136E (Figure 7). The pre-1963 landslide tag No. 07SE01324E is marked at the same location as identified under the NTLI but the positions of the older pre-1956 landslides are amended to have crowns further to the north than previously indicated in the NTLI, which are closer to the position of the pre-1963 landslide and closer to locations identified from API and from site inspection. The August 2005 landslide and the distressed hillside are not located within a Historical Landslide Catchment (Wong *et al*, 2006).

Table of Contents
Table of Contents
Table of Contents
Table of Contents

GEO's large landslide database (Scott Wilson, 1999) contains records of a large landslide with tag No. 7SECL016 in the catchment to the west (Figure 7). This is coincident with NTLI landslide tag Nos. 07SEC0164 and 07SEC0165. This landslide feature is located at the head of a drainage line and is described as a combination of debris slide and debris flow with estimated dimensions of about 25 m by 25 m. No large landslide is indicated within the topographical depression where the August 2005 landslide and the distressed hillside are situated.

3.2.2 Aerial Photograph Interpretation

In the 1963 aerial photograph, the terrain along the western side of the linear topographical depression appears hummocky, which may be indicative of possible disturbance through landsliding or slope instability as well as from wartime activities (e.g. trenches and tracks) observed on the hillside, while the eastern side, although partly covered with vegetation, appears to have a more uniform morphology. Within the mid-portion of the linear depression, two rounded breaks-in-slope (Figure A3) may have developed as a result of much older landslides, the scars of which have since degraded considerably. There is a series of parallel convex breaks-in-slope along the rounded spurline that bounds the eastern side of the topographical depression, which may be related to the underlying geological structure or formation of wartime tracks. Relict landslides R3 and R5 observed to the west of the spurline (Figure 7) on the western boundary of the linear depression, appear to have a straight edge (which trends north-northwest to south-southeast) for at least part of the scar, suggesting possible structural control to these landslides (Figure A5).

At the mouth and northern end of the topographical depression, a clear arcuate break-in-slope is discernable, possibly a relict landslide scar or the coalescence of two relict landslide scars, into which poorly defined ephemeral drainage lines, which are observed to pass through the depression, appear to drain. In the 1963 aerial photographs, an incised gully can be seen at the western side of this break-in-slope (Figure A5). About 5 m to 10 m west of the depression mouth, two (approximately 4 m wide by about 5 m long) clearly defined relict landslide scars, R1 and R2 (Figure 7) are visible, with a possible third small degraded relict landslide immediately in front of the toe of these landslides. Landslides R1 and R2 are identified under the ENTLI as tag Nos. 07SEC0136E and 07SEC0135E. The terrain in front of the two relict landslides, where the possible third landslide is identified, was affected by a landslide between 1956 and 1963. A lack of vegetation in the scar of this landslide by 1963 suggests that it occurred in 1961 or 1962 (see Figures 7 and A4), and the area encompassing that two relict landslides identified in the 1956 aerial photographs, was affected by the August 2005 landslide which occurred about 30 m upslope of the pre-1963 landslide. Both landslides occurred in the steeper part of the hillside, i.e. in the lower part of the topographical depression. Concurrent with the pre-1963 landslide there appears to have been a reactivation of one of the smaller pre-1956 landslides (landslide labelled R2 in Figure 7).

3.2.3 GEO's Landslide Database

According to the GEO's landslide database, no landslide incidents have been reported to the GEO in the immediate vicinity of the study area. One of the nearest recorded

Table of Contents
Table of Contents
Table of Contents
Table of Contents

landslides is Incident No. K98/6/5 (with a failure volume of about 2,500 m³), which occurred in June 1998 and affected cut slope No. 7SE-C/C42 along Fei Ngo Shan Road below the Police Post at Tate's Ridge, some 400 m southeast of the August 2005 landslide (Figure 1). According to FSW (1999), the surface of rupture passed through completely decomposed tuff (CDT) "which has an extensive network of kaolin and manganiferous veins through the fabric of the material". Slope No. 7SE-C/C42 has a history of failures since 1993, and the previous deformation noted at the slope toe and significant tension cracks that were observed on the hillside above may represent "the progressive development of a deep-seated instability within the CDT".

4. THE AUGUST 2005 LANDSLIDE AND POST-FAILURE OBSERVATIONS

4.1 General

According to the Incident Report prepared by GEO, the August 2005 landslide was reported to the GEO at 10:48 a.m. on 22 August 2005. Based on an eyewitness account, the landslide was first observed at about 7 a.m. on the morning of 22 August 2005 and the eyewitness noted the landslide appeared to be "fresh". Given the remote location of the site and the inclement weather between 19 and 20 August 2005, the landslide may have occurred much earlier than reported. The exact time of failure is unknown. The landslide destroyed an approximately 10 m section of the MacLehose Trail located about 30 m downhill of the landslide source area (the Trail was subsequently re-aligned by AFCD in October 2005), and came to rest about 330 m down the streamcourse below. No casualties were reported as a result of the landslide.

MGSL first inspected the landslide on 24 August 2005 and commenced detailed field mapping. A plan of the landslide scar is shown on Figure 2 and engineering geological mapping of the landslide is shown on Drawing No. 1. A general view of the landslide source area is shown in Plate 6. To provide a reference for field mapping and fixing the positions of features within the debris trail, a chainage was established along the centreline of the landslide scar starting with 0 m (chainage CH 0) at the upslope extremity of the crown of the landslide source and extending to the toe of the debris trail at 332 m (*viz.* chainage CH 332).

The landslide involved a total displaced volume of about 2,350 m³. About 1,000 m³ of the material detached from the source area, with about 170 m³ of material entrained mostly in the vicinity of the MacLehose Trail below the toe of the source area, (see Figure 3). A large portion of the displaced material (about 1,350 m³) remained within the source area as intact rafts separated by a series of stepped tension cracks (see Section 4.2). About 50 m³ of the detached debris was deposited within the source area of the August 2005 landslide. The rest of the detached material (i.e. about 950 m³) from the source area entered the ephemeral drainage line below, and developed into a channelised debris flow. The landslide debris travelled a total distance of about 330 m down the drainage line and came to rest at two distinct boulder dams within the drainage line. A longitudinal section of the landslide, together with the estimated volumes of material entrained and deposited, is presented in Figure 3.

The difference in elevations between the landslide source and the end of the debris trail was approximately 138 m. The elevation of the source area ranged between about 448 mPD

Table of Contents
Table of Contents
Table of Contents
Table of Contents

and 430 mPD and the elevation at the boulder dams at the end of debris trail is about 310 mPD. The landslide scar has an average aspect of about 035° for the upper 220 m, changing to 346° for the lower 110 m. The travel angle (Wong & Ho, 1996) of the landslide debris was about 24°.

Longitudinal sections through the August 2005 landslide and source area are presented in Figures 3 and 4. A map of the debris trail is presented in Drawing No. 1, and cross sections through the source area and drainage line are presented in Appendix B.

4.2 Source Area

The total area occupied by the source of the August 2005 landslide measured about 36 m long by 22 m wide. The displaced material that remained below the crown and along the eastern flank of the source area measured about 26 m long and varied in widths from 8 m to 16 m (Plate 7). The series of stepped tension cracks within this material were about 0.5 m to 1 m high. The scar left by the material that detached from the source measured about 29 m long by 15 m wide with a maximum depth of about 5.5 m (Drawing No. 1 and Plate 6). The main scarp of the detached material was about 3 m high and inclined at an angle of about 60°. The floor of the scar from the detached material was inclined at about 26° to 28°. Since the source area of the August 2005 landslide was covered with erosion control mat as part of the urgent repair works by AFCD in October 2005, only part of the scar was exposed and logged by MGSL. A map of the exposures logged within the landslide scar is shown in Drawing No. 1.

The August 2005 landslide source is located immediately above a convex break-in-slope, where the terrain gradient changes from about 25° to 28° above to about 30° to 35° below. The break-in-slope probably developed as the result of the recent landslide as identified in the 1963 aerial photographs (i.e. the pre-1963 landslide described in Section 3.2, the scar of which is situated in front of the toe of the August 2005 landslide).

The maximum depth of the August 2005 landslide was about 5.5 m, based on site measurements and a comparison of the pre failure 1:1,000 topographical plan and the post-failure topographical survey. Evidence from API indicates that two smaller pre-1956 landslides may have occupied the same location as the August 2005 landslide, which would have somewhat reduced the estimated landslide depth and failure volume. However, this has not been accounted for in the above estimates.

Materials encountered within the landslide scar are described in detail in Drawing No. 1. The detached material primarily comprised boulder-rich colluvium of about 3 m thick, described as young colluvium (see section 5.3) consisting of reddish brown slightly sandy silty clay with many cobbles and boulders of coarse ash crystal tuff. The material below the young colluvium was initially described as a disturbed CDT by MGSL but was subsequently reclassified as ‘old colluvium’ (see Section 5.3). This material was observed on the western flank (less than 1 m thick) and near the crest of the landslide (about 2.9 m thick), but was absent in the eastern flank (Drawing No. 1). The old colluvium comprised sandy clayey silt with some to many cobbles and boulders of coarse ash crystal tuff and abundant kaolin, in patches and veins. Local soil piping was observed in the lower portion of the old colluvium (Plate 8), where it appears that preferential groundwater flow has exploited a burrow or decayed tree root. CDT was observed at the floor of the landslide scar,

Table of Contents
Table of Contents
Table of Contents
Table of Contents

which comprised light yellowish brown to reddish brown sandy clayey silt.

The eastern flank of the landslide scar exhibits lateral tension cracks (Plates 9 and 10) that extend towards the westernmost of the two large erosion gully features.

The surface of rupture appears to have been primarily along the colluvium/saprolite interface with the deepest part of the landslide passing through the upper CDT that contains several thin kaolin veins (Drawing No. 1 and Plate 11).

No evidence of the feldsparphyric rhyolite dyke, shown on the HKGS 1:20 000 scale Solid and Superficial Geology Map Sheet No. 7 to be underlying the location of the August 2005 landslide source, was found during the field mapping of the landslide scar and surrounding area.

4.3 Debris Trail

4.3.1 Source Area to MacLehose Trail (CH35 to CH65)

The detached mass entrained a portion of the colluvial material immediately below the landslide source area (Plate 12 and Drawing No. 1), with the entrainment extending to about chainage CH75. The estimated total entrainment through this portion of the landslide was about 150 m³, and included the destruction of a 10 m long section of the MacLehose Trail (Plate 12).

About 20 m³ of remoulded debris (Material type MT8, refer to Drawing No. 1 for detailed description) was deposited in the scar of the pre-1963 landslide, which is located below the western flank of the August 2005 landslide. There was also evidence of older landslide debris at about the location of the pre-1963 landslide (Plate 13). Deposition of debris from the August 2005 landslide of up to 0.5 m thick also took place on the eastern flank of the debris trail.

Several trees alongside the trail were observed to have been toppled by the debris with several noted to have been displaced and many were likely to have been entrained together with the debris (Plates 12 and 14).

4.3.2 Upper Debris Trail (CH65 to CH188)

The landslide debris entered a minor ephemeral drainage line, the head of which is marked by the scar of the pre-1963 landslide (Drawing No. 1). Material within the upper portion of the drainage line, which is likely to be debris from the pre-1963 instability, was entrained along with the severed section of MacLehose Trail. Beyond CH75, entrainment became minor with entrainment/erosion within the drainage line below possibly related to earlier landslide events (possibly the pre-1963 landslide). Evidence in support of this includes the observation of the insitu topsoil, which had been stripped of vegetation, beneath the August 2005 landslide debris (Plate 15).

The inclination of the drainage line between CH65 and CH75 is about 30°, steepening up to about 40° between CH75 and CH142. The lower portion of the upper debris trail

Table of Contents
Table of Contents
Table of Contents
Table of Contents

reduces to about 20° at CH188. The channelisation ratio of the ephemeral drainage line at the upper debris trail decreases from 5.5 at CH88 to a minimum of 2 at CH 173.

There was much deposition of remoulded debris (Material type MT8) with a large proportion of small tree trunks along the flanks of the upper debris trail despite the steepness (30° to 40°) of the terrain (Plate 16). Generally, debris was deposited in lobes and pressed up against trees on the original ground surface, on either side of the deeper central portion of the drainage line. Debris splatter was observed on the trees alongside the debris trail, with some debris splatter reaching several metres up the tree trunks and on branches. The extent of the debris splatter suggests wet debris probably travelling in a turbulent manner.

Moderately decomposed coarse ash crystal tuff with a light brown weathered surface layer was exposed at the base of the drainage line, between CH101 and CH108. Impact marks observed on the exposed rock were indicative of the bouldery nature of the debris. Other smaller exposures of moderately decomposed tuff (MDT) occurred at several locations along the drainage line between CH118 and CH188.

Between CH150 and just beyond CH188, a central sinuous streamcourse developed along the ephemeral drainage line and the shape of the channel noticeably changes. The western side of the drainage line is steeply dipping, locally up to 70°, while the eastern side is 3 m to 4 m high and sub-vertical with flat ground beyond. Consequently there is much deposition of debris in levees along the flat ground above the eastern side of the drainage line, with debris splatter marks observed on trees alongside the debris trail up to 4 m above the drainage line bank level. The western flank essentially marks an area of transportation with only thin (less than 0.2 m) fine debris (Material type MT7, see Drawing No. 1) remaining over the surface after the passage of the debris flow.

At about CH175, a constant flow of water emerged from a spring in the streamcourse and a minor landslide with an estimated volume of about 20 m³ was located on the western side of the drainage line (Drawing No. 1). The timing of the minor landslide is uncertain but it may have been triggered by the passing debris flow.

4.3.3 Lower Debris Trail (CH188 to CH330)

Between CH188 and CH203, the shape of the drainage line opens out into a broader form as the ephemeral drainage line approaches the confluence with a broader streamcourse that flows from the east (Plate 17). The gradient of the debris trail at this location decreases from about 20° to a shallower gradient of between 8° and 15°. The channelisation ratio of the streamcourse at the lower debris trail ranged from 5 to 7.8, with the higher ratio between CH185 and CH220.

On entering the larger streamcourse, the debris changed direction from an approximately northeast (035°) heading towards a northwest (346°) heading. This sharp change in the direction of flow resulted in a superelevation of about 6.8 m up the north-eastern flank of the streamcourse. Debris splatter and boulder impact marks on the trees at about the location of the maximum superelevation (CH220) reached about 4.5 m.

On the inside bend (western side) of the streamcourse opposite the maximum superelevation, there was considerable deposition (about 250 m³) of debris in a levee

Table of Contents
Table of Contents
Table of Contents
Table of Contents

(Plate 18). The levee measured between 8 m and 10 m wide, about 30 m long and up to 1.5 m thick. The debris comprised gravelly sandy silt with many cobbles and boulders (primarily Material type MT8).

The debris flow continued through the area with a shallow gradient along the streamcourse, with some boulder deposition. However, the majority of the boulders within the streamcourse appeared to have been deposited by earlier event(s) and were not entrained or transported by the August 2005 landslide. Boulders that were inferred to have been transported by the 2005 landslide (based on the appearance of previously buried surfaces on the boulders) are labelled on Drawing No. 1

Between CH250 and CH280, buried trees and soil from previous landsliding (Plate 19) were observed on both sides of the streamcourse. Given the degree of decomposition of the buried trees, it is apparent that they had been in place for some time, and may be related to the pre-1963 landslide event.

At CH270 and CH276, boulders of feldsparphyric rhyolite were observed (Drawing No. 1). These were the only pieces of evidence of the local presence of feldsparphyric rhyolite that is indicated on the HKGS 1:20 000 Solid and Superficial Geology Map Sheet No. 7 (Plate 20).

The major area of deposition, comprising boulder jammed logs, boulders and finer debris, occurred at two distinct boulder dams (Plates 21 and 22). An upper boulder dam located between CH292 and CH303 and a lower boulder dam between CH321 and CH332. The lower dam is located just above a break-in-slope within the drainage line where the streamcourse gradient increases from 8° to 10° to about 30° below the lower dam.

The boulder dams were probably formed in previous landslide incident(s) since it was observed that buried logs within the debris had decomposed since deposition. Several boulders within the dam were observed to have a thick moss and lichen cover, suggesting that the August 2005 landslide had not affected them.

Debris splash marks indicated limited debris movement beyond CH332, though debris-rich water flow was observed to pass the lower dam in the post-landslide inspection carried out on 24 August 2005 (Plates 23 and 24).

4.4 Distressed Hillside Adjacent to the August 2005 Landslide

A more detailed inspection of the hillside above the August 2005 landslide in March 2006 revealed an extensive system of tension cracks with a cumulative length of about 100 m, and observed to be continuous for about 70 m along the eastern and southern flanks of the distressed hillside. The system of tension cracks, included two prominent features (with throw up to about 1.1 m) of about 25 m to 30 m in length with a maximum horizontal separation of up to 300 mm that is open to a maximum depth of approximately 1.7 m (Drawing No. 2 and Plate 3). The tension cracks appeared fresh with an absence of any algal growth, though a portion of the southernmost tension crack (i.e. the uppermost scarp) appeared to have a weathered patina (Drawing No. 2), which are signs of having been exposed for some time.

Table of Contents
Table of Contents
Table of Contents
Table of Contents

The August 2005 landslide source area abuts the northwest side of the distressed hillside. While the southern and eastern flanks of the distressed hillside are delineated by distinct tension cracks, the western boundary of the distressed hillside becomes less well defined above the August 2005 landslide source area. The western side of the distressed hillside is weakly delineated by a series of en-echelon discontinuous tension cracks (Drawing No. 2 and Plate 25). Less extensive, discrete tension cracks are also evident within the main body of the distressed hillside (Plate 26).

The distressed ground (measuring about 3,000 m² in plan) did not behave as a rigid mass. Instead, the distressed ground probably underwent internal distortion, fragmentation and dislocation forming minor terraces/benches akin to local breaks-in-slope.

Well defined concave and convex breaks-in-slope are present within the distressed hillside. It is postulated that the observed breaks-in-slope are most likely to have been present before the August 2005 landslide. These breaks-in-slope, together with the signs of the uppermost scarp (i.e. the southernmost tension crack) having been exposed for some time, suggests that the distress on the hillside may have developed over a considerable period of time. At the eastern side of the distressed hillside, a concave break-in-slope defines a basinal morphology, while a hummocky morphology is present on the western side. A series of convex and concave breaks-in-slope are present between elevations 433 mPD and 445 mPD and may mark the toe of the distressed hillside.

Ground collapse features, possibly associated with groundwater flow removing fines from between boulders, were identified in the area above the source of the August 2005 landslide (Plate 27). A group of cavities/collapsed features was also located to the east of the uppermost tension crack. Boulders were scattered across the middle and upper parts of the distressed hillside and numerous boulders were present near the toe of the distressed hillside. Small gaps up to 100 mm across (Plate 28) were observed between boulders and the surrounding soil at several locations (Drawing No. 2), which may be indicative of ground movement below the boulders.

Possible further evidence of a history of movement of the distressed hillside was given by several leaning trees, which had changed their direction of growth to return to vertical. These were observed near the eastern boundary and near the toe of the distressed hillside (Plate 29). Some of the trees had been disturbed and toppled by boulder movement due to ground collapse (Plate 30).

Two trees at the western boundary of the distressed hillside were split along the tension cracks (Drawing No. 2 and Plate 31). The direction and magnitude of the observed movement are summarised in Figure 8.

Two prominent gully features (namely the western gully and eastern gully, see Drawing No. 2 and Plate 32) are located immediately adjacent to the August 2005 landslide source area. These features were probably initiated from ground collapse into large subsurface voids and developed further following removal of fines from the boulder-rich colluvium and due to side-wall collapses. Soakaways are present at the northernmost ends of both gullies.

Two wartime tunnels (Plate 4) were located 5 m to 10 m uphill of the distressed hillside, one of which was inspected using CCTV. The CCTV survey revealed a larger

Table of Contents
Table of Contents
Table of Contents
Table of Contents

subsurface cavity below the narrow entrance. The wartime trenches located on the hillside above the distressed hillside were also inspected. The trenches (Plate 5) are about 1 m wide by 1 m deep and up to 40 m long and appear as a chevron pattern when viewed in plan. The trenches were overgrown with scrubs and long grass. The trenches showed signs of erosion and loose soil was observed at the base of the trenches.

4.5 Emergency Remedial Works on the August 2005 Landslide and the Distressed Hillside and Field Observations

Emergency remedial works were carried out on the August 2005 landslide source area and the hillside above, following the identification of the extensive distress in the hillside. The remedial works include installation of 634 soil nails of between 16 m and 20 m in length (consisting of 32 mm diameter steel bar in 100 mm drillhole inclined at 20° to horizontal) with 1,320 m of reinforced concrete nail head tie beams, provision of 31 Nos. temporary and about 70 Nos. permanent Type II prescriptive raking drains of up to 20 m long and 320 m of surface drainage channels. As a contingency measure, two flexible debris-resisting wire mesh barriers will be provided on the lower part of the hillside near Kwun Ping Road and a debris deflector wall will be provided along the streamcourse near Kwun Yam Fa Yuen (Figure 1) in order to minimise the possible impact from the potential debris flow from the hillside. The remedial works were designed by the Geotechnical Projects Division of the GEO and the construction works, which commenced in late June 2006 and were substantially completed by March 2007. The works were carried out under the supervision of the LPM Division 3 of the GEO.

During the emergency remedial works to the August 2005 landslide scar, a notable problem was encountered during the drilling of some of the soil nail holes, particularly in close proximity to the August 2005 landslide source. Despite excessive drilling time, some soil nail holes were not able to advance beyond a depth of about 16 m. Subsequent ground investigation (see Section 5.2) revealed that no apparently unusual ground conditions were encountered at that depth and that the problem might have been associated with the difficulties in air-lifting the cuttings out of the hole, loss of circulation, high groundwater and presence of soil of high plasticity.

During the drilling of hole No. AG22 at the lower portion of the distressed hillside (Figure 9), prior to installation of the soil nail, groundwater encountered at a depth of about 19 m was observed to rise in the hole to a point about 8 m from the ground surface. This corresponded to a 3 m vertical rise in water level. As drilling of hole No. G22 continued, water was observed to be blown out of adjacent hole No. AG23. During the installation of raking drain No. RDK4, a blow out (about 0.2 m diameter) and ground collapse (about 0.5 m by 0.5 m) occurred near drillhole No. BH1. The approximate locations of the incidents are shown in Figure 9, which can be seen to roughly align suggesting that a subsurface void might have been intercepted by the drilling of the raking drain drillhole.

Selected raking drains within the distressed hillside have been monitored daily since their installation. Several showed signs of water flow or dripping and the flows were seen to increase after periods of rainfall (Figure 9). Seepage was observed from the drains installed along the eastern flank of the August 2005 landslide and from the raking drains along the toe of the source area and the distressed hillside was observed.

Table of Contents
Table of Contents
Table of Contents
Table of Contents

5. GEOLOGY, GEOMORPHOLOGY AND GROUND INVESTIGATION

5.1 General

The geology and geomorphology of the site was determined using information from desk and field studies. The desk study comprised a review of all the available data and published geological information, whilst the field study included detailed field mapping and a ground investigation (GI). Engineering geological mapping of the site was carried out between early March 2006 and August 2006, when access was made available for the GI works.

5.2 Ground Investigation

There are no records of any previous GI within the immediate vicinity of the study area. As part of this detailed study, GI works which comprised five vertical drillholes (Nos.BH1 to BH5), one inclined drillhole (No. IBH1), nine trial pits (Nos. TP1 to TP6 and TP8 to TP10) and 41 GCO probes (Nos. GC1 to GC41) were carried out by DrilTech Ground Engineering Ltd. between late May 2006 and the end of August 2006. Due to the on-going remedial works, no GI stations were installed in the August 2005 landslide area. The locations of the GI stations are shown in Figure 10. Falling head permeability tests were carried out in the drillholes, and three double ring constant-head infiltration tests were carried out on the ground surface of the distressed hillside.

Standpipes and piezometers were installed in drillholes Nos. BH1, BH2 and BH5. The depths to the tips of the installations are shown in Table C1 (Appendix C). Two piezometers were installed in each borehole, one at rockhead level (with rockhead defined as the top of a 5 m section of Grade III rock or better with at least 85% core recovery) and a second shallow standpipe or piezometer in order to monitor for any potential perched groundwater. The tip of the shallow piezometer in drillhole No. BH1 was located at the old colluvium/CDT interface, whereas the tip of the shallow standpipe in drillhole No. BH2 was located at the young colluvium/CDT interface. The shallow piezometer in drillhole No. BH5 was located at the young colluvium/old colluvium interface**.**

Water levels in drillholes Nos. BH1 and BH2 were monitored using automatic vibrating wire piezometers, with remote transmission of the data to the GEO for real-time monitoring between mid-August and early September 2006 (due to the on-going remedial works on site, the automatic piezometers were temporarily removed in September 2006 with manual readings taken twice daily since). The piezometers in drillhole No. BH5 included Halcrow buckets (buckets were also installed in piezometers of drillholes Nos. BH1 and BH2 prior to the installation of real-time monitoring devices). A discussion of the groundwater conditions at the site is presented in Section 7.2.

In-place inclinometers, also with remote transmission of data to the GEO and real-time monitoring, were installed in drillholes Nos. BH3 and BH4, with sensors placed at 2 m centres between depths of 1 m and 11 m and at 3.3 m centres for the remaining 16.5 m. Due to the on-going works on site, the in-place inclinometers have been temporarily removed since September 2006 and weekly manual readings have been taken subsequently. Real-time monitoring (in-place inclinometers and automatic piezometers) resumed at the site in March 2007 after the completion of the slope improvement works. The monitoring

Table of Contents
Table of Contents
Table of Contents
Table of Contents

records have so far not shown any abnormal movement or a trend of downhill movement within the distressed hillside.

A total of 36 settlement markers were installed on the distressed hillside (Figure 10). The monitoring of the markers since April 2006 has not identified any noticeable movement.

The vertical drillholes were sunk to depths of between 36.4 m and 53.1 m below ground surface and terminated in 5 m of Grade III rock or better using air-foam as the flushing medium. Drillhole No. IBH1 was drilled at an angle of 20° to the horizontal (i.e. the same inclination as the soil nails) to examine the ground conditions that may have caused the difficulties in soil nail installation (Section 4.5). There were no apparent unusual or adverse ground conditions encountered by drillhole No. IBH1 which was terminated at a length of 25.1 m. A summary of the materials encountered in each drillhole is presented in Table C1.

Continuous Mazier samples were taken in all drillholes to a depth of 34 m below ground surface and most of these samples (about 85%, except for those recovered between corestones at depth) were split and logged in the Public Works Central Laboratory (PWCL).

Trial pits Nos. TP1 to TP3 and TP10 were excavated through the tension cracks in the distressed hillside to examine the nature of the distressed surface. Trial pits Nos. TP6 and TP9 were excavated north of the distressed hillside in an attempt to delineate the toe of the distressed zone. Logs of trial pits Nos. TP1, TP2, TP8 and TP10 are presented in Appendix C.

GCO probes Nos. GC1 to GC41 were carried out along the tension cracks and around the distressed hillside. The GCO probes met refusal at depths of between 1.35 m and 7.99 m. A summary of the GCO probes results are presented in Appendix C.

Sections A'-A' and B-B through the August 2005 landslide source area and the distressed hillside are shown in Figures 11 and 12 respectively.

5.3 Superficial Deposits

The superficial deposits encountered at the site essentially comprise colluvium below an approximately 200 mm thick mantle of organic rich dark brown sandy silt/clay (topsoil). Two types of colluvium were identified. For the purposes of differentiation, the terms ‘young colluvium’ and ’old colluvium’ have been adopted for the upper material and the underlying material respectively.

5.3.1 Young Colluvium

The young colluvium was encountered in all exploratory holes and was exposed in the tension cracks bounding the distressed hillside. The young colluvium is up to 2.9 m thick and generally comprises a soft to firm, reddish brown, slightly sandy clayey silt with some sub-angular to sub-rounded cobbles and occasional boulders of coarse ash crystal tuff. The young colluvium appears to have been derived entirely from landslide debris. In trial pits Nos. TP8 and TP10, distinct stone line (an identifiable alignment of cobbles, typically within

Table of Contents
Table of Contents
Table of Contents
Table of Contents

the soil mass), marking the probable base of a landslide, support the likely landslide debris related origin of the young colluvium (Plate 33). Where the young colluvium was exposed in the tension cracks, its consistency was firm to stiff.

5.3.2 Old Colluvium

The old colluvium, which was between 2 m and 3 m thick, appears to be disturbed with discontinuous structure and apparent localised sedimentary layering (Plate 34a). In drillhole No. BH5, the disturbance resulted in the development of voids that were subsequently infilled with kaolin up to 5 mm thick (Plate 34b). The old colluvium generally comprised firm to stiff, reddish brown, light yellowish brown and greenish grey, sandy clayey silt with occasional quartz gravel and some to many cobbles of CDT. The old colluvium was encountered in most exploratory holes, except drillhole No. BH2 and trial pits Nos. TP6 and TP9.

The origin of the old colluvium is uncertain. It is possible that moderately decomposed cobbles associated with a significantly older landslide, have subsequently decomposed completely. The sedimentary layering possibly represents a material that was deposited within a series of subsurface voids/soil pipes through the old landslide debris. The old colluvium is found in all drillholes except BH2. The confinement of the old colluvium within the topographical depression is illustrated by its thickening towards the centre of the depression (see BH1) and thinning out towards the edge of the depression (see TP8), and the absence of the old colluvium beyond the convex break-in-slope near BH2. The above observations suggest that the extent of the old landslide, with which the old colluvium could be associated, may be confined to the linear topographical depression.

The old colluvium observed in trial pit No. TP10 and drillhole No. BH3 (Plates 34c and 34d) differs in appearance from that observed elsewhere. The sedimentary structure appears to be absent and there is less variability in colour, which is more consistently reddish to dark reddish brown. This may be due to a different origin of the material on the eastern flanks of the topographical depression (Figure 10).

5.4 Solid Geology

The solid geology comprises completely decomposed to moderately decomposed coarse ash crystal tuff. The CDT was generally extremely weak, greyish brown, reddish brown, yellowish brown and greenish grey locally streaked white and black, with very closely to closely spaced planar, occasionally undulating kaolin infilled and manganese coated, mostly slickensided joints (slightly sandy silty CLAY to sandy clayey SILT with occasional fine gravel).

The CDT appears to be homogeneous coarse ash tuff but a closer examination reveals a greater variability from coarse-ash to fine-ash and lapilli bearing tuff. The variability in grain size is clearly evident and often identified through the presence of finer and coarser quartz. The most obvious indication of variability is the range of concentrations of lithic inclusions from none to abundant, small (typically less than 10 mm diameter) lithics, which have commonly decomposed to a dark grey silt/clay.

Table of Contents
Table of Contents
Table of Contents
Table of Contents

The depth to the base of the CDT ranged between 31 m in drillhole No. BH2 to 48.3 m in drillhole No. BH1 (Figures 10 and 12). Corestones of MDT were encountered within the CDT at various levels in the drillholes (see Section B-B in Figure 12), and towards the base of the saprolite highly decomposed tuff (HDT) is present. Furthermore, it appears that the transition from CDT to MDT occurs with little or possibly no HDT. During the splitting of the Mazier samples, it was observed that even at the deepest levels (i.e. deeper than 25 m), small samples of the decomposed tuff would slake quite readily suggesting a completely decomposed grade.

Joints within the saprolite, primarily observed from split Mazier samples, vary in dip from sub-horizontal to sub-vertical but the largest proportion dip at between 40° and 50° and most joints are slickensided. The orientations of the slickensides identified in most of the joints appear to be variable, with the majority plunging down dip. Joints are typically planar and all are manganese coated with the manganese up to 2 mm thick. Kaolin infill is common within the joints and is generally about 3 mm thick with a maximum thickness of 10 mm. Occasionally, ladder veins and boxwork veining of the kaolin were observed (Plate 35). There was little evidence of significant movement along the relict joints although small-scale movement was observed in drillhole No. BH4 (Plate 36).

Campbell & Parry (2002) suggest, in relation to observations made at the June 1998 landslide below Tate's Ridge (FSW, 1999), that the kaolin observed in veins throughout the saprolite and along the joints is a product of weathering with the boxwork veining being related to hydrothermal activity. This supports the suggestion by Addison (1986) that the tuffs at Tate's ridge are thermally metamorphosed (i.e. hornfelsed), which is a likely consequence of the close proximity to the intruding underlying fine-grained granite. Campbell & Parry (2002) also note that manganese oxide lines the margins of the kaolin veins and is likely to be a more recent product of weathering.

The tentative rockhead contours based on the limited information from the GI are presented in Figure 10. The deep weathering may be structurally controlled (e.g. possible presence of steeply dipping very closely spaced persistent joints) promoting preferential weathering of the tuff at this location

The MDT comprised a moderately strong to strong, dark greenish grey, light grey, locally light green and occasionally light reddish brown, moderately decomposed coarse ash crystal tuff. Joints are closely to very closely spaced planar to planar rough dipping between 20° and 70° but mostly between 40° and 50°, occasionally iron stained and infilled with kaolin in places. The presence of a green mineral (probably chlorite), suggests that the tuff has been thermally altered. Possible evidence for a fault was observed near the base of the core in drillhole No. BH2. The core was highly fractured and a possible fault gouge up to 20 mm thick was observed on a steeply dipping (about 55°) planar joint at a depth of about 30.8 m (Plate 37).

Examination of MDT from field samples, mostly colluvial boulders, indicated that the rock was commonly coarse ash crystal tuffs with lithic inclusions. Volcanic stratification and subsequent metamorphism, including chlorite veins, a hornfelsic texture and localised shearing, were also exhibited. The reported feldsparphyric rhyolite dyke (GCO, 1986) has not been identified at the landslide site but boulders of feldsparphyric rhyolite were noted in the drainage line below the August 2005 landslide about 300 m down the debris trail below the confluence with the larger streamcourse (Figure 2). The rock comprises a fine

Table of Contents
Table of Contents
Table of Contents
Table of Contents

groundmass with quartz and occasional tabular mica and feldspar, which is indicative of a minor intrusive body.

Inspection of the original, unpublished Hong Kong Geological Survey field notes made during the preparation of the 1:20 000 scale Solid and Superficial Geological Map Sheet No. 7, indicates that the record of a feldsparphyric rhyolite dyke was based on a single exposure in the vicinity of the August 2005 landslide, while the remaining area is blanketed by boulder-rich colluvium. The lack of either an outcrop or topographical expression of more resistant rock at this location suggests that the indicated dyke probably had little relevance to the present landslide study. The granitic rock indicated as being present in the lower part of the debris trail also has not been identified, whilst the area indicated as granite is mostly covered by colluvium of between 2 m and 5 m thick.

5.4.1 Clay Bands

Clay bands comprising 3 mm to 5 mm thick of soft to firm, sandy clay, were identified in four of the five drillholes, *viz.* drillholes Nos. BH1, BH3, BH4 and BH5.

The clay bands were encountered at depths of 10 m in drillhole No. BH1, 4.2 m in drillhole No. BH3, 4.2 m and 11.5 m in drillhole No. BH4, and 5.7 m, 9 m and 18.6 m in drillhole No. BH5. The locations of the clay bands have been plotted on Section B-B (Figure 12), and photographs of the local clay bands are shown in Plates 38 to 44.

The clay bands observed in drillhole No. BH1 comprised a thin, soft, moist light brown clay of about 5 mm maximum thickness dipping at about 45°, with a sub-horizontal lens of soft moist light brown slightly sandy clay located about 60 mm below (Plate 38). Bands of wet sandy clay up to 200 mm thick were also observed in drillhole No. BH1 between depths of about 3.7 m and 3.8 m, and about 4.8 m and 5 m within the old colluvium. The lower sandy clay band was marked by an abrupt horizontal boundary with the material below. The origin of these clayey bands is unclear. Thin clay laminae/bands are not uncommon in a weathered volcanic tuff sequence. Sewell et al (2000) note that possible pyroclastic fall deposits “include finely laminated, white to light grey and orangish brown, very fine ash tuffs with variable crystal components”. However, none of the clay bands observed at the subject site appeared finely laminated, and the consistency in the sub-horizontal orientation and relatively consistent thickness suggest a different origin to that of pyroclastic fall.

In drillhole No. BH3, the clay band encountered at a depth of 4.2 m (taken through old colluvium) was soft, moist, dark reddish brown sandy clay of about 20 mm thickness (Plate 39). The clay bands in drillhole No. BH4 encountered at a depth of 4.3 m (at old colluvium) comprised a bifurcating band of soft to firm greenish brown clay of about 2 mm to 5 mm thickness located about 60 mm above an undulating 5 mm thick soft to firm greenish brown clay (Plate 40).

At a depth of 11.5 m in drillhole No. BH4 (within the CDT layer), the clay band comprises 5 mm thick sub-horizontal soft light reddish brown slightly sandy clay (Plate 41). There appears to be no obvious evidence of displacement of the CDT on either side of the clay band, although there is a lack of distinct structure (e.g. a joint or bedding plane) from which observation of displacement can be made readily.

Table of Contents
Table of Contents
Table of Contents
Table of Contents

Clay bands were encountered in drillhole No. BH5 at three different levels. The uppermost bands were encountered at a depth of 5.7 m within the old colluvium and comprised three parallel sub-horizontal soft to firm reddish brown clay bands (Plate 42), spaced at about 20 mm to 30 mm apart. The corresponding Mazier sample was taken after a falling head permeability test was carried out (between depths of 4.4 m and 5.4 m). There is evidence of disturbance to the material recovered in the top of the sample and this may also account for the disturbance of the material below the sands. The subject Mazier sample was taken immediately above a large MDT corestone, which was encountered between depths of about 5.8 m and 7.6 m.

The second level of clay bands in drillhole No. BH5 was observed at about 9 m depth within the CDT. The clay bands comprised soft to firm light reddish brown clay of about 3 mm to 8 mm in thickness (Plate 43). There were 12 bands, which were sub-horizontal and very regularly spaced at between 25 mm and 35 mm. The clay bands prevail in a portion of the CDT that has a concentration of kaolin in the form of boxwork veins. Displacement appeared negligible across the upper bands whereas an apparent cutting of the boxwork veining was evident towards a depth of 9.2 m.

The third and deepest set of clay bands encountered in drillhole BH5 was observed in the sample taken from depths of about 18.6 m and 18.8 m (Plate 44). The clay bands are in the form of a series of sub-parallel, 5 mm to 10 mm thick, very soft, moist, light greenish brown sandy clay. The sample was taken below the main ground water level (measured at about 17 m depth) and from between two MDT corestones.

5.5 Laboratory Testing, Permeability Testing and Soil Properties

A series of laboratory tests was conducted at the PWCL and the Public Works Regional Laboratories on samples retrieved during the GI, in accordance with Geospec 3 (GEO, 2001). The testing programme included classification tests (moisture content tests, particle size distribution (PSD) and Atterberg Limits tests), together with and multi-stage consolidated undrained (CU) triaxial compression tests.

The average silt and sand contents of the young colluvium were 36% (ranging from 18% to 51%) and 29% (ranging from 18% to 69%) respectively, whilst that of the old colluvium were 43% (ranging from 29% to 52%) and 33% (ranging from 25% to 37%) respectively. The average silt and sand contents of the CDT were 44% (with a range of 24% to 60%) and 41% (ranging from 24% to 56%) respectively. The average clay content for young and old colluvium was 24% (ranging from 5% to 40%) and 18% (ranging from 11% to 35%) respectively, while the average clay content for CDT was about 9% (ranging from 3% to 17%).

The plasticity index of the fines of the young colluvium ranged from 15% to 43%, and the liquid limit ranged from 47% to 80%, which was classified as high to very high plasticity silt with occasional very high plasticity clay. The plasticity index of the fines of the old colluvium ranged from 15% to 40%, and the liquid limit ranged from 46% to 79%, which was classified as intermediate to highly plasticity silt with occasional very high plasticity. The plasticity index of the fines of the CDT ranged from 6% to 26%, and the liquid limit ranged from 29% to 66%, which was classified as low to intermediate plasticity silt with occasional high plasticity silt and low to intermediate plasticity clay (Figure 13 and 14).

Table of Contents
Table of Contents
Table of Contents
Table of Contents

Twenty-one falling head permeability tests were carried out in the vertical drillholes, mostly in CDT (except for one which was in colluvium) and also within the upper portion of the rock. The permeability of colluvium is 5.9×10^{-7} m/s. The permeability of CDT ranged from 2.1×10^{-6} m/s to 2.4×10^{-5} m/s with an average value of 7.5×10^{-6} m/s. The permeability of fractured rock ranged from 2.2×10^{-6} m/s to 6.5×10^{-7} m/s with an average value of 1.3×10^{-6} m/s. Double ring infiltration tests (DRIT) were carried out on the top of the young colluvium layer at three locations within the distressed hillside, *viz.* above the southern main scarp, immediately below the southern main scarp and centrally within the distressed hillside. The permeability from DRIT ranged from 1.5×10^{-5} m/s to 4.5×10^{-5} m/s with an average of 3.0×10^{-5} m/s. The permeability test results are plotted in Figure 15. The permeability shows a wide variability within individual strata but with a general trend of decreasing with depth.

Three permeability tests (at 4 m and 32 m depth in drillhole No. BH1 and at 11 m depth in drillhole No. BH5) were unsuccessful as the water level dropped too slowly, suggesting a very low permeability. In contrast, water drained away from the bottom of drillhole No. BH3 during an attempt to carry out a permeability test at a depth of 18.3 m (within CDT), despite adding water for more than 20 minutes (Figure 15).

A large number of Mazier samples of young colluvium and CDT were split for the purposes of inspection and examination, which therefore necessitated multi-stage triaxial tests being carried out on a limited number of Mazier and block samples. The p'-q plots for young colluvium and CDT are presented in Figure 16. The shear strength parameters of CDT from the triaxial tests correspond to c' = 9 kPa and $\phi' = 37°$, whereas the shear strength parameters of young colluvium from the triaxial tests correspond to c' = 3 kPa and $\phi' = 30°$.

Only limited Mazier samples of old colluvium were taken and all were split for inspection and examination. Based on the particle size distribution test results (see Section 5.5), the old colluvium has only a marginally higher sand content than the young colluvium. Only a marginally higher ϕ' value would be anticipated. For the purpose of theoretical stability analysis, the same shear strength parameters have been adopted for both old and young colluvium.

5.6 Geomorphology

The August 2005 landslide and area of distressed hillside are located on north-facing bouldery natural terrain, comprising rounded ridgelines bounding a linear topographical depression (Figure 2 and A2). The landslide is situated at the head of a drainage line and immediately above a break-in-slope associated with an older landslide scar. The distressed hillside where extensive tension cracks are present is situated within the linear topographical depression through which poorly defined ephemeral drainage lines run. The mouth of the depression is marked by a series of convex and concave breaks-in-slope with the terrain inclination observed to steepen from between 20° and 25° above the breaks-in-slope to between 30° and 35° below.

The hummocky ground surface morphology of the distressed hillside is indicative of a colluvial terrain with a history of instability. However, the footpaths and military activities on the hillside (Section 3.1) might also have contributed to the hummocky appearance of the

Table of Contents
Table of Contents
Table of Contents
Table of Contents

hillside by adversely changing the surface infiltration characteristic and potentially promoting concentrated water ingress.

The volcanic terrain is deeply weathered with up to 30 m of saprolite above Grade III rock. The presence of photolineaments and evidence from API (Section 3.2.2 and Appendix A) of a possible structural control to landslides in the vicinity and possible parallel breaks-in-slope along the eastern flank of the depression suggest that there may be an underlying structural influence on slope instability within the study area.

6. GEOLOGICAL AND GEOMORPHOLOGICAL MODEL

The study area is characterised by a deeply weathered thermally metamorphosed volcanic terrain with a mantle of colluvium. The colluvium is bouldery and about 5 m thick, while the underlying volcanic tuff saprolite is up to 30 m thick and in which corestone development appears relatively common. Many of the relict joints in the saprolite have a kaolin infill, a manganese oxide coating and are slickensided.

The feldsparphyric rhyolite dyke indicated on the HKGS 1:20 000 Solid and Superficial Geological Map Sheet No. 7, was not identified on site. The possible effects related to the presence of the dyke, such as damming of groundwater flow, have therefore been discounted from the geological model.

The location of the August 2005 landslide, which is above a prominent break-in-slope on a site previously affected by natural terrain landslides, appears to be typical of hillside retreat. Based on the geomorphological model of landform evolution in Hong Kong proposed by Hansen (1984), hillside retreat is a land forming process characterized by a zone of instability between the upper (older) landforms and the younger (lower) landforms. The hillside retreat occurs as the zone of instability propagates progressively upslope. The break-in-slope probably marks the upper limit of the erosion front between the older and younger landforms.

The distressed hillside (Section 4.2) adjacent to the August 2005 landslide lies within an elongate topographical depression, which appears to differ in shape from the broader catchments observed elsewhere in the vicinity. The sub-catchment in which the topographical depression lies is also elongate in shape. It would appear that the shape of the sub-catchment is somewhat structurally controlled. This postulation is supported by a possible photolineament based on API (Section 3.2.2), and a possible steeply dipping fault near the base of drillhole No. BH2 (Section 5.4).

The origin of the old colluvium (Section 5.3.2) is postulated to be remnant of landslide debris from an ancient landslide, which appears to be confined to the topographical depression. This suggests that the depression itself may be a degraded landslide scar (or multiple relict landslides). However, variations observed in the nature of the old colluvium towards the edges of the depression (Section 5.3.2) indicate that the depression has likely been shaped by several landslide events.

Table of Contents
Table of Contents
Table of Contents
Table of Contents

6.1 Landslide Susceptibility

Three or possibly four landslides have been identified from API (Section 3.2) to have occurred at about the same location as the August 2005 landslide. Two small landslides were identified in the 1956 aerial photographs and a larger pre-1963 landslide had affected the hillside in front of the future toe of the August 2005 landslide. API also indicated that concurrent with the pre-1963 landslide, there was reactivation of one of the smaller pre-1956 landslides. To the west of the spurline above the August 2005 landslide, several relict landslides have been identified and some appear to have had at least a partial structural influence (Section 3.2.2).

Two possible degraded landslide scars were identified from API (Appendix A) within the linear depression in which the distressed hillside is located and the northern-most ends of the eastern and western gullies (Section 4.4) appear to be coincident with possible relict landslides.

Large accumulations of boulders are present in the drainage lines and on the natural terrain below the landslide site with some colluvial boulders several metres across, all indicative of previous instability. Accumulation of colluvium within the drainage line appeared thin (typically less than 1 m thick), suggesting that while the terrain exhibits a susceptibility to landsliding, the historical landslide scale has been fairly small with the fine materials probably washed out, leaving the larger boulders along the drainage line.

7. HYDROGEOLOGY

7.1 General

Results from limited field permeability tests carried out during the GI indicate a general decreasing trend of permeability with depth (Figure 15). The possible decreasing trend and the variability of the colluvial soil material suggest that there is a potential for transient perched water tables to develop at the young colluvium/old colluvium interface and the old colluvium/CDT interface due to contrasts in permeability values. Based on the results of two field tests, the permeability of the fractured upper portion of the MDT appears to be quite low. Though the evidence is not strong, it appears unlikely that there is a confined aquifer in the upper portion of the MDT.

Numerous military trenches and other wartime excavations on the hillside above, within and close to the distressed hillside are likely to have influenced the pattern of surface runoff and promoted the ingress of water into the hillside during periods of heavy rainfall.

The near-surface hydrogeology at the site is likely to have been significantly influenced by the presence of soil pipes (Section 7.3) in the young and old colluvium. Evidence from the ground collapse features (Section 4.4), the connectivity of a subsurface erosion pipe near the August 2005 landslide (Section 4.5) and the soil pipes identified during the splitting of the Mazier samples (Section 7.3), suggests that the near-surface soil/erosion pipes are likely to be part of a complex interconnected subsurface drainage network.

There is a possible local depression in the rockhead profile around the location of drillhole No. BH1 (Figure 10) but this is based tentatively on the data from only five

Table of Contents
Table of Contents
Table of Contents
Table of Contents

drillholes. The rockhead contours indicate that there is a general dip in rockhead level towards the north and generally following the surface topography.

7.2 Groundwater Conditions

Post-landslide groundwater monitoring in drillholes Nos. BH1, BH2 and BH5 was carried out between July and October 2006 during the GI fieldwork and emergency works (Figure 17). Base groundwater levels within the lower piezometers in drillholes Nos. BH1, BH2, and BH5 varied between depths of 17.4 m and 20.1 m, 16.0 m and 22.0 m and 13.1 m and 16.9 m respectively. Following the rainstorm in mid September 2006, with a daily rainfall of 327 mm recorded on 13 September 2006 corresponding to a maximum return period of about 7 years, the base groundwater rose by a maximum of 3.7 m in drillhole No. BH2. Rises in the base groundwater of 3.5 m and 2 m were recorded in drillholes Nos. BH5 and BH1 respectively.

Transient perched water levels were recorded in the shallow standpipes and piezometers installed in drillholes Nos. BH1, BH2 and BH5 (Section 5.2), after the mid September 2006 rainstorm. A perched water table developed in drillhole No. BH1 rising to a maximum of about 2.5 m above the old colluvium/CDT interface, and corresponding to a water level about 2.8 m below ground level. A transient perched water levels of about 1.6 m and 0.4 m above the young colluvium/CDT and young colluvium/old colluvium interfaces in drillholes Nos. BH2 and BH5 respectively. The recorded transient water levels in both drillholes Nos. BH2 and BH5, corresponded to a maximum water level of about 1.4 m below ground level within the young colluvium.

The responses of piezometer and standpipe in the mid September 2006 rainstorm were rapid, though dissipation was slower with base groundwater levels steadily declining over a period of 10 to 12 days following the rainstorm. The slowest dissipation was observed in the upper piezometer in drillhole No. BH1, where the perched water above the old colluvium/CDT interface took over 22 days to drop to levels close to that recorded before the rainstorm. The corresponding perched water recorded in drillholes Nos. BH2 and BH5 declined over about six days. The sharp response in all piezometers probably relates to direct infiltration and groundwater flow through the subsurface drainage network or secondary porosity system, i.e. relict discontinuities, fissures and soil pipes (GEO, 2006b). A slower dissipation subsequent to a rainstorm could be associated with recharge from upslope. The particularly slow decline in the transient water levels observed in drillhole No. BH1 may be related to its location but probably reflects the condition of the secondary porosity system intercepted by the drillhole. Choked soil pipes were identified in the old colluvium in drillhole No. BH1 during the GI (Section 7.3), and these may have impeded groundwater drainage.

7.3 Underground Streams and Cavities

Numerous underground cavities and soil pipes up to 1 m across are present below the subject hillside, some of which were only identified as a result of the cavities causing ground surface collapse. Most of the cavities appear to be present in the top 2 m below ground surface within the young colluvium. Soil pipes were also encountered during the GI in the old colluvium and incipient soil pipe development was observed throughout the CDT.

Table of Contents
Table of Contents
Table of Contents
Table of Contents

Soil pipes were observed in trial pits Nos. TP2 and TP8 (Figures C2 and C3 in Appendix C). The soil pipe in trial pit No. TP2 was observed at a depth of about 2.7 m below ground level within old colluvium. The soil pipe had a maximum width of 0.8 m and was probed to a depth of 0.6 m. Further probing was not possible since the roof of the soil pipe collapsed during the excavation of the pit. A 0.6 m diameter boulder of MDT was located above and to one side of the cavity and a 0.3 m to 0.4 m thick alternating sequence of clay and sand was observed at the base of the soil pipe (Plate 45**)**.

The cavity in trial pit No. TP8 was observed at depths of between about 0.8 m and 1.8 m within the young colluvium and was over 1 m across. It was probed downhill (i.e. northwards towards the distressed hillside) up to 2 m. The cavity was first identified as a result of ground surface collapse and during the excavation of the pit, a large accumulation of sandy clay was observed above silty sand (Plate 46). The observations in trial pits Nos. TP2 and TP8 of alternating clayey and sandy layers appear to indicate periods when the interconnected soil pipe system had been choked leading to deposition of fines (clay or silt/clay), and other periods when the system was open and ground water had flowed more easily, depositing sands. The soil pipes observed in both trial pits Nos. TP2 and TP8 were noted to extend uphill beyond the area of distressed hillside as delineated by the extensive tension cracks.

In drillhole No. BH1, erosion pipes were encountered at depths of between 1.7 m and 1.9 m in young colluvium, and between 2.9 m and 3.1 m in old colluvium. The deposit in the lower erosion pipe was observed to be a ‘fining up’ sequence of sands (Plate 47), with a sub-horizontal 10 mm thick clay layer at about the mid-height of the choked soil pipe (Plate 48).

The connectivity of the subsurface drainage network was revealed during the drilling of drillhole No. BH1, when the loss of circulation of drilling flush was observed to correspond to the emergence of drilling foam from a raking drain installed into the August 2005 landslide scar**.**

A soil pipe was observed in drillhole No. BH4 at a depth of about 4 m, measuring up to 60 mm across with a sandy infill and a 10 mm to 20 mm thick band of clay deposit above the sand.

Dark reddish brown stained patches were observed throughout the CDT (Plate 49). These patches appeared to be the incipient stages of soil pipe development. The stained patches varied in size from several millimetres up to 80 mm across, and were characterised by the presence of reddish brown iron oxide stained quartz and a reduction or absence of fine material, in contrast to the surrounding CDT.

8. ANALYSIS OF RAINFALL RECORDS

Rainfall data were obtained from the nearest GEO automatic raingauge No. K07, which is located approximately 1.67 km to the southwest of the August 2005 landslide on the roof of Ching Tak House, Tsz Ching Estate, Tsz Wan Shan (Figure 1). The raingauge records and transmits rainfall data at 5-minute intervals to the GEO and the Hong Kong Observatory (HKO). The daily rainfall recorded by raingauge No. K07 from 20 July to 24 August 2005, together with the hourly rainfall readings for the period of 19 to 22 August 2005,

Table of Contents
Table of Contents
Table of Contents
Table of Contents

are presented in Figure 18. Records from another nearby GEO automatic raingauge No. N43, which is about 2.5 km to the north of the August 2005 landslide, were also examined. The pattern of rainfall recorded at this raingauge was broadly similar to that recorded at raingauge No. K07, although the rainfall was slightly less intense.

Amber Rainstorm Warnings were hoisted on the evening of 19 August 2005 and in the morning of 20 August 2005. Intense rainfall was recorded until the evening of 20 August 2005. According to an eyewitness, the landslide was first observed at about 7 a.m. in the morning of 22 August 2005 (see Section 4). Given the remote location of the site and the inclement weather, the landslide may have occurred anytime between 19 and 22 August 2005 when it was first identified. Since the exact time of the landslide is not certain, it has been assumed that the landslide occurred before 7:00 a.m. on 22 August 2005. No rainfall was recorded between 10:00 p.m. on 21 August 2005 and 7:00 a.m. on 22 August 2005. The daily rainfall on 21 August 2005 was 23.5 mm. The maximum 12-hour and 24-hour rolling rainfalls before the incident were 266 mm and 473.5 mm respectively, which were recorded on 20 August 2005. The maximum 1-hour rolling rainfall was recorded as 44.5 mm between 10:10 a.m. and 11:10 a.m. on 20 August 2005 (Table 1).

An analysis of the return periods for various durations of rolling rainfall recorded at raingauge No K07, with reference to the historical rainfall data at the HKO at Tsim Sha Tsui where records began in 1884 (Lam & Leung, 1994), shows that a rainfall duration of 10 days or more before the landslide was the most severe with corresponding return periods ranging from 80 years to 119 years (Table 1).

The return periods were also assessed based on the statistical parameters derived by Evans & Yu (2001) from rainfall data recorded by the local raingauge No. K07 between 1984 and 1997. The 24-hour and 48-hour rainfalls were assessed to be most critical with return periods of 47 years and 31 years respectively (Table 1), which are less than those estimated using the historical rainfall data at the HKO.

The maximum rolling rainfall for the August 2005 rainstorm has been compared with the past major rainstorms recorded by raingauge No. K07 between 1983 and 2004 (Figure 19). The 20 August 2005 rainstorm was the most severe for rainfall durations between 24 hours and 15 days.

9. THEORETICAL STABILITY ANALYSES

9.1 The August 2005 Landslide

Theoretical stability analyses were carried out to assist the diagnosis of the mechanism and causes of the August 2005 landslide. These analyses were carried out to investigate the likely operative range of shear strength parameters along the failure surface corresponding to different possible groundwater levels at the time of the failure.

A cross-section of the August 2005 landslide site and the input parameters adopted in the analyses are shown in Figure 20. The pre-failure ground profile within the failed area was interpolated from the detailed topographical survey of the two flanks of the landslide undertaken after the failure, with suitable adjustment of ground levels based on the evidence from API that a smaller landslide may have occurred at the same location as the 2005

Table of Contents
Table of Contents
Table of Contents
Table of Contents

landslide (see Section 3.2.2). The geological profile of the analysed failure surface was determined from field mapping and ground investigation information. Based on geological mapping, the failure surface of the August 2005 landslide was primarily along the interface between colluvium and CDT. A range of groundwater levels was assumed in the analyses to simulate the possible groundwater conditions at the time of failure.

The results of the analyses are presented in Figure 20 for shear strength parameters of c' = 0 to 4 kPa and ϕ' = 28° to 36°. The results indicate that for the ranges of shear strength parameters along the failure surface, a groundwater level of between 1.2 m and 3.1 m below ground surface would have been sufficient for failure to occur. Using the shear strength parameters of c' = 3 kPa and ϕ' = 30° for colluvium (both young and old colluvium are assumed to have the same shear strength parameters, see Section 5.5) that were derived from laboratory tests, a groundwater level of about 2.6 m below ground surface, corresponding to a rise of about 2.5 m above the colluvium/CDT interface, would have been sufficient for failure.

9.2 The Distressed Hillside

Theoretical stability analyses of the distressed hillside were carried out to evaluate potential failures with respect to different possible groundwater regimes and shear strength parameters along a pre-defined failure surface. Based on the geological model, the following two cases were examined:

(a) Case A - failure along the interface of old colluvium and CDT, at a depth of about 5 m below ground level with a build-up of perched water table (corresponds to a failure of about 12,000 m³ in volume).

(b) Case B - failure exploiting potentially weaker material within the CDT, with lower shear strength, at a depth of about 10 m below ground surface and a rise in the main groundwater table (corresponds to a failure of about 30,000 m³ in volume).

A cross-section of the distressed hillside and the input parameters adopted in the analyses are shown in Figures 21 and 22. The ground profile of the hillside was obtained from topographical survey and the geological profile of the section was determined from field mapping and ground investigation information. A range of groundwater profiles was assumed in the analyses to simulate the possible groundwater conditions.

The results of the analyses are presented in Figures 21 and 22.

(a) Case A: For failure along the interface between old colluvium and CDT, the results indicate that a rise in perched groundwater to about 1.3 m below ground surface (i.e. about 3.8 m above the inferred failure surface) would be sufficient to initiate failure assuming shear strength parameters of c' = 3 kPa and ϕ' = 30° for colluvium that

Table of Contents
Table of Contents
Table of Contents
Table of Contents

were derived from laboratory tests.

(b) Case B: For failure exploiting weaker materials, assuming shear strength parameters for c' of between 0 kPa and 2 kPa and ϕ' between 26° and 32° and a maximum depth of 10 m within the CDT, the results indicate that groundwater would need to rise between 6.3 m and 9.0 m above the inferred failure surface to be sufficient for the failure to occur.

The results for Case A indicate that a shallow failure (i.e. along the interface between old colluvium and CDT) would be plausible with a perched groundwater of about 1.3 m below ground surface. A perched water level of 1.4 m below ground was recorded once in the upper piezometer at drillhole No. BH2 after the September 2006 rainstorm, which suggests the perched water level required for the shallow failure to initiate, is viable.

The results for Case B show that if the shear strength parameters of the materials along the failure surface are of c' = 0 kPa and 2 kPa and ϕ' = 26°, a deep-seated failure (i.e. along the possible weaker materials within CDT at a depth of about 10 m depth) would be feasible with a rise in base groundwater level of about 8.5 m to 9 m (assuming a base groundwater level of about 13 m to 14 m below ground level during the wet season, see Section 7.2). When c' = 0 kPa and 2 kPa and ϕ' = 32°, the base groundwater level would need to rise between 12.5 m and 13 m to reduce the factor of safety to below 1.0 and potentially initiate failure (Figure 22).

The rapid groundwater rise (3.7 m rise in the base groundwater table) and the slow rate of dissipation of water (10 to 12 days after the initial rise) observed following the September 2006 rainstorm (see Figure 17) suggest that prolonged intense rainfall, such as that of the August 2005 rainstorm, may invoke some unusual hydrogeological conditions and could potentially lead to a significant rise in the base groundwater, despite a fairly small catchment area of about 20,000 m^2 plan area.

10. DIAGNOSIS OF THE PROBABLE CAUSES OF THE AUGUST 2005 LANDSLIDE AND THE DISTRESS ON THE HILLSIDE

10.1 The August 2005 Landslide

The close correlation between the August 2005 landslide and the preceding heavy rainstorm suggests that the failure was triggered by rainfall. The landslide was reported to the GEO in the morning of 22 August 2005, almost two days after the end of the rainstorm on 20 ugust 2005. If failure did occur on 22 August 2005, the apparent two-day delay would suggest that a slow rise in groundwater might have been a contributory factor to the landslide. However, following the mid September 2006 rainstorm (maximum 24-hr rolling rainfall of 327 mm compared with a maximum 24 hr rolling rainfall of 473.5 mm for the 22 August 2005 rainstorm), rapid rises in both the main groundwater as well as the perched groundwater in the surface mantle of colluvium were recorded in the piezometers and standpipes. Several raking drains (see Figure 9) installed in the 2005 landslide scar showed rapid increases in groundwater flow subsequent to the September 2006 rainstorm, which also suggests a rapid infiltration into the subsurface material. Therefore, a relatively rapid rise in groundwater would seem more credible given the permeable nature of the colluvium, and a

Table of Contents
Table of Contents
Table of Contents
Table of Contents

delayed response was probably unlikely.

The August 2005 landslide involved a failure of both young and old colluvium. The surface of rupture appears to have been primarily along the old colluvium/CDT interface, though the deepest portion of the landslide near the toe of the surface of rupture appeared to be through the top of the underlying CDT. The likely mechanism of failure involved a wetting up of the ground mass due to direct infiltration and subsurface seepage from the uphill catchment leading to the transient development of perched groundwater pressure above the old colluvium/CDT interface.

Theoretical stability analyses of the August 2005 landslide indicate that a transient perched water table of between 1.2 m and 3.1 m below ground surface, i.e. about 3.8 m to 1.9 m above the old colluvium/CDT interface respectively, would be sufficient for failure to occur. Rises in the perched water table approaching those required to initiate failure were recorded in standpipes and piezometers, following a rainstorm in mid September 2006 (Section 7.2).

The geomorphological setting of the August 2005 landslide is likely to have played a key role in the failure. The landslide is located above a prominent break-in-slope which may mark the limit of a zone of instability, indicative of a hillside retreat process. The August 2005 landslide is also located at the head of an ephemeral drainage line, where convergent surface runoff and subsurface seepage would likely occur during periods of heavy rainfall.

After the mid September 2006 rainstorm, groundwater flow rates from some of the raking drains were observed to be greater than from others (Figure 9). The drains with the higher flow rates had probably intercepted more transmissive groundwater pathways, indicating that preferential flow paths are present in the subsurface material, which are likely to have promoted rapid groundwater flow towards the landslide site.

The choked soil pipes encountered in drillhole No. BH1, located to the east and upslope of the August 2005 landslide, and the established connectivity of the subsurface drainage network between the distressed hillside near drillhole No. BH1 and the August 2005 landslide scar (Section 7.3) could have also resulted in a greater concentration of groundwater flow towards the August 2005 landslide site.

10.2 The Distress on the Hillside

The generally hummocky morphology of the distressed hillside and the extensive system of tension cracks with a varied and occasionally intermittent surface expression, are indicative of a large ground mass undergoing a complex movement in terms of its kinematics. The presence of numerous underground cavities and soil pipes, some with layered deposits and others blocked, together with ground surface collapse features, indicate that the distressed hillside has a complicated and highly variable hydrogeology.

The extent over which the tension cracks have developed along the eastern and southern flanks of the distressed hillside is indicative of a single surface of rupture controlling movement at that location. In contrast, the series of en echelon tension cracks along the western flank of the distressed hillside, are possibly related to a poorly developed or

Table of Contents
Table of Contents
Table of Contents
Table of Contents

discontinuous slip surface, possibly below separate blocks.

The contrasting surface expressions between the distinct tension cracks on the eastern and southern main scarps of the distressed hillside, with up to 1.1 m of vertical displacement, and the less distinct en echelon tension cracks on the western flank with a vertical displacement of about 0.2 m, support the postulation that the large ground mass undergoing displacement probably comprises separate blocks of material possibly moving in different directions (Figure 8).

The probable toe of the distressed hillside appears to be delineated by a series of prominent convex and concave breaks-in-slope on the hillside directly east of the August 2005 landslide. The absence of old colluvium in drillhole No. BH2 and trial pits Nos. TP6 and TP9 and no obvious signs of movement, (e.g. tension cracks, disturbance of soil around boulders, etc.), in the hillside below the breaks-in-slope support the above postulation.

Theoretical stability analyses were carried out to examine the possible presence of developing failure surfaces at differing depths (see Section 9.2). For the soil parameters adopted, these indicate that a perched water table of between 2.5 m and 3.5 m above the old colluvium/CDT interface is required to initiate failure. To initiate failure along an assumed deeper weak layer/slip surface within the CDT (at about 10 m below ground level), the base groundwater would need to rise between about 8.5 m and 13 m. Although the available information does not point to the presence of a continuous weak layer below the distressed hillside, the completely decomposed tuff contains a high kaolin content which could weaken the soil mass along localised zones.

11. DISCUSSION

The location of the August 2005 landslide is probably associated with the geomorphological setting, above a prominent break in slope at the head of a drainage line. The aerial photographic records indicate that the August 2005 landslide occurred at about the same location as two smaller pre-1956 landslides (Section 3.2.2), and the surface of rupture was observed to pass through colluvium, along the old colluvium/CDT interface and partly through completely decomposed tuff (Section 4.2). The previous instability and progressive degradation of the hillside appears typical of a hillside retreat process. Both surface runoff and subsurface flow would be directed towards the landslide site at the head of a drainage line and the presence of an interconnected subsurface drainage network would have promoted rapid groundwater flow to the landslide site. In overall terms, the August 2005 landslide was not a surprise.

The distressed hillside delineated by the extensive tension cracks within the topographical depression adjacent to the August 2005 landslide was identified in March 2006. The majority of the tension cracks as identified in March 2006 appeared fresh and may have occurred subsequent to the August 2005 landslide. Evidence on the distressed hillside, *viz.* hummocky morphology, leaning trees, possible weathered patina on the southernmost tension crack (Section 4.4), however suggests that initial movement of the distressed hillside most likely predates the August 2005 landslide and that initial development of at least part of the tension cracks may have been a result of earlier rainstorms. Given that the majority of the tension crack faces appeared fresh, the largest proportion of movement is postulated to have likely been triggered by the August 2005 rainstorm. The possibility of the fresh tension

Table of Contents
Table of Contents
Table of Contents
Table of Contents

cracks being a reactivation of the distressed hillside due to the severe rainstorm in August 2005 cannot be ruled out.

Theoretical stability analyses and groundwater monitoring data to date, suggest that the development of a perched water table above the old colluvium/CDT interface, indicative of a fairly shallow failure with an average depth of about 4 m (maximum 6 m), could initiate a failure along the old colluvium/CDT interface potentially leading to the formation of the main scarps. However, it is noteworthy that the limited GI did not indicate any shear surface or any other obvious indication of movement at the old colluvium/CDT interface. It may be possible that for a large hillside, significant shear and volumetric strains could have developed in the ground mass as a result of heavy rainstorms and progressive deterioration of the hillside, giving rise to major settlements and tension cracks at the ground surface without resulting in a distinct and complete rupture surface.

The extent of the tension cracks and the large area of the distressed hillside delineated by the cracks are indicative of a large mass undergoing intermittent movement. It may also be possible that the August 2005 landslide was a local detachment of a larger unstable ground mass undergoing intermittent movement and progressive deterioration following heavy rainfall.

The extensive distress on a shallowly dipping hillside (*viz*. about 20°), suggests the presence of weak geological material and/or adverse ground conditions. The spatial distribution of drillholes across the distressed hillside (Figure 10) was determined with a view to identifying the possible presence of a developing slip surface below the disturbed mass. During the GI, clay-rich bands were identified in four of the five vertical drillholes (see Section 5.4.1) at depths of between about 4 m and 18 m. In three of the four drillholes (i.e. drillholes Nos. BH1, BH4 and BH5), the clay-rich bands were identified between about 9 m and 11 m below ground surface. However, there was no discernable evidence of movement associated with the clay-rich bands and their origins are not certain. It is noteworthy that laboratory testing determined that the clay-rich bands were a clayey silt of high plasticity (see Section 5.5). Although the available information does not point to the presence of a continuous weak layer below the distressed hillside, the completely decomposed tuff possesses a high kaolin content which could weaken the soil mass along localised zones.

In trial pits Nos. TP1 to TP3, through the eastern and southern tension cracks (Figure 10), the slip surface was observed to dip steeply and run through the front of the trial pit with no apparent indication of a flattening off of the slip surface towards a shallow basal surface (see Appendix C). Notably, possible evidence of shearing along discontinuous planar joint surfaces as indicated by a light brown discolouration of kaolin within the joints, was identified at about 2.5 m below ground level and in the upslope sides of trial pits Nos. TP1 and TP2 (see Appendix C). The discontinuous surfaces were shallow dipping at 12°/005° in trial pit No. TP1 and 12°/015° in trial pit No. TP2 (Figure 8). This compares with an apparent overall downhill direction of movement of the distressed hillside towards a bearing of 025°. The significance of these discontinuous apparently sheared surfaces is unclear; their presence, however, highlights the complex nature of the movement and kinematics of the large ground mass. The monitoring records from the in-place inclinometers have not shown a trend of downhill movement within the distressed hillside (see Section 5.2).

The presence of a basal slip surface within the distressed hillside was not positively

Table of Contents
Table of Contents
Table of Contents
Table of Contents

established by the available GI information. The difficulty in establishing whether or not such a surface was present may be the result of the surface not having yet fully developed. The poorly developed failure surface may also be discontinuous between separate blocks of material with internal distortions and local concentrated strains within the distressed hillside.

Although a well-developed incipient slip surface could not be identified from the limited drillholes, the observations of displacement structures from field mapping (Section 4.4), *viz*. scarps and en-echelon tension cracks, could potentially be the surface expression of a developing large-scale landslide. Similar displacement structures were reported by Parry & Campbell (2003) for a slow moving, deep-seated failure in a slope in weathered andesite lava. The observed displacement structures at the subject site suggest that the mode of deformation of the distressed hillside may correspond to local fracture surfaces slipping approximately parallel to the fracture front, *viz*. Mode III deformation, as discussed by Parry & Campbell (2003). The disposition and areal extent of the tension cracks within the distressed hillside suggests the possibility of a developing instability, which could be deep seated and involve progressive failure (see Section 9.2), cannot be entirely discounted, although the likelihood of this occurring cannot be established from the limited GI and groundwater monitoring.

With the intermittent ground movement and the developing tension cracks, the condition of the hillside is subject to progressive deterioration. The distressed hillside is likely to be more vulnerable to sudden uncontrolled detachments (the ductile movement mode may transform into a brittle detachment mode), as the distressed ground mass is liable to become weaker and more susceptible to water ingress with further movement.

The stability analyses and the rather limited groundwater monitoring suggest that the failure of the old colluvium is plausible, which could be a possible mechanism for the formation of the main scarps. This would be consistent with Case A (see Section 9.2) shallow failure scenario which is supported by the extensive near-surface anthropogenic activities (e.g. military trenches, tunnels, pits and tracks) providing direct access of surface water into the shallow subsurface and affecting the pattern of surface runoff, the connectivity of subsurface drainage network (e.g. loss of circulation during soil nail construction, and other observations cited in Section 7.3), and the observation during rainy periods of a constant flow of groundwater in some raking drains in and near the August 2005 landslide scar and erosion gullies. However, it should be noted that the Case A scenario, while appearing to be a credible plausible failure mechanism, does not satisfactorily explain some of the observations, e.g. the very widespread tension cracks and other displacement features in a distressed hillside which is inclined at an average angle of only 20°; no obvious indication of any shearing between the base of the old colluvium and the top of the CDT in any of the split Mazier samples; the subsurface trace of the tension cracks appears to continue beyond 3 m below the ground level; no indication of flattening off of the tension cracks to a shallow slip surface, etc. The mode of displacement of the groundmass within the distressed hillside and the hydrogeology of the site are very complex.

The available drillhole data have not revealed strong evidence of a deep-seated failure mode, such as shear zones or slip planes. A significant rise in the base groundwater level would be necessary to cause deep-seated instability which would need to involve some fairly unusual hydrogeological conditions given a fairly small catchment of about 20,000 m^2 plan area. However, given the extensive distress and displacement structures, the presence of clay-rich bands and a high kaolin content in the saprolite, together with the rather limited GI

Table of Contents
Table of Contents
Table of Contents
Table of Contents

and groundwater monitoring, the possibility of a developing deep-seated progressive failure cannot be entirely ruled out.

12. CONCLUSIONS

The August 2005 landslide was probably triggered by the preceding intense rainstorm. It involved the failure of up to 5 m of colluvium, primarily along the old colluvium/CDT interface in an uncontrolled manner giving rise to fast-moving debris. Debris from the landslide travelled a total distance of 330 m down the drainage line below the landslide source area and appeared to be wet and mobile. There was little entrainment other than at the location near the MacLehose Trail below the landslide source. Deposition of debris took place on the sides of the debris trail for almost the entire length of the landslide trail.

The August 2005 landslide, the crest of which is some 30 m upslope of the crest of the pre-1963 landslide, was probably influenced by its adverse geomorphological setting, *viz*. immediately above a break-in-slope on deeply weathered volcanic terrain with a surface mantle of colluvium at a site with a history of landslides. The 2005 landslide location is typical of an erosion front advancing uphill through the natural hillside as part of the progressive degradation of the hillside in the form of a hillside retreat process. Both surface runoff and subsurface flow would be directed towards the landslide site at the head of a drainage line and the presence of an interconnected subsurface drainage network would have promoted rapid groundwater flow to the landslide site. The extensive near-surface anthropogenic activities (e.g. military trenches, tunnels, pits and tracks) will also have affected the pattern of surface runoff and provided direct access of surface water into the ground mass.

The development of the extensive tension cracks with intermittent surface opening and other displacement structures within the distressed hillside are indicative of a large ground mass undergoing a complex mode of instability. Whether the controlling slip surface below the large unstable mass is relatively shallow or deep-seated could not be positively established based on the evidence obtained from the available GI information. Theoretical stability analyses and groundwater monitoring data to date, suggest that the development of a perched water table above the old colluvium/CDT interface, corresponding to a relatively shallow failure, would appear to be a plausible means of initiating instability. However, given the disposition and areal extent of the tension cracks within the distressed hillside, the possibility of a developing instability, which could be deep seated and involve progressive failure, cannot be entirely ruled out based on the rather limited GI and groundwater monitoring data.

The geometry of the old colluvium, which thickens towards the centre of the depression in which the distressed hillside is located, and the geographical association of the old colluvium with the topographical depression which may be a degraded relict landslide scar (or multiple relict landslide scars), suggest that the old colluvium is probably the remnant of the landslide debris associated with relict failure(s).

13. REFERENCES

Addison, R. (1986). Geology of Sha Tin. Hong Kong Geological Survey Memoir No. 1. Geotechnical Control Office, Civil Engineering Services Department, Hong Kong

Table of Contents
Table of Contents
Table of Contents
Table of Contents

Government, 85 p.

Agriculture, Fisheries and Conservation Department (2005). War Relics (Stage 5 of MacLehose Trail). <http://www.afcd.gov.hk/parks/trails/Eng/hiking/wrtrail/wrtrail.htm>. Agriculture, Fisheries and Conservation Department, Government of the Hong Kong SAR.

Campbell, S.D.G. & Parry, S. (2002). Report on the Investigation of Kaolin-Rich Zones in Weathered Rocks in Hong Kong. (GEO Report No. 132). Geotechnical Engineering Office, Civil Engineering Department, Government of the Hong Kong SAR, 75 p.

Campbell, S.D.G., Sewell, R.J. & Westnidge, R. (2000). Report on the Geology of the Landslide Site at Tate's Ridge, Fei Ngo Shan Road. Geotechnical Engineering Office, Civil Engineering Department, Government of the Hong Kong SAR, 34 p. plus 2 drgs. (unpublished).

Cruden, D.N. & Varnes, D.J. (1996). Landslide Types and Processes. Landslides: Investigation and Mitigation (Ed. Turner, A.K. and Schuster, R.L.), Special Report 247 of the Transport Research Board, National Research Council, National Academy press, Washington D.C. Chapter 3, pp. 36 - 75.

Evans, N.C., Huang, S.W. & King, J.P. (1997). The Natural Terrain Landslide Study Phases I and II. Special Project Report No. SPR 5/97, Geotechnical Engineering Office, Civil Engineering Department, Government of the Hong Kong SAR, 199 p. plus 2 drgs.

Evans, N.C. & Yu, Y.F. (2001). Regional Variation in Extreme Rainfall Values. (GEO Report No. 115). Geotechnical Engineering Office, Civil Engineering Department, Government of the Hong Kong SAR, 81 p.

Fugro Scott Wilson Joint Venture (1999). Detailed study of the Landslide at Tate's Ridge, Fei Ngo Shan Road on 9 June 1998. Landslide Study Report No. LSR 16/99, Geotechnical Engineering Office, Civil Engineering Department, Government of the Hong Kong SAR, 69 p.

Geotechnical Control Office (1984). Geotechnical Manual for Slopes (Second Edition). Geotechnical Control Office, Civil Engineering Services Department, Hong Kong Government, 295 p.

Geotechnical Control Office (1986). Sha Tin: Solid and Superficial Geology, Hong Kong Geology Survey, Map Series HGM20, Sheet 7, 1:20 000 scale. Geotechnical Control Office, Civil Engineering Services Department, Hong Kong Government.

Geotechnical Control Office (1987a). Geotechnical Area Studies Programme - Central New Territories. GASP Report No. II, Geotechnical Control Office, Civil Engineering Department, Hong Kong Government, 165 p. plus 4 maps.

Geotechnical Control Office (1987b). Guide to Site Investigation (Geoguide 2). Geotechnical Control Office, Civil Engineering Department, Hong Kong Government, 359 p.

Table of Contents
Table of Contents
Table of Contents
Table of Contents

Geotechnical Control Office (1988). Guide to Rock and Soil Descriptions (Geoguide 3). Geotechnical Control Office, Civil Engineering Department, Hong Kong Government, 186 p.

Geotechnical Engineering Office (2001). Model Specification for Soil Testing - Geospec 3. Geotechnical Engineering Office, Civil Engineering Department, Government of the Hong Kong SAR, 340 p.

Geotechnical Engineering Office (2007). Engineering Geological Practice in Hong Kong. GEO Publication No. 1/2007, Geotechnical Engineering Office, Civil Engineering and Development Department, Government of the Hong Kong SAR, 278 p.

Hansen, A. (1984). Engineering geomorphology: The application of an evolutionary model of Hong Kong's terrain. Zeitschrift fur Geomorphologie, supplementary vol. 51, pp 39 - 50.

King, J.P. (1999). Natural Terrain Landslide Study - The Natural Terrain Landslide Inventory. (GEO Report No. 74). Geotechnical Engineering Office, Civil Engineering Department, Government of the Hong Kong SAR, 116 p.

Lam, C.C. & Leung, Y.K. (1994). Extreme Rainfall Statistics and Design Rainstorm Profiles at Selected Locations in Hong Kong. Technical Note No. 86, Royal Observatory, Hong Kong Government, 89 p.

Parry, S. & Campbell, S.D.G. (2003). A Large Scale Slow Moving Natural Terrain Landslide in the Leung King Valley. Geological Report No. GR 2/2003, Geotechnical Engineering Office, Civil Engineering Department, Government of the Hong Kong SAR, 60 p.

Scott Wilson (Hong Kong) Ltd. (1999). Specialist API Services for the Natural Terrain Landslide Study - Task B Final Report. Report to Geotechnical Engineering Office, Civil Engineering Department, Government of the Hong Kong SAR, 9 p. plus 4 maps.

Sewell, R.J., Campbell, S.D.G., Fletcher, C.J.N., Lai, K.W. & Kirk, P.A. (2000). The Pre-Quaternary Geology of Hong Kong. Geotechnical Engineering Office, Civil Engineering Department, Government of the Hong Kong SAR, 181 p. plus 4 maps.

Wong, H.N. & Ho, K.K.S. (1996). Travel distance of landslide debris. Proceedings of the Seventh International Symposium on Landslides, Trondheim, Norway, vol. 1, pp. 417 - 422.

Wong, H.N., Ko, F.W.Y. & Hui, T.H.H. (2006). Assessment of Landslide Risk of Natural Hillsides in Hong Kong. (GEO Report No. 191). Geotechnical Engineering Office, Civil Engineering and Development Department, Government of the Hong Kong SAR, 117 p.

Table of Contents
Table of Contents
Table of Contents
Table of Contents

LIST OF TABLES

Table No.		Page No.
1	Maximum Rolling Rainfall at GEO Raingauge No. K07 for Selected Durations Preceding the 22 August 2005 Landslides and Estimated Return Periods	43

Table of Contents
Table of Contents
Table of Contents
Table of Contents

Table 1 - Maximum Rolling Rainfall at GEO Raingauge No. K07 for Selected Durations Preceding the 22 August 2005 Landslide and the Estimated Return Periods

Duration	Maximum Rolling Rainfall (mm)	End of Period	Estimated Return Period (Year)	
			By Lam & Leung (1994)	By Data of K07 from Evans & Yu (2001)
5 Minutes	6.0	11:00a.m. on 20 August 2005	< 2	< 2
15 Minutes	17.0	11:10a.m. on 20 August 2005	< 2	< 2
1 Hour	44.0	11:10a.m. on 20 August 2005	< 2	< 2
2 Hours	82.5	11:10a.m. on 20 August 2005	< 2	< 2
4 Hours	128.0	11:10a.m. on 20 August 2005	2	3
12 Hours	266.0	6:55 p.m. 20 August 2005	7	7
24 Hours	473.5	6:30 p.m. 20 August 2005	33	47
48 Hours	624.0	9:45 p.m. 20 August 2005	68	31
4 Days	726.50	8:30 p.m. 20 August 2005	58	15
7 Days	832.0	8:45 p.m. 20 August 2005	79	20
10 Days	927.5	9:15 p.m. 21 August 2005	93	17
12 Days	1011.5	11:40 p.m. 20 August 2005	119	17
15 Days	1035.0	9:15 p.m. 21 August 2005	81	11
31 Days	1296.0	8:45 p.m. 20 August 2005	90	7

Notes:
(1) Maximum rolling rainfall was calulated from 5-minute rainfall data.
(2) Return periods were derived from Table 3 of Lam & Leung (1994) and using data from Evans & Yu (2001) with interpolation of rainfall parameters for 10 days and 12 days.
(3) According to the eyewitness, the landslide was first observed at about 7:00 a.m. on 22 August 2005.
(4) The nearest GEO automatic raingauge to the landslide site is raingauge No. K07 located about 1.67 km to the southwest of the landslide site.

Table of Contents
Table of Contents
Table of Contents
Table of Contents

LIST OF FIGURES

Figure No.		Page No.
1	Location Plan	46
2	Site Layout Plan	47
3	Section A-A Through the August 2005 Landslide	48
4	Section B-B Through the Distressed Hillside	49
5	Regional Geology	50
6	Site History	51
7	Past Instabilities	52
8	Movement Observed within the Distressed Hillside	53
9	Field Observations During the Remedial Works	54
10	Ground Investigation Layout and Rockhead Contour	55
11	Geological Section A'-A' through the August 2005 Landslide Source Area	56
12	Geological Section B-B through the Distressed Hillside	57
13	Plasticity Charts	58
14	Atterberg Limits and Moisture Content	59
15	Summary of Field Permeability Tests	60
16	p'-q Plots	61
17	Records of Groundwater Monitoring between July 2006 and October 2006	62
18	Daily and Hourly Rainfall Recorded at GEO Raingauge No. K07	63
19	Maximum Rolling Rainfall for Previous Major Rainstorms at GEO Raingauges No. K07	64
20	Summary of Theoretical Stability Analysis of the August 2005 Landslide	65

Table of Contents
Table of Contents
Table of Contents
Table of Contents

Figure No.		Page No.
21	Summary of Theoretical Stability Analysis of the Distressed Hillside (Shallow Failure)	66
22	Summary of Theoretical Stability Analysis of the Distressed Hillside (Deep Seated Failure)	67
23	Locations and Directions of Photographs	68

Table of Contents
Table of Contents
Table of Contents
Table of Contents

Table of Contents
Table of Contents
Table of Contents

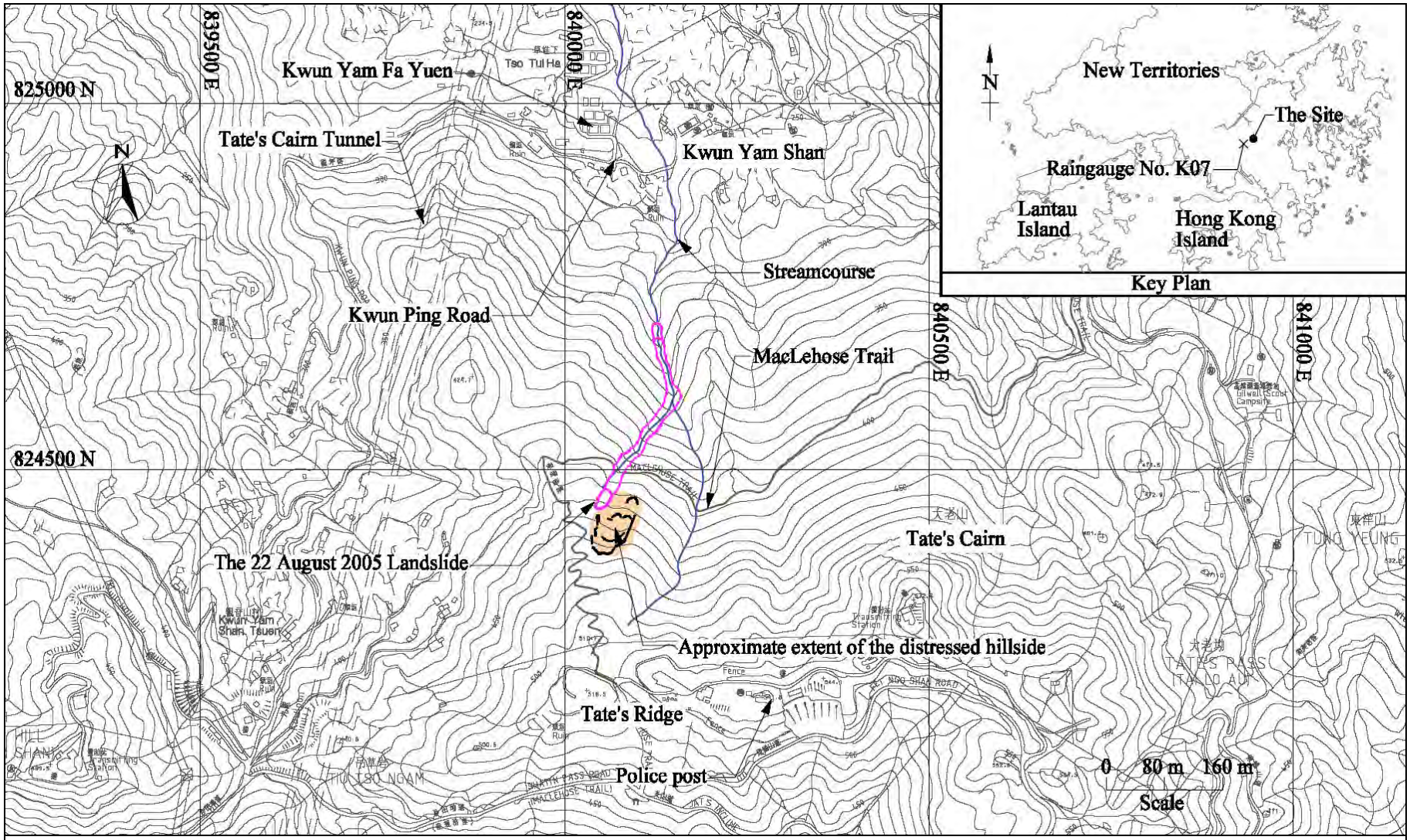

Note: Base plan is extracted from 1:5000 survey sheet No. 7SE-C dated March 2004.

Figure 1 - Location Plan

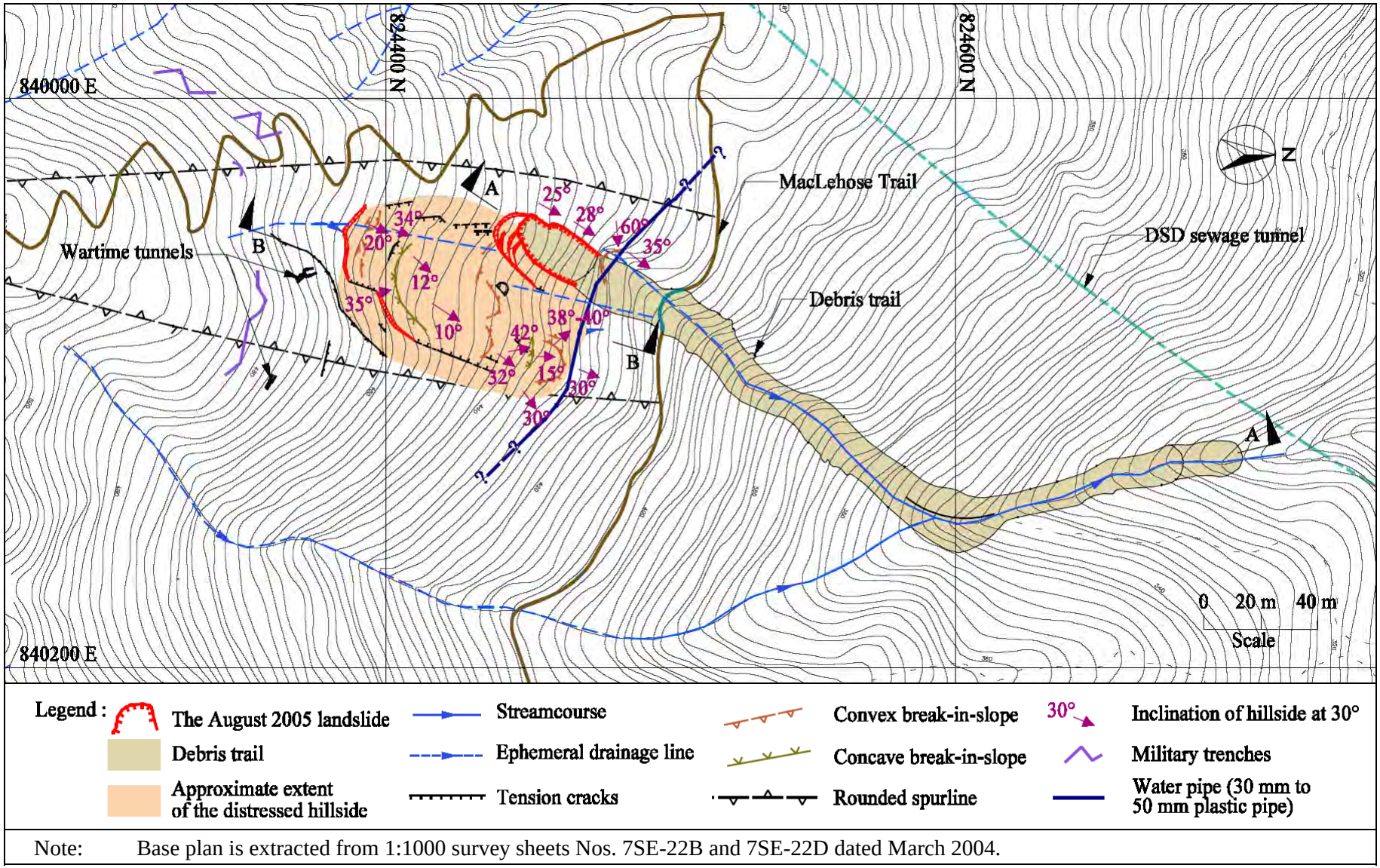

Note: Base plan is extracted from 1:1000 survey sheets Nos. 7SE-22B and 7SE-22D dated March 2004.

Figure 2 - Site Layout Plan

Table of Contents
Table of Contents
Table of Contents
Table of Contents

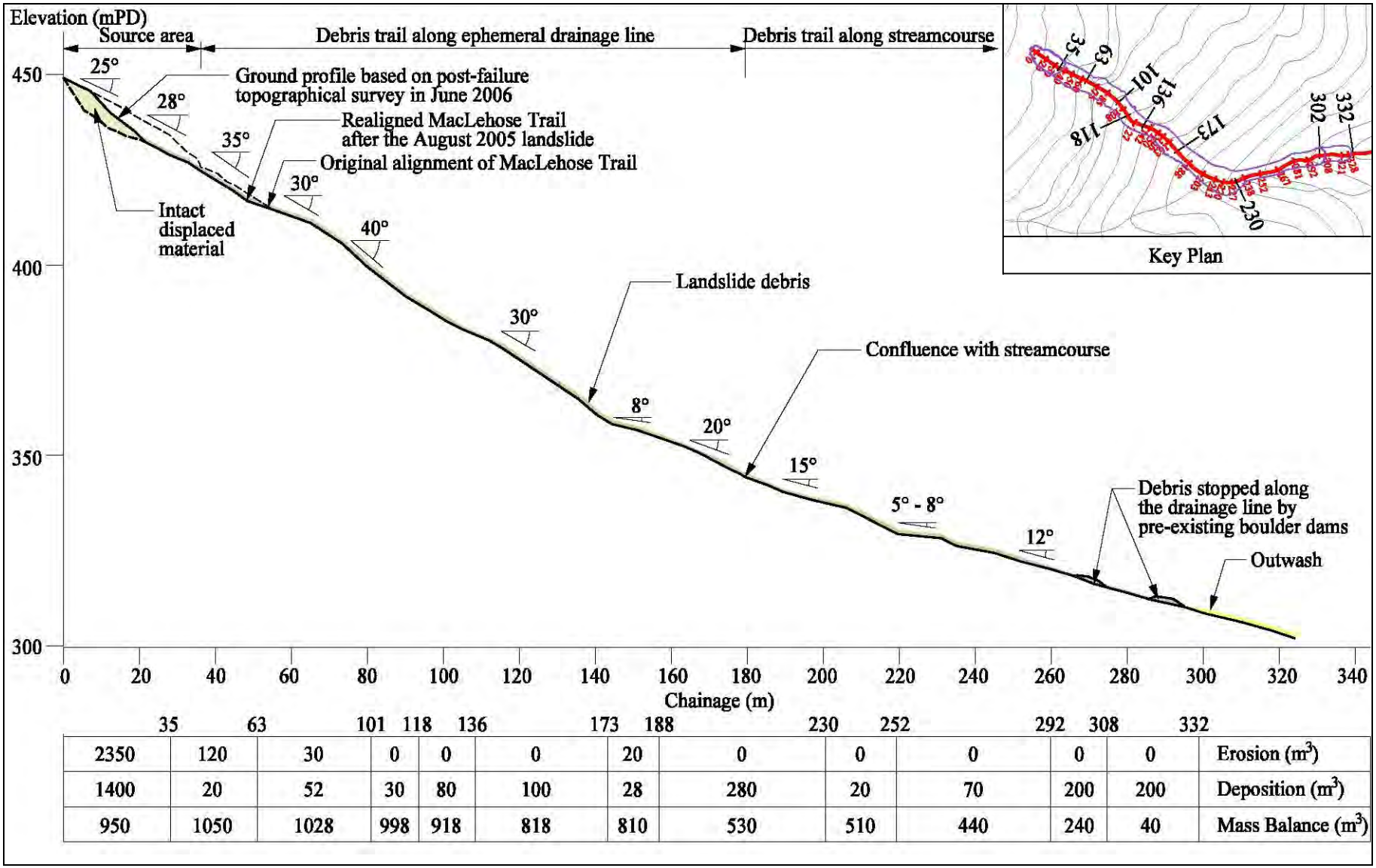

35	63	101	118	136	173	188	230	252	292	308	332	
2350	120	30	0	0	0	20	0	0	0	0	0	Erosion (m^3)
1400	20	52	30	80	100	28	280	20	70	200	200	Deposition (m^3)
950	1050	1028	998	918	818	810	530	510	440	240	40	Mass Balance (m^3)

Figure 3 - Section A-A through the August 2005 Landslide

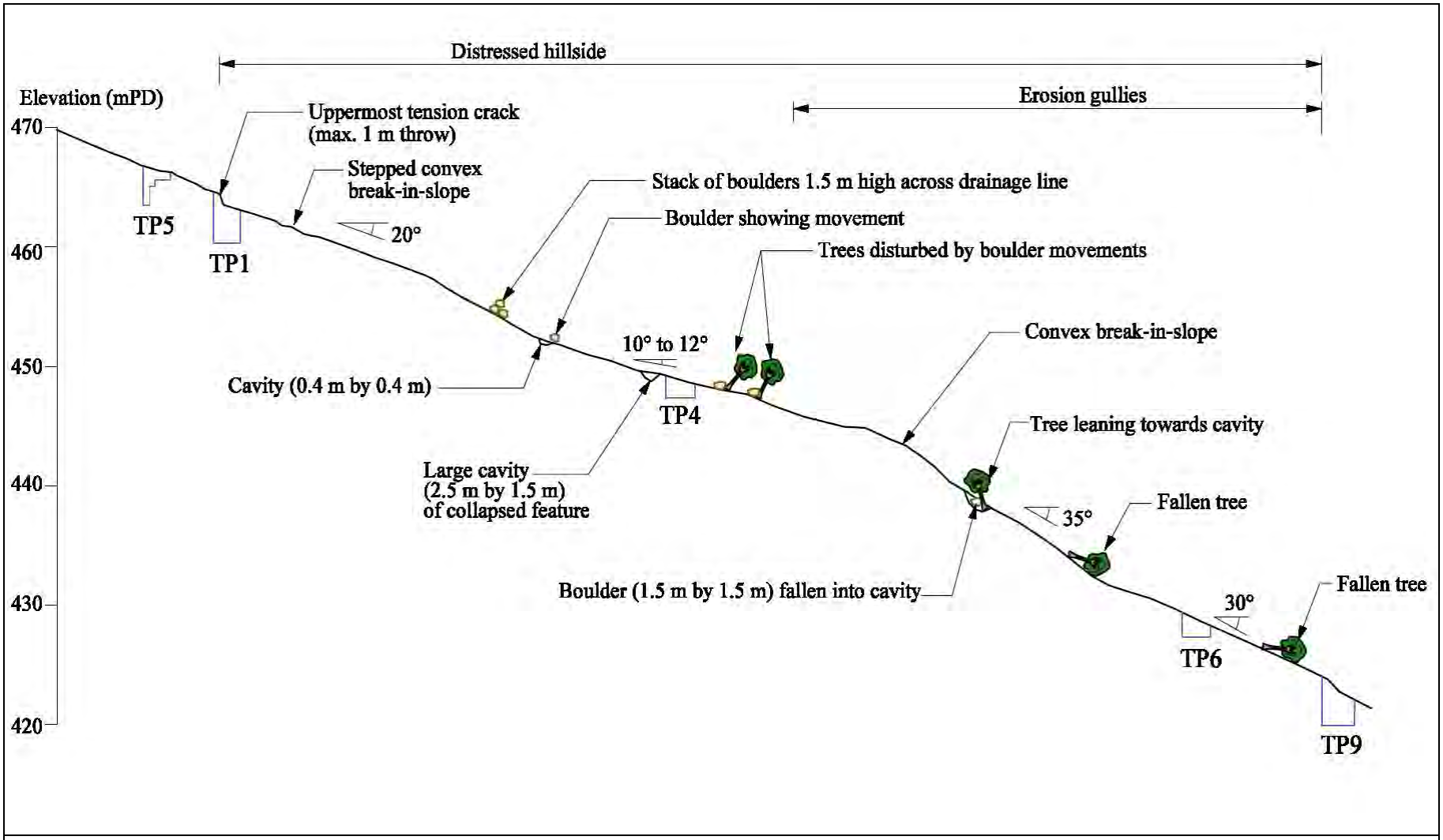

Note: See Figure 2 for location of section, Figure 12 for geological Section B-B of the distressed hillside and Drawing No. 2 for detailed field mapping.

Figure 4 - Section B-B through the Distressed Hillslide

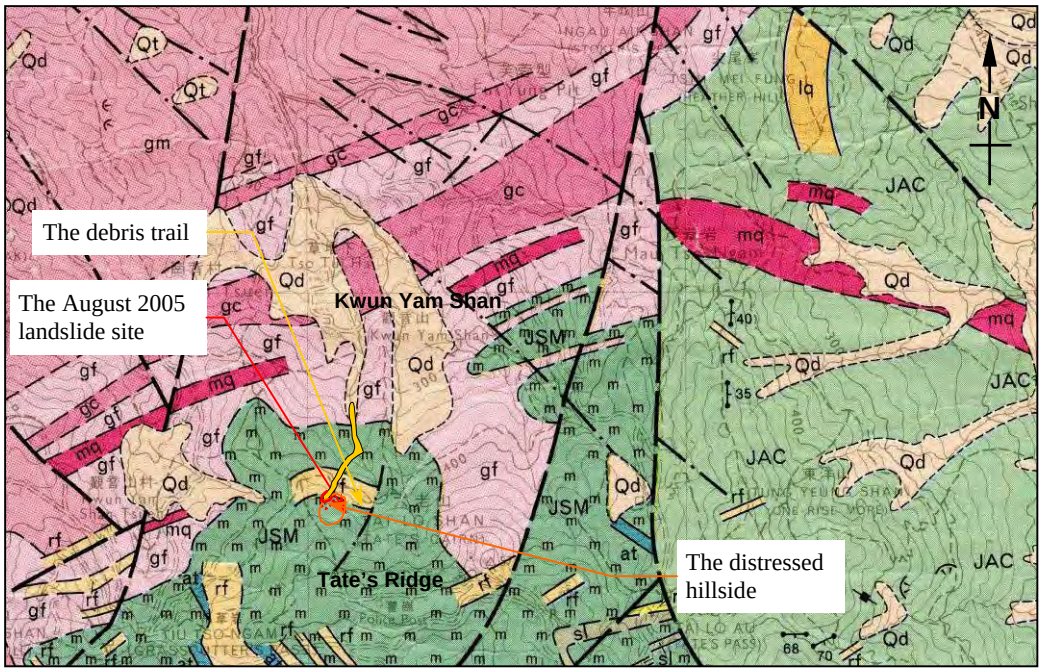

LEGEND:

SUPERFICAL DEPOSITS

Qd	Sand, gravel, cobbles and boulders in clay/silt matrix (Debris flow deposits)	Qdl	Material of the regolith and bedrodk (Slide deposits)

SOLID GEOLOGY

JAC	Vitric tuff, with biotite	JSM	Crystal and lithic tuff, tuff-breccia and tuffite
gc	Coarse-grained granite	sl	Silstone nad mudstone
gm	Medium-grained granite	lq	Quartz latite
gf	Fine-grained granite	mq	Quarrtz monzonite
rf	Feldsparphyric rhytolite	m m m	Hornfels

GEOLOGICAL LINES

- Geological boundary, superficial deposits
- Geological boundary, solid rock
- Fault (crossmark indicated downthrow side)
- Mineral vein
- Photogeological lineament

STRUCTURAL SYMBOLS

- Intrusive contact
- Jointing for vertical

Note: Extracted from Hong Kong Geological Survey, Map Series HGM20, Sheet No. 7, 1:20 000 scale (GCO, 1986)

Figure 5 - Regional Geology

Table of Contents
Table of Contents
Table of Contents
Table of Contents

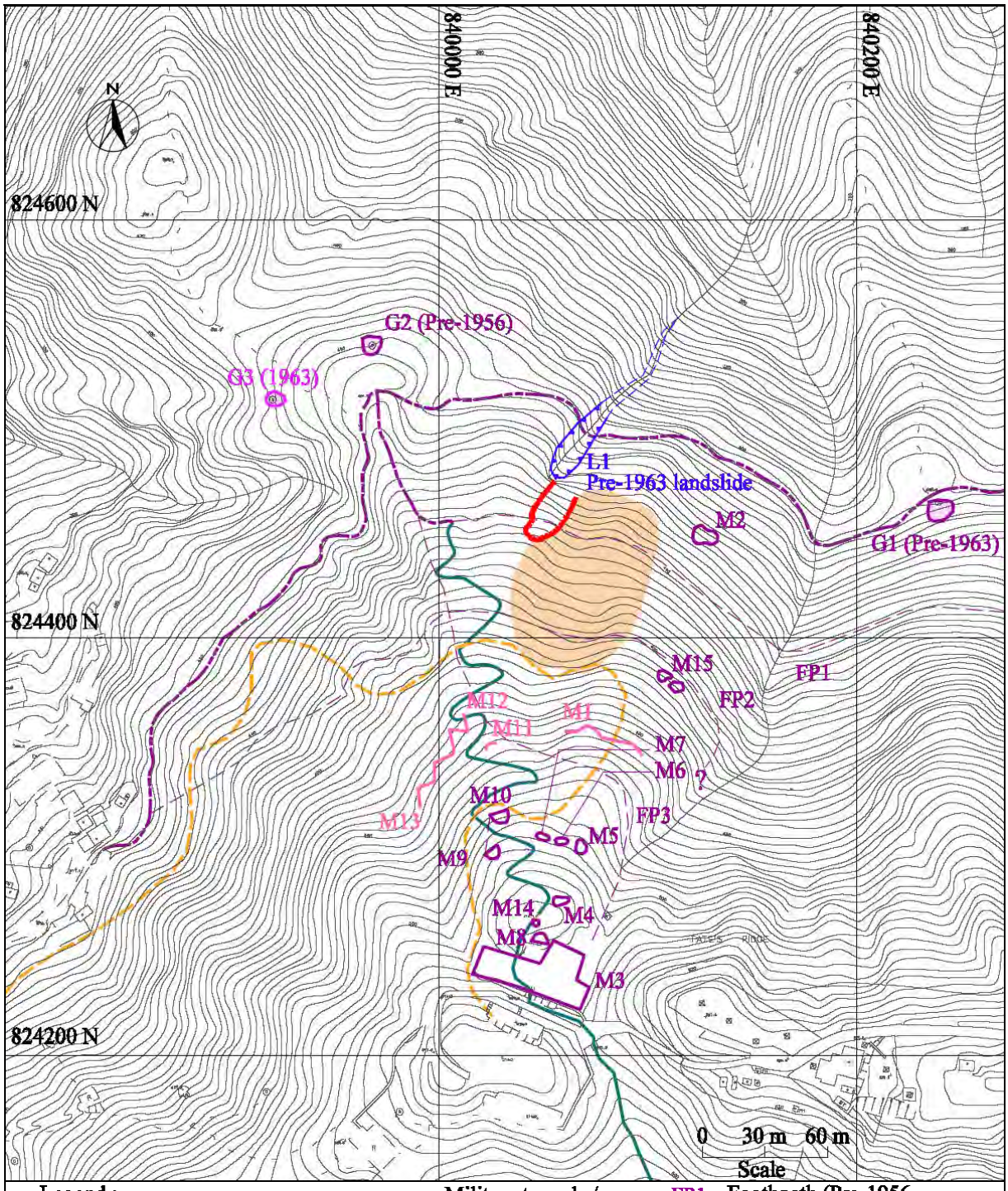

Notes: (1) Base plan is extracted from 1:1000 survey sheets Nos. 7SE-22B and 7SE-22D dated March 2004.
(2) The aligment of militrary trenches M1 was mapped on site.

Figure 6 - Site History

Table of Contents
Table of Contents
Table of Contents
Table of Contents

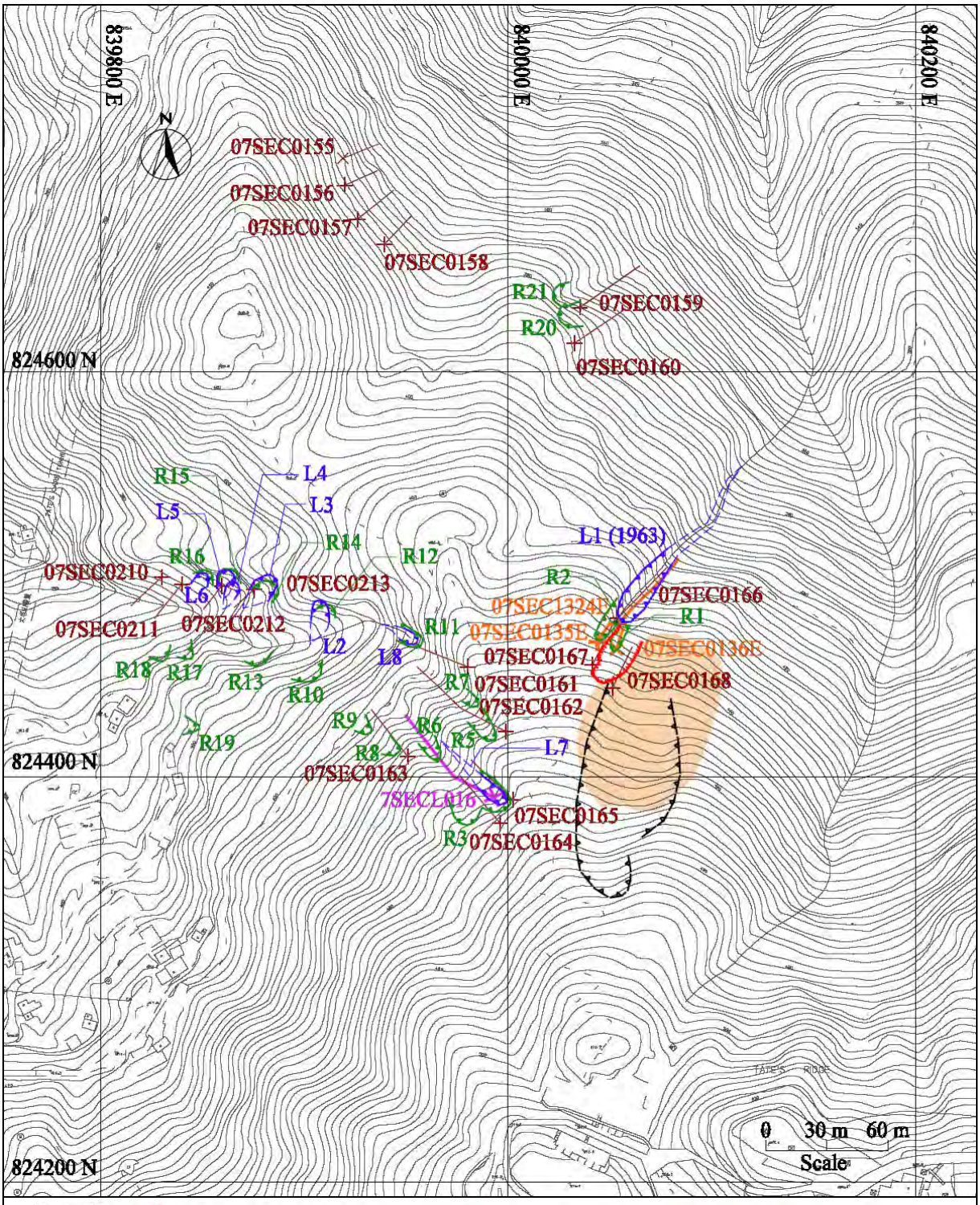

Note: Base plan is extracted from 1:1000 survey sheets Nos. 7SE-22B and 7SE-22D dated March 2004.

Figure 7 - Past Instabilities

Table of Contents
Table of Contents
Table of Contents
Table of Contents

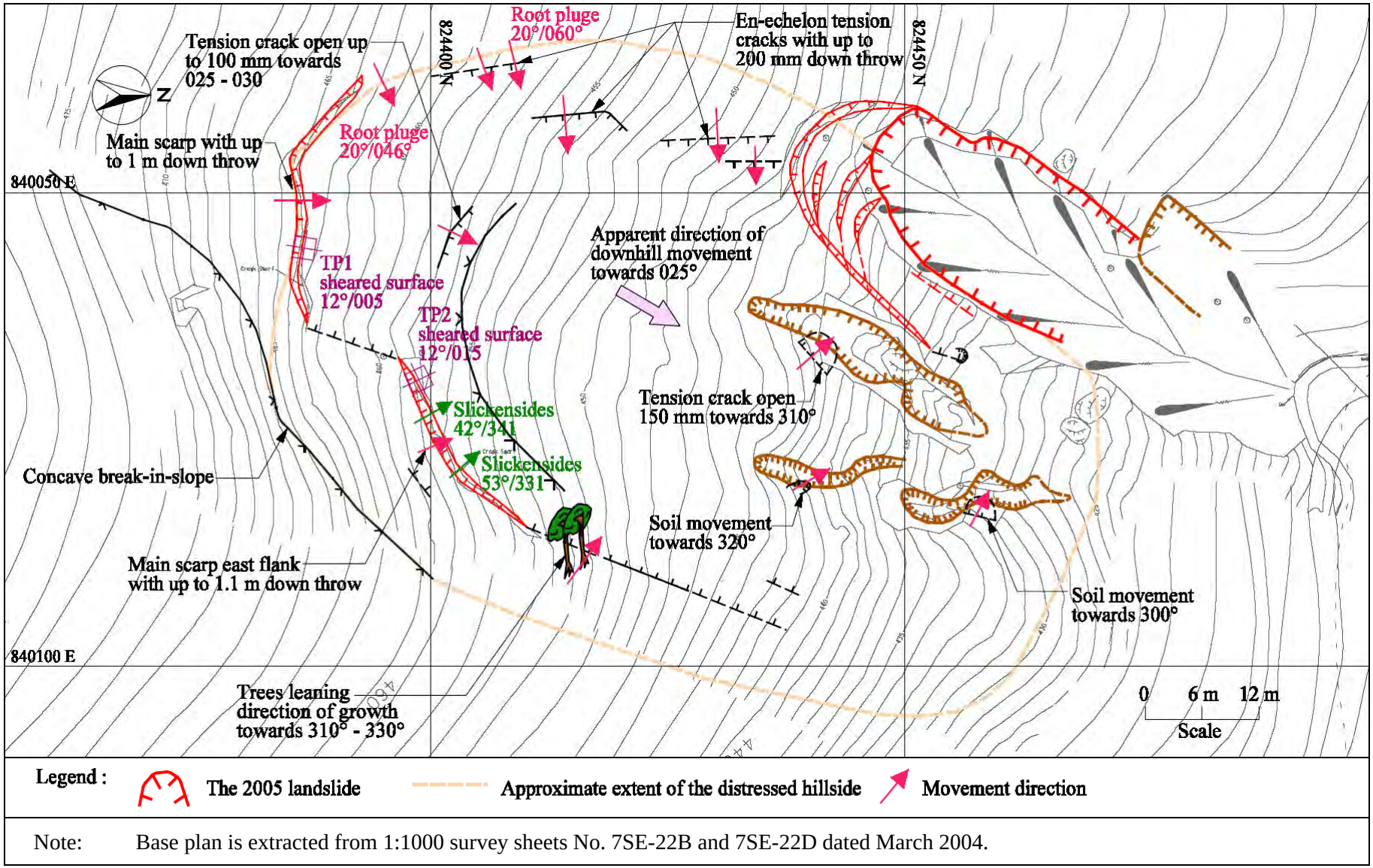

Note: Base plan is extracted from 1:1000 survey sheets No. 7SE-22B and 7SE-22D dated March 2004.

Figure 8 - Movement Observated within the Distressed Hillside

Table of Contents
Table of Contents
Table of Contents
Table of Contents

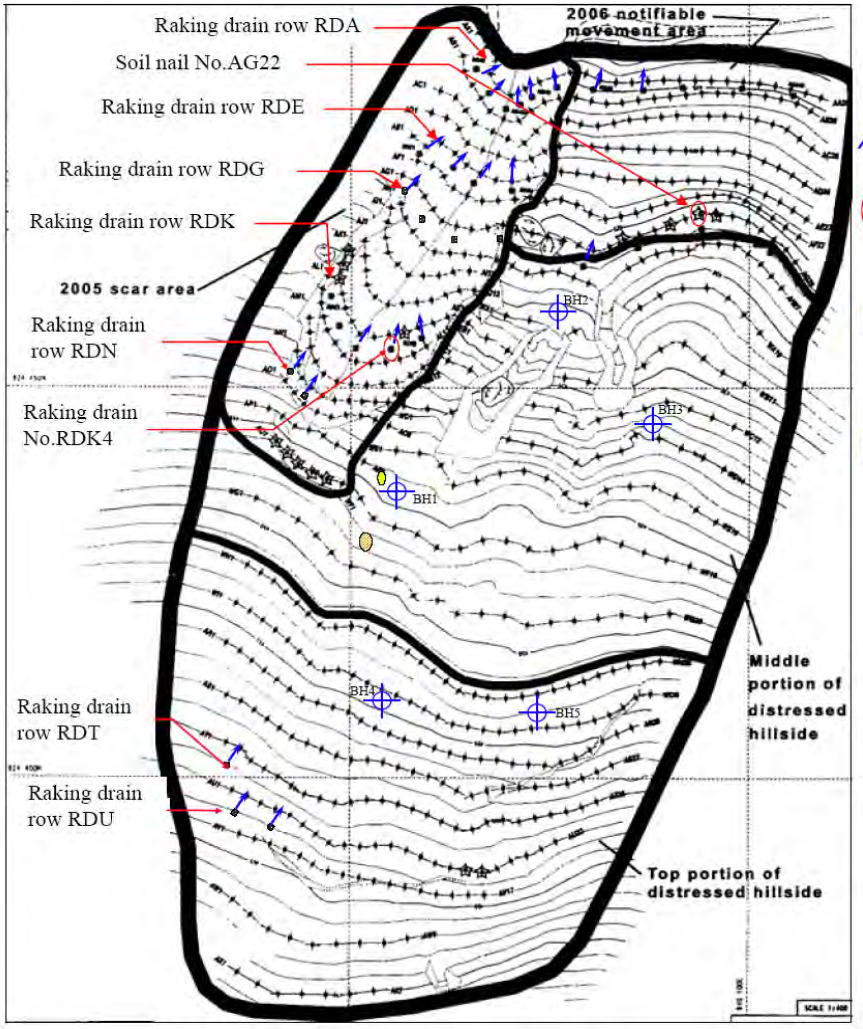

Observation of watrerflow from raking drains

	Raking Drain No.	Length of Raking Drain (m)	September 2006																													October 2006													
			1	2	3	4	5	6	7	8	9	10	11	12	13	14	15	16	17	18	19	20	21	22	23	24	25	26	27	28	29	30	1	2	3	4	5	6	7	8	9	10	11	12	13	14
Weather		(a.m.)	F	F	F	F	F	F	R	F	R	F	F	R	R	R	F	F	F	F	F	F	F	F	F	F	F	F	F	F	F	F	F	F	F	F	F	F	F	F	F	F	F	F	F	F
		(p.m.)	F	F	F	F	F	F	R	F	R	F	F	R	R	R	F	F	F	F	F	F	F	F	F	F	F	F	F	F	F	F	F	F	F	F	F	F	F	F	F	F	F	F	F	F
August 2005 landslide scar	RDN1	20.0	N	N		N	N	N	D	D	D		N	N		S	S	S		N	N	N	N	N	N		N	N	N	N	N	N			N	N	N			N	N	N	N	N	N
	RDN2	18.0	S	S		S	S	S	S	S	S		D	S		S	S	S		D	D	D	D	D	D		D	D	D	D	D	D			D	D	D			D	D	D	D	D	D
	RDK1	16.0	N	N		N	N	N	N	N	N		N	N		N	N	N		N	N	N	N	N	N		N	N	N	N	N	N			N	N	N			N	D	D	D	D	D
	RDK2	16.0	N	N		N	N	N	N	N	N		N	N		N	N	N		N	N	N	N	N	N		N	N	N	N	N	N			N	N	N			N	N	N	N	N	N
	RDK3	16.0	D	D		D	D	D	S	S	S		D	D		S	S	S		S	S	S	S	S	S		S	D	D	D	D	D			D	D	D			D	D	D	D	D	D
	RDK4	16.0	N	N		N	N	N	D	D	D		N	N		S	S	S		D	D	D	D	D	D		D	D	D	D	D	D			D	D	D			D	D	D	D	D	D
	RDK5	12.0	N	N		N	N	N	N	N	N		N	N		S	S	S		S	D	D	D	D	D		D	N	N	N	N	N			N	N	N			N	D	D	D	D	D
	RDE1	20.0	D	D		D	D	D	D	D	D		N	N		D	D	D		S	S	S	S	S	S		S	D	D	D	D	D			D	D	D			D	N	N	N	N	N
	RDE2	20.0	D	D		D	D	D	S	S	S		D	D		D	D	D		D	D	D	D	D	D		D	D	D	D	D	D			D	D	D			D	N	N	N	N	N
	RDE3	20.0	N	N		N	N	N	D	D	D		N	N		S	S	S		D	D	D	D	D	D		D	D	D	D	D	D			D	D	D			D	N	N	N	N	N
	RDE4	20.0	N	N		N	N	N	D	D	D		N	N		S	S	S		N	N	N	N	N	N		N	N	N	N	N	N			N	N	N			N	D	D	D	D	D
	RDA1	18.0	D	D		D	D	D	D	D	D		N	N		D	D	D		D	D	D	D	D	D		D	N	N	N	N	N			N	N	N			N	S	S	S	S	S
	RDA2	16.0	D	D		D	D	D	S	S	S		D	D		D	D	D		D	D	D	D	D	D		D	N	N	N	N	N			N	N	N			N	S	S	S	S	S
	RDA2a	20.0	S	S		S	S	S	S	S	S		S	S		S	S	S		S	S	S	S	S	S		S	D	D	D	D	D			D	D	D			D	S	S	S	S	S
	RDA3	16.0	S	S		S	S	S	S	S	S		S	S		S	S	S		S	S	S	S	S	S		S	S	S	S	S	S			S	S	S			S	S	D	D	D	D
	RDA3a	22.0	S	S		S	S	S	S	S	S		D	D		S	S	S		S	S	S	S	S	S		S	S	S	S	S	S			S	S	S			S	S	S	S	S	S
	RDA4	20.0	D	D		D	D	D	D	D	D		D	D		S	S	S		S	S	S	S	S	S		S	S	S	S	S	S			S	S	S			S	S	N	N	N	N
	RDA5	20.0	N	N		N	N	N	N	N	N		N	N		D	D	D		D	D	D	D	D	D		D	D	D	D	D	D			D	D	D			D	D	N	N	N	N
Toe portion of distressed hillside	RDG1	20.0	S	S		S	S	S	S	S	S		S	S		S	S	S		S	S	S	S	S	S		S	S	S	S	S	S			S	S	S			S	S	N	N	N	N
	RDG5	10.0	N	N		N	N	N	S	S	S		N	N		S	S	S		S	N	N	N	N	N		N	N	N	N	N	N			N	N	N			N	N	N	N	N	N
	RDG2	20.0	N	N		N	N	N	N	N	N		N	N		N	N	N		N	N	N	N	N	N		N	N	N	N	N	N			N	N	N			N	N	N	N	N	N
	RDG3	20.0	N	N		N	N	N	N	N	N		N	N		N	N	N		N	N	N	N	N	N		N	N	N	N	N	N			N	N	N			N	D	D	D	D	D
	RDG4	20.0	N	N		N	N	N	N	N	N		N	N		N	N	N		N	N	N	N	N	N		N	N	N	N	N	N			N	N	N			N	N	N	N	N	N
	RDA6	20.0	D	D		D	D	D	S	S	S		D	D		D	D	D		D	D	D	D	D	D		D	N	N	N	N	N			N	N	N			N	N	N	N	N	N
	RDA7	20.0	S	S		S	S	S	S	S	S		S	S		S	S	S		S	S	S	S	S	S		S	D	D	D	D	D			D	D	D			D	N	N	N	N	N
	RDA8	20.0	N	N		N	N	N	D	D	D		N	N		N	N	N		N	N	N	N	N	N		N	N	N	N	N	N			N	N	N			N	N	N	N	N	N
	RDA9	20.0	N	N		N	N	N	N	N	N		N	N		N	N	N		N	N	N	N	N	N		N	N	N	N	N	N			N	N	N			N	N	N	N	N	N
	RDA10	20.0	N	N		N	N	N	N	N	N		N	N		N	N	N		N	N	N	N	N	N		N	N	N	N	N	N			N	N	N			N	N	N	N	N	N
Top portion of distressed hillside	RDU1	20.0	N	N		N	N	N	N	N	N		N	N		D	D	D		N	N	N	N	N	N		N	N	N	N	N	N			N	N	N			N	N	N	N	N	N
	RDT1	20.0	N	N		N	N	N	N	N	N		N	N		S	S	S		N	N	N	N	N	N		N	N	N	N	N	N			N	N	N			N	N	N	N	N	N
	RDT2	20.0	N	N		N	N	N	N	N	N		N	N		S	S	S		N	N	N	N	N	N		N	N	N	N	N	N			N	N	N			N	N	N	N	N	N

Legend : N - No water outflow or dripping D - With water dripping S - With water outflow Weather : F - Fine R - Raining

Note: Observations were made by LIC and LPM Division 3 of GEO as of 14 October 2006.

Figure 9 - Field Observations during the Remedial Works

Table of Contents
Table of Contents
Table of Contents
Table of Contents

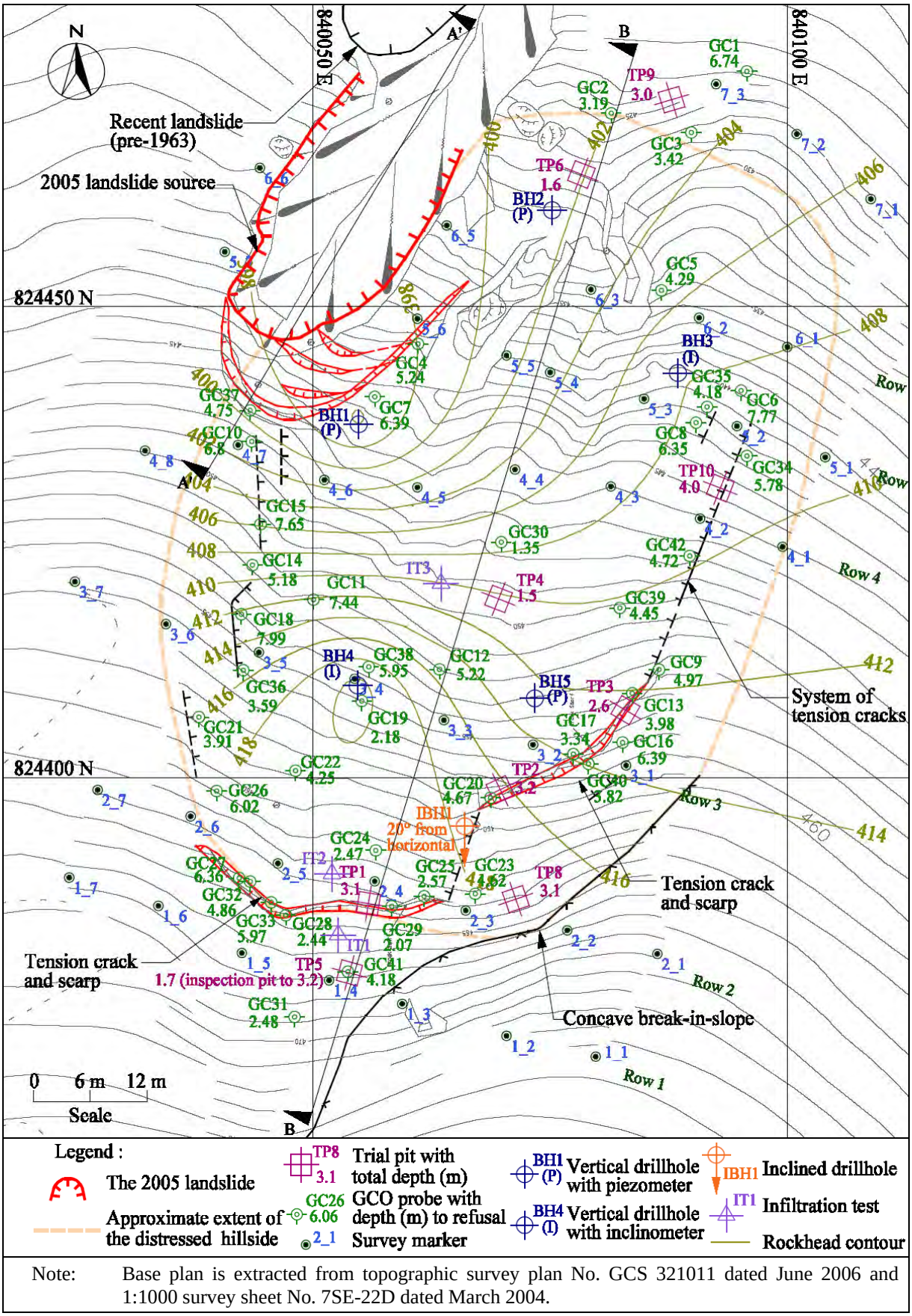

Note: Base plan is extracted from topographic survey plan No. GCS 321011 dated June 2006 and 1:1000 survey sheet No. 7SE-22D dated March 2004.

Figure 10 - Ground Investigation Layout and Rockhead Contour

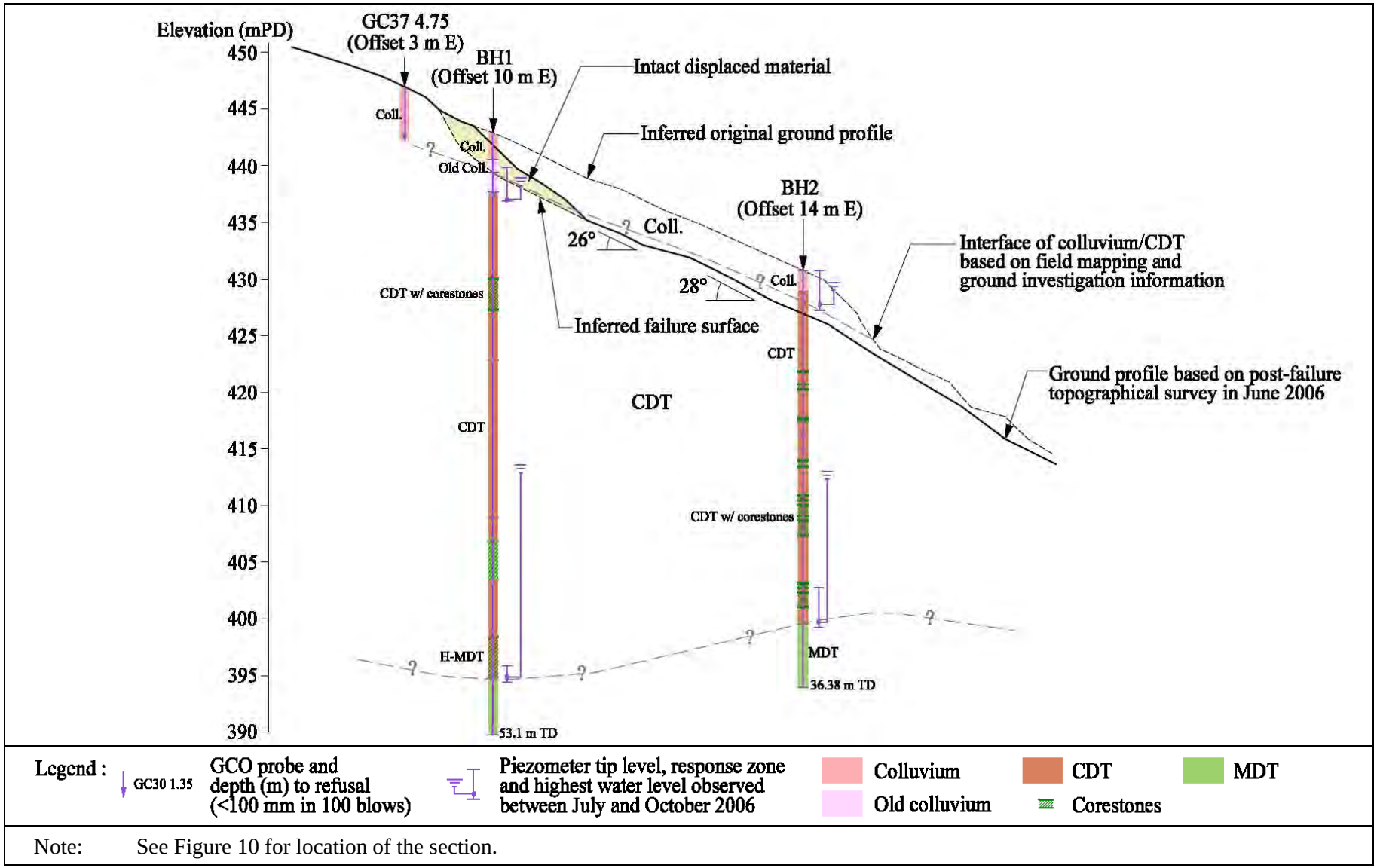

Note: See Figure 10 for location of the section.

Figure 11 - Geological Section A'-A' through the 2005 Landslide Source Area

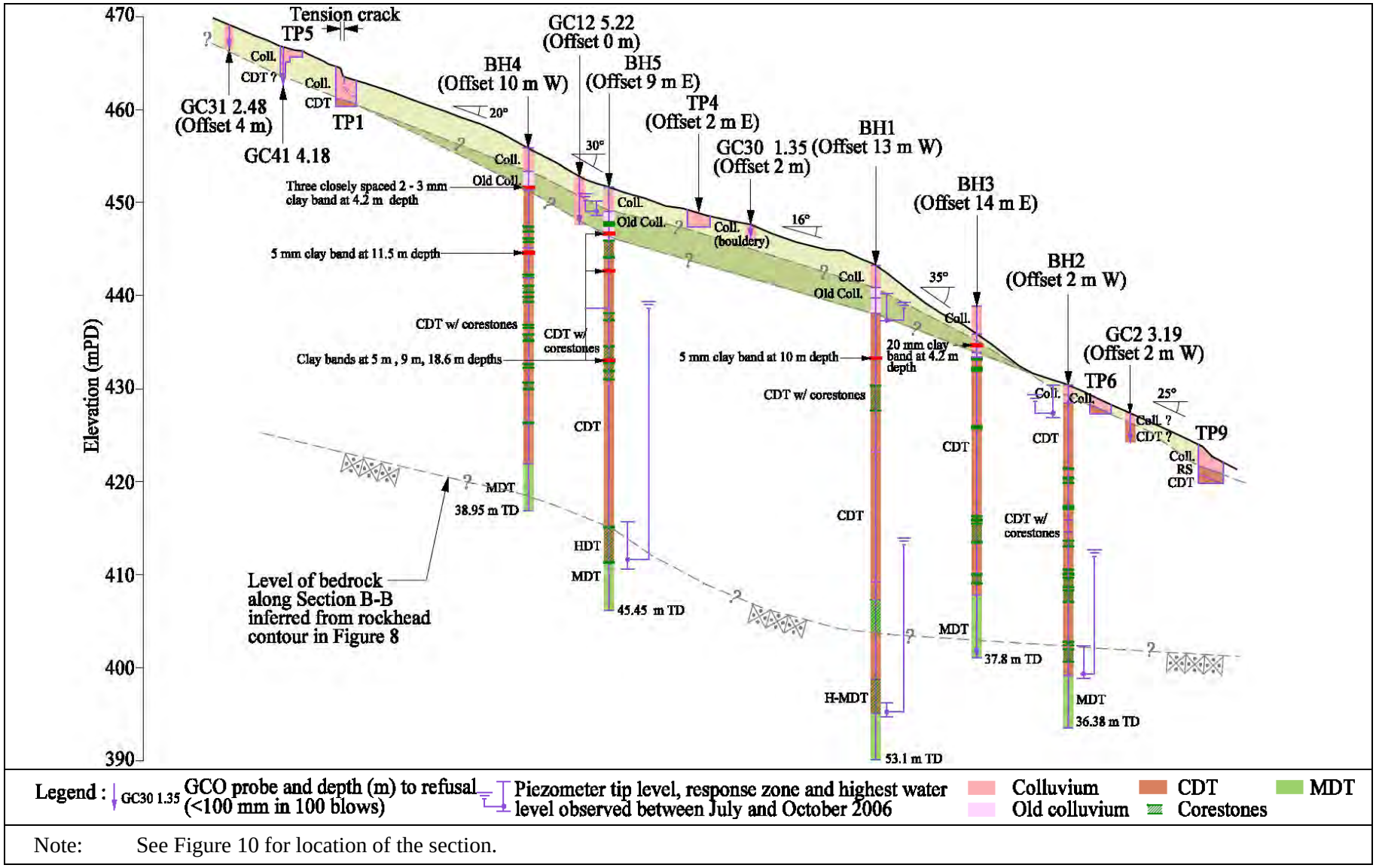

Note: See Figure 10 for location of the section.

Figure 12 - Geological Section B-B through the Distressed Landslide

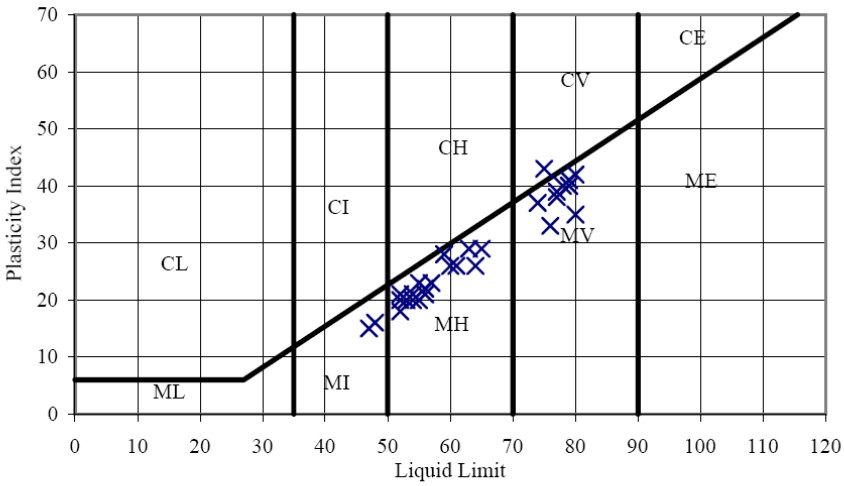

(a) Young colluvium

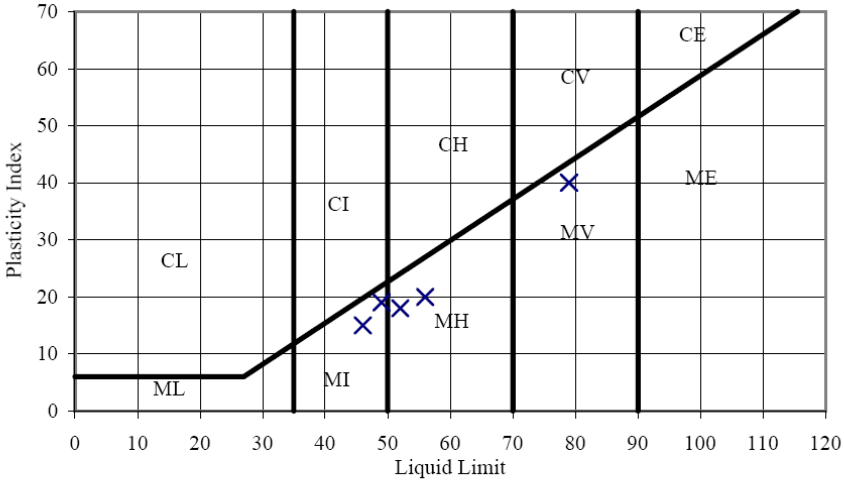

(b) Old colluvium

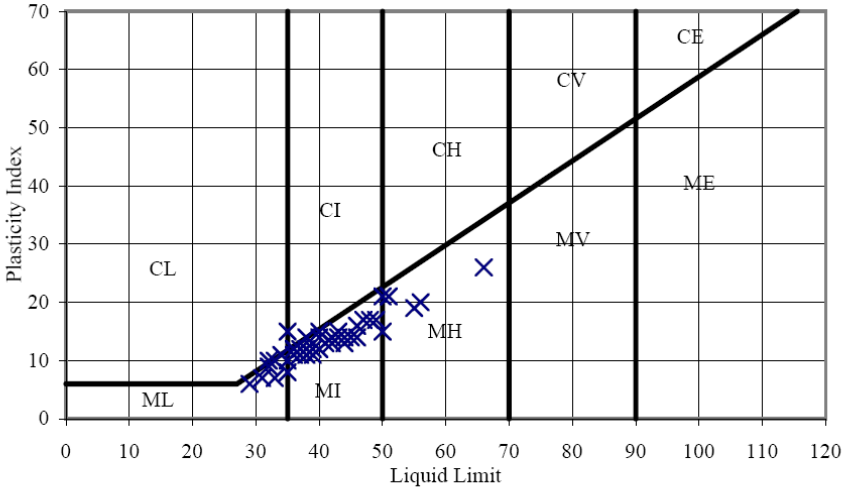

(c) Completely decomposed tuff

Figure 13 - Plasticity Charts

Table of Contents
Table of Contents
Table of Contents
Table of Contents

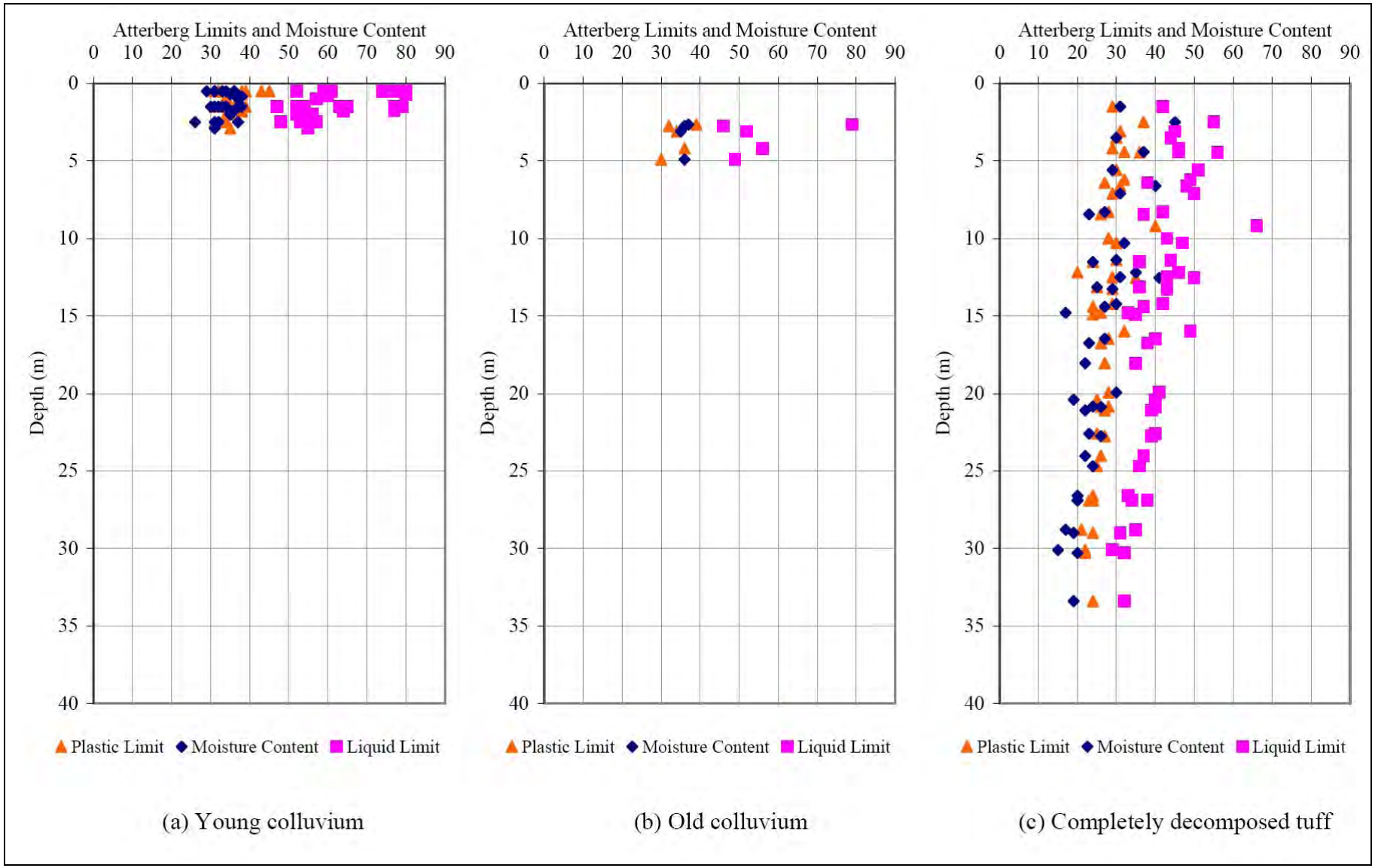

Figure 14 - Atterberg Limits and Moisture Content

Table of Contents
Table of Contents
Table of Contents
Table of Contents

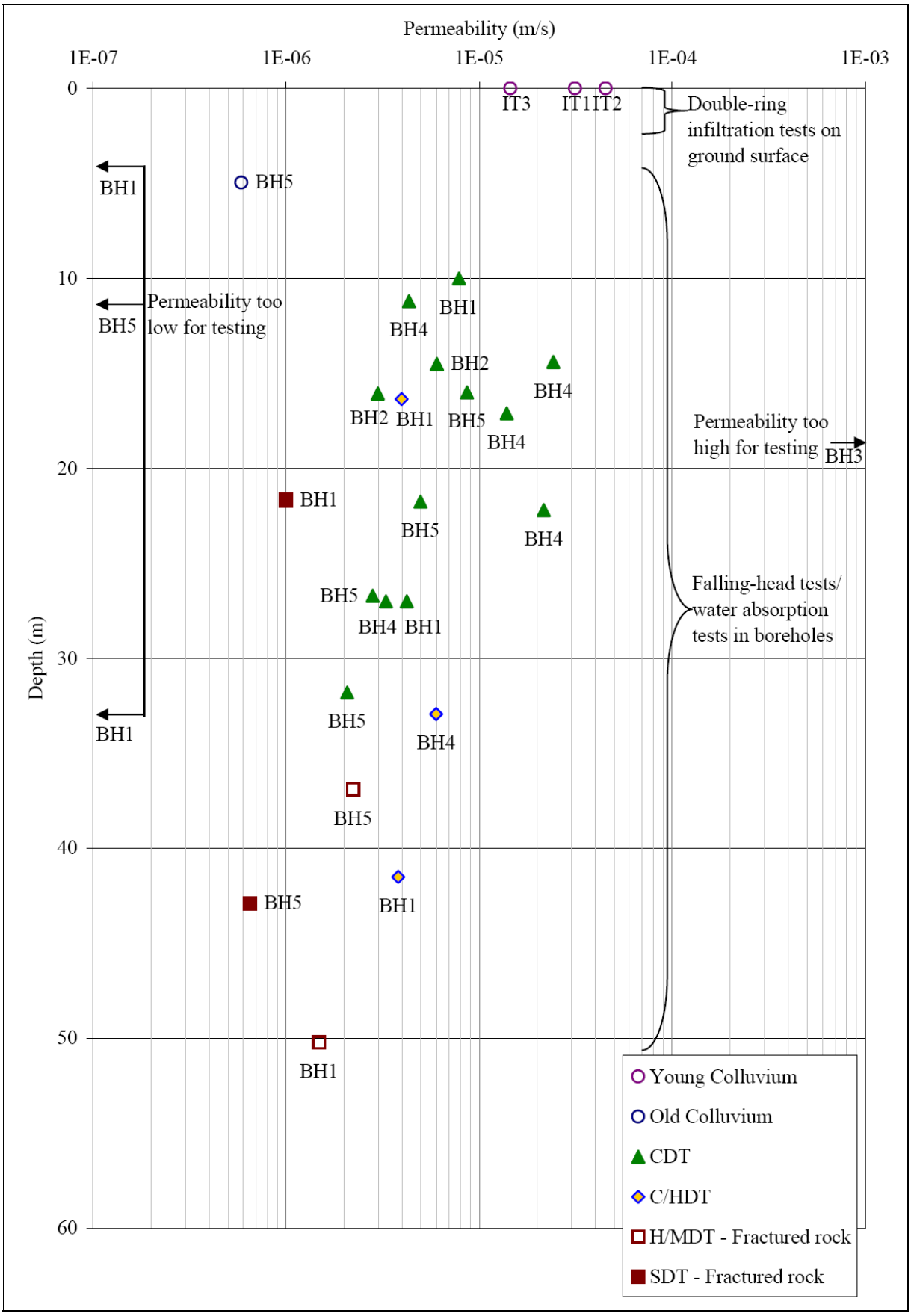

Figure 15 - Summary of Feild Permeability Tests

Table of Contents
Table of Contents
Table of Contents
Table of Contents

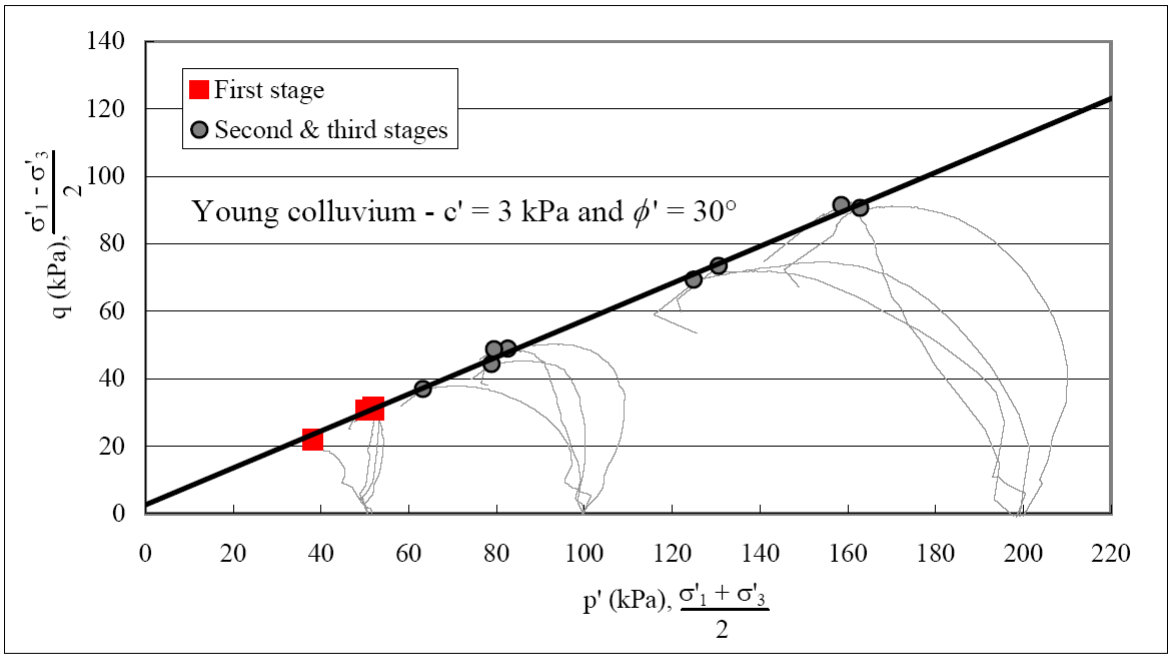

(a) Colluvium

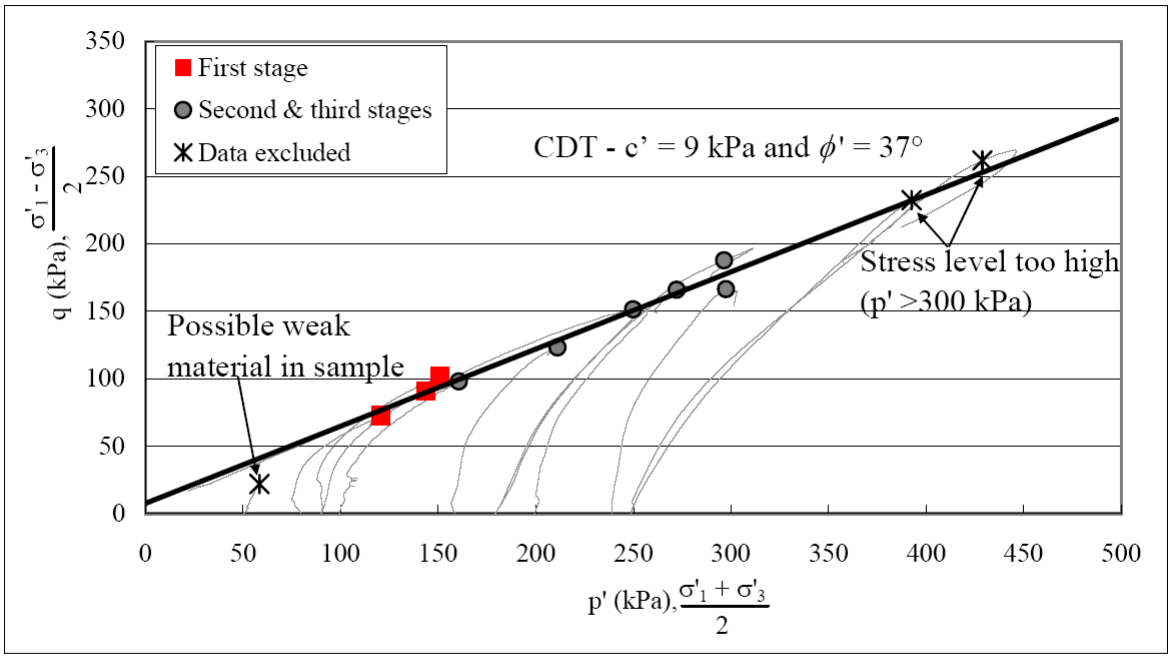

(b) Completely Decomposed Tuff

Legend:

c'	cohesion	ϕ'	angle of shearing resistance
σ_1'	major principal stress	σ_3'	minor principal stress

Figure 16 - p'-q Plots

Table of Contents
Table of Contents
Table of Contents
Table of Contents

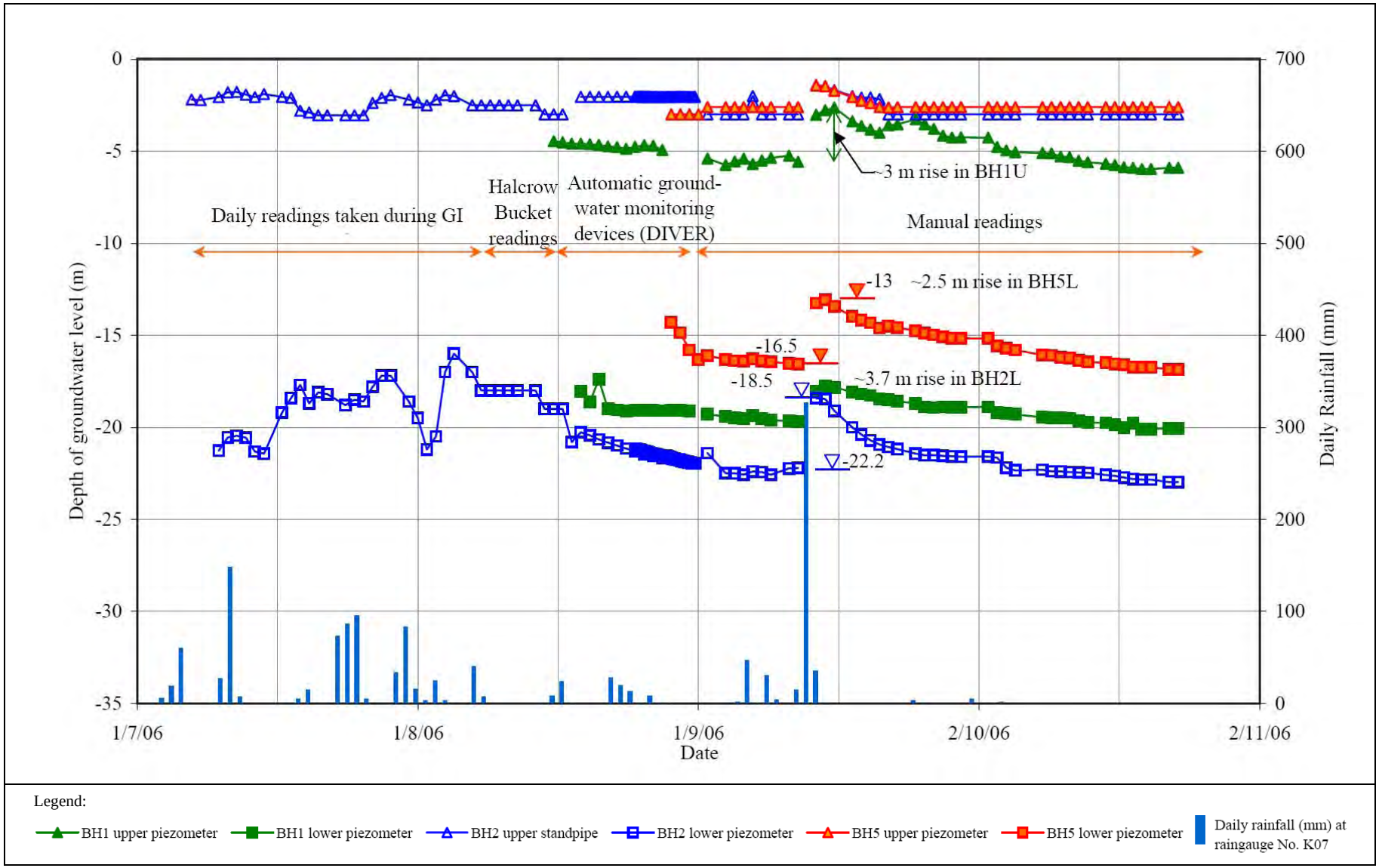

Figure 17 - Records of Groundwater Monitoring between July 2006 and October 2006

Table of Contents
Table of Contents
Table of Contents
Table of Contents

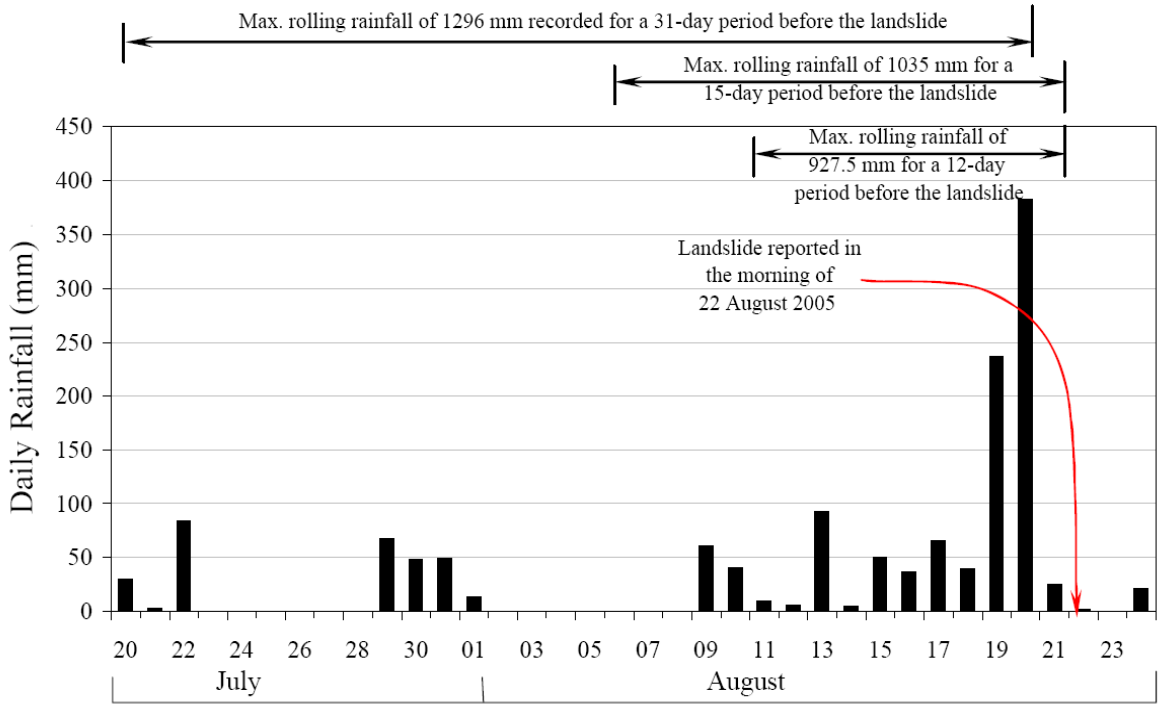

(a) Daily Rainfall Recorded at GEO Raingauge No. K07 between 20 July 2005 and 24 August 2005

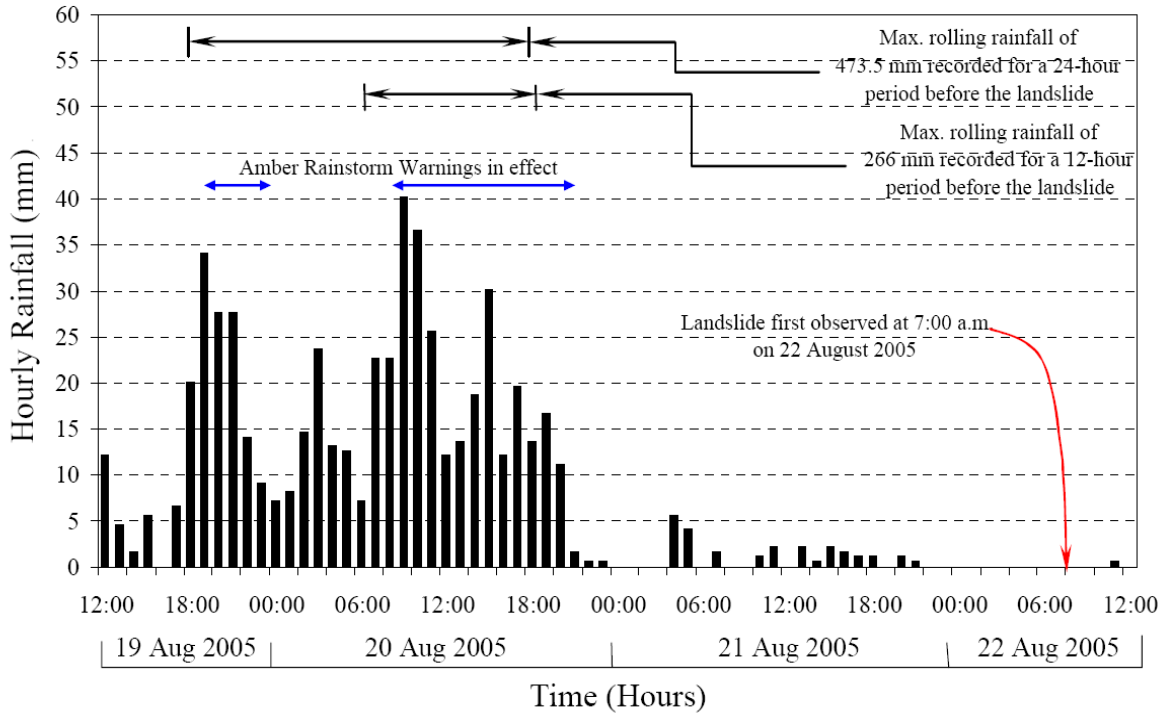

(b) Hourly Rainfall Recorded at GEO Raingauge No. K07 between 19 August 2005 and 22 August 2005

Figure 18 - Daily and Hourly Rainfall Recorded at GEO Raingauge No. K07

Table of Contents
Table of Contents
Table of Contents
Table of Contents

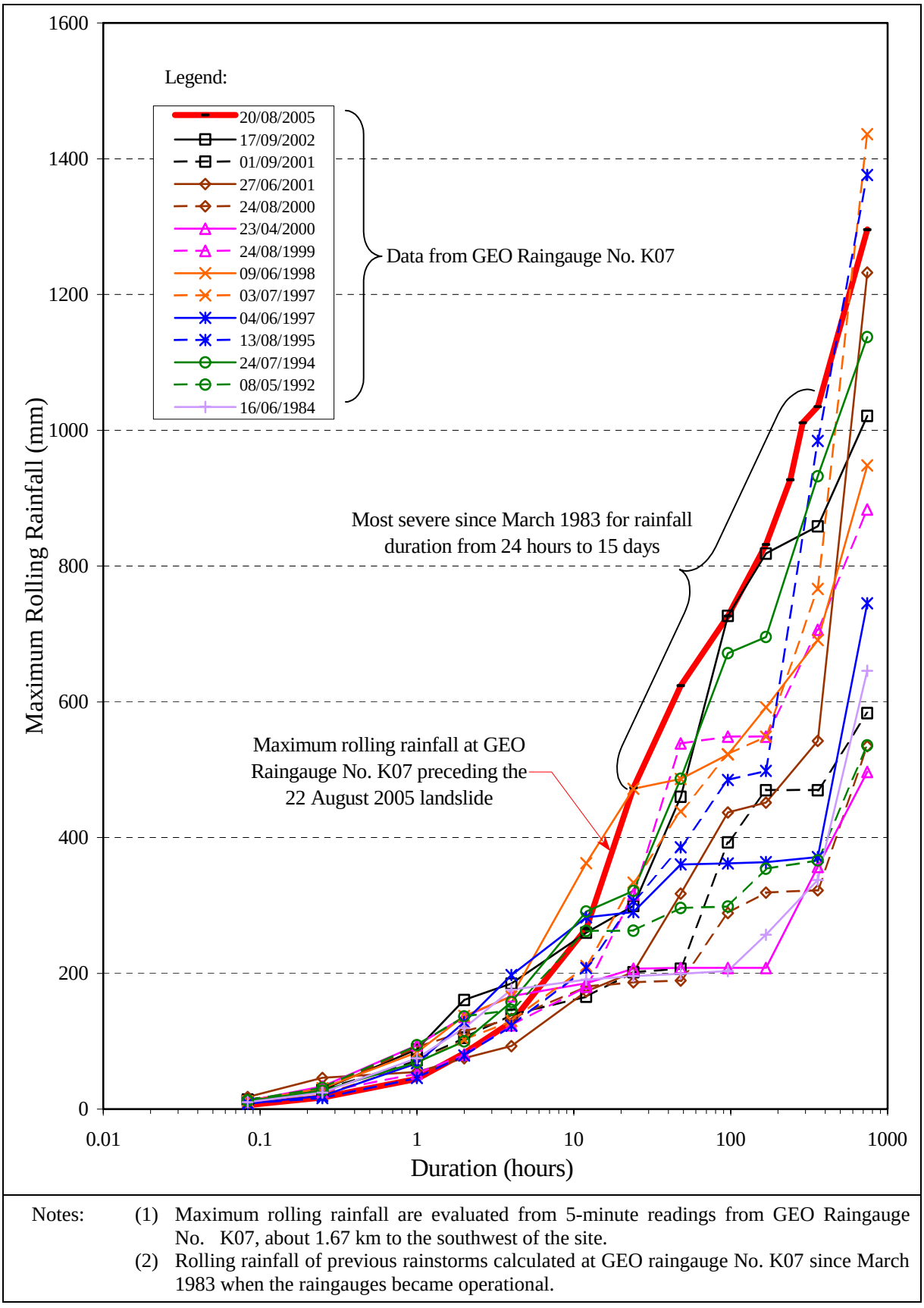

Notes:
(1) Maximum rolling rainfall are evaluated from 5-minute readings from GEO Raingauge No. K07, about 1.67 km to the southwest of the site.
(2) Rolling rainfall of previous rainstorms calculated at GEO raingauge No. K07 since March 1983 when the raingauges became operational.

Figure 19 - Maximum Rolling Rainfall for Previous Major Rainstorms at GEO Raingauge No. K07

Table of Contents
Table of Contents
Table of Contents
Table of Contents

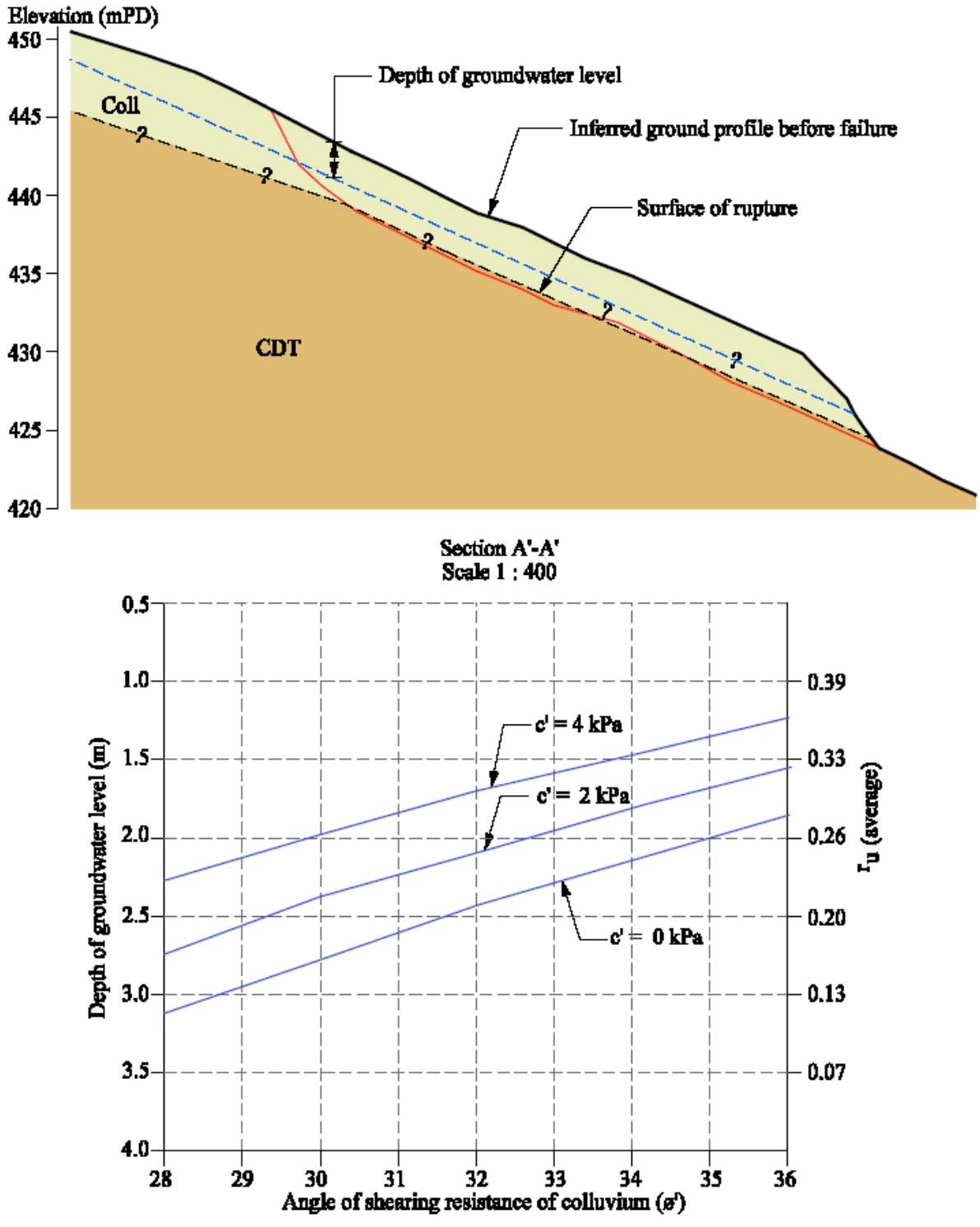

Legend:

——— Factor of safely equal to unity

Notes: (1) The pre-failure ground profile and the failure surface are based on topographical survey, photographic records, post-failure observations and field mapping.

(2) See Figure 10 for location of cross section.

Figure 20 - Summary of Theoretical Stability Analyses of the August 2005 Landslide

Table of Contents
Table of Contents
Table of Contents
Table of Contents

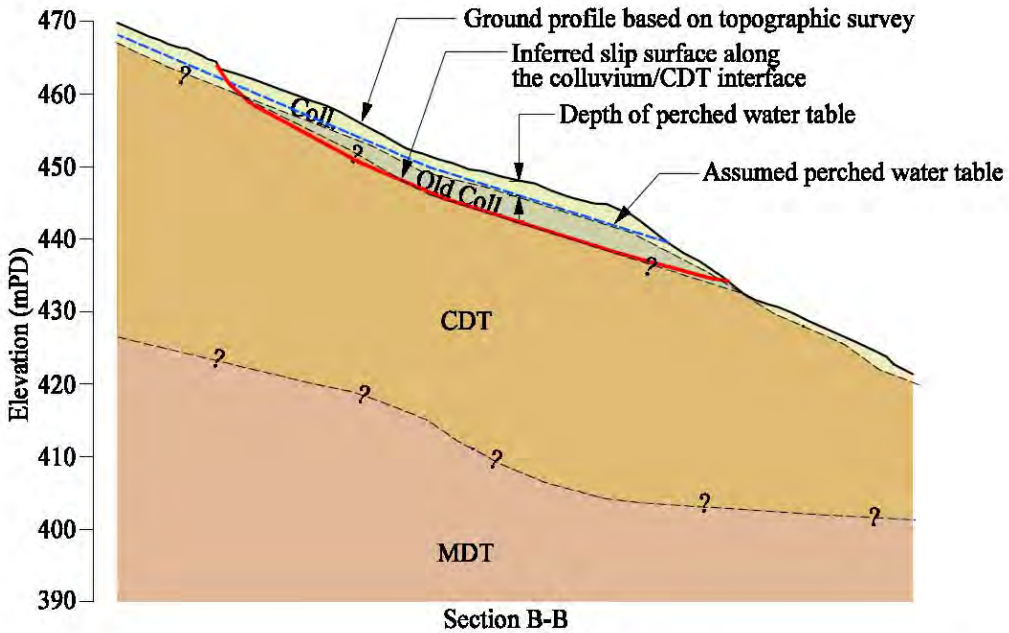

Section B-B
Scale 1 : 1000

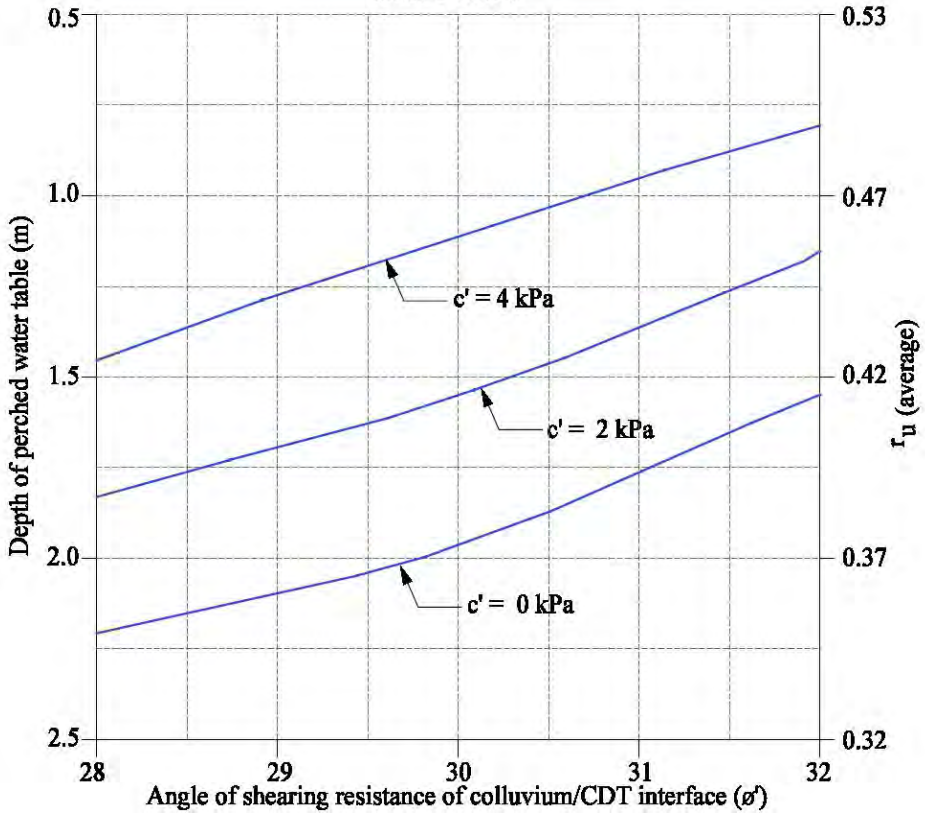

Legend:

——— Factor of safely equal to unity

Notes: (1) The ground profile and the inferred slip surface are based on topographical survey, ground investigation, post-failure observations and field mapping.

(2) See Figure 10 for location of cross section.

Figure 21 - Summary of Theoretical Stability Analyses of the Distressed Hillside (Shallow Failure)

Table of Contents
Table of Contents
Table of Contents
Table of Contents

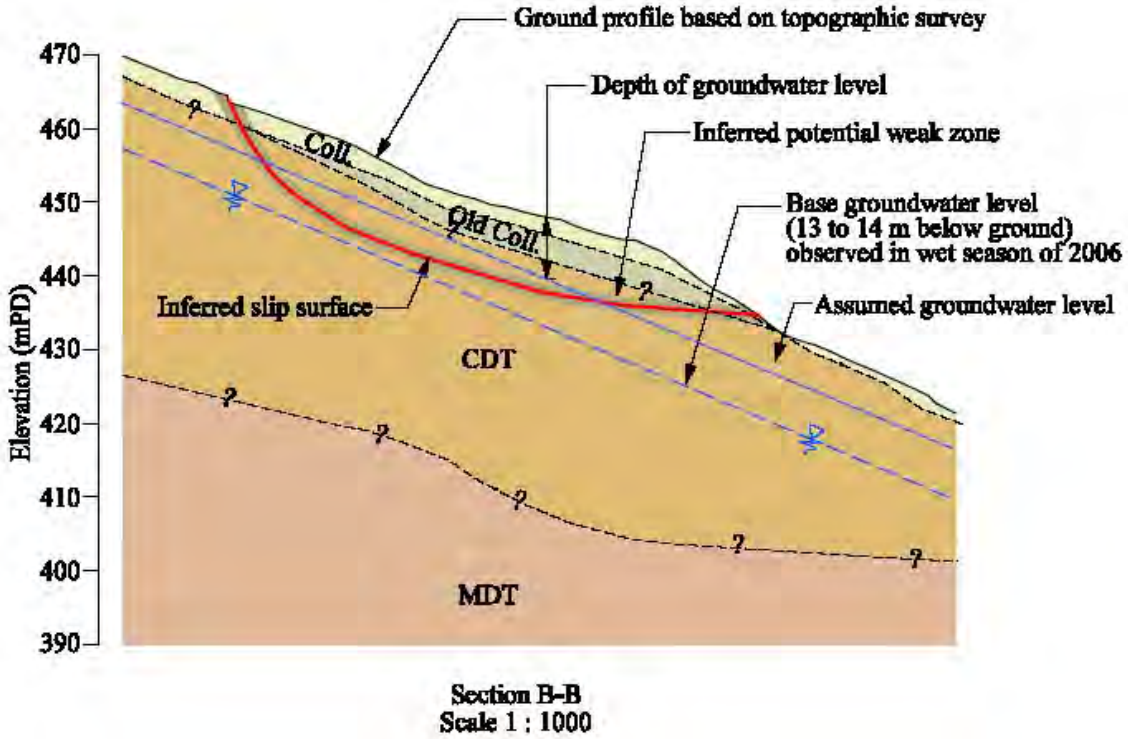

Section B-B
Scale 1 : 1000

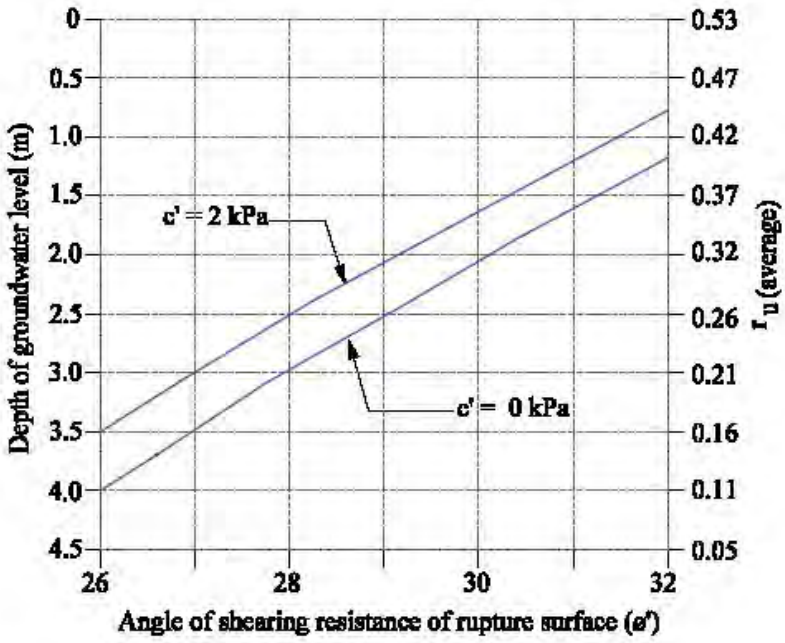

Legend:

——— Factor of safely equal to unity

Notes:
(1) The ground profile and the inferred slip surface are based on topographical survey, ground investigation, post-failure observations and field mapping.
(2) See Figure 10 for location of cross section.

Figure 22 - Summary of Theoretical Stability Analyses of the Distressed Hillside (Deep-seated Failure)

Table of Contents
Table of Contents
Table of Contents
Table of Contents

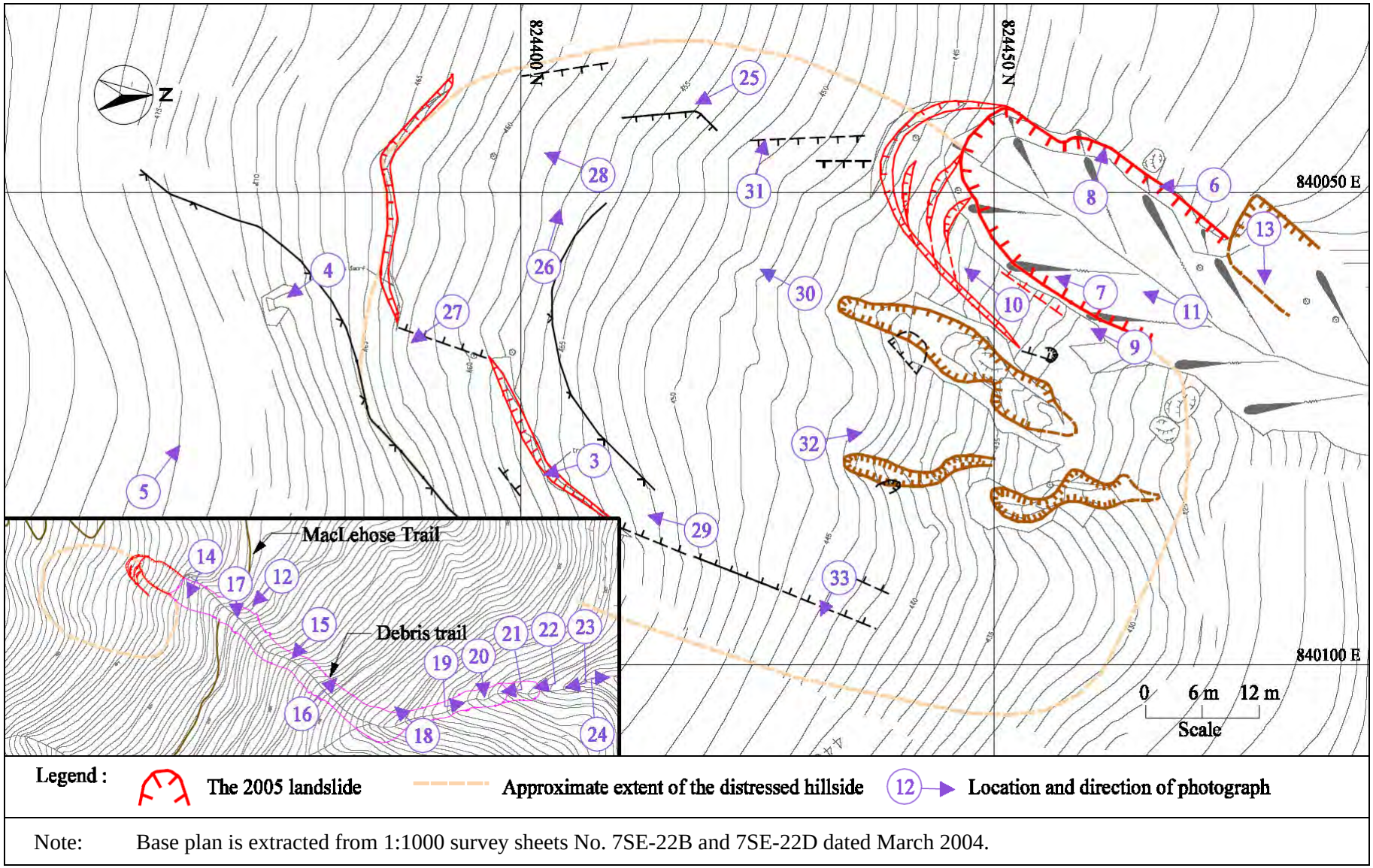

Figure 23 - Locations and Directions of Photographs

LIST OF PLATES

Plate No.		Page No.
1	Oblique Aerial View of the August 2005 Landslide (Photograph taken on 28 August 2005)	73
2	Oblique Aerial View of the August 2005 Landslide and the Facilities at Kwun Ping Road (Photograph taken on 28 August 2005)	74
3	Central Part of the Eastern Flank of the Main Scarp within the Distressed Hillside (Photograph taken on 8 March 2006)	75
4	Entrance to Wartime Tunnel (Photograph taken on 10 March 2006)	76
5	Wartime Trench above the Distressed Hillside (Photograph taken on 29 May 2006)	76
6	General View of Main Scarp of the August 2005 Landslide (Photograph taken on 24 August 2005)	77
7	Displaced Mass below Stepped Tension Cracks on Eastern Flank of the August 2005 Landslide Source (Photograph taken on 5 June 2006)	78
8	Old Colluvium Exposed in the Western Flank of the August 2005 Landslide (Photograph taken on 14 March 2006)	78
9	Lateral Tension Crack Immediately West of the August 2005 Landslide (Photograph taken on 10 March 2006)	79
10	Upslope Extension of the Lateral Tension Crack Immediately West of the August 2005 Landslide above the Main Scarp (Photograph taken on 10 March 2006)	79
11	Completely Decomposed Tuff with Kaolin Veins Exposed in the Base of the August 2005 Landslide (Photograph taken on 14 March 2006)	80
12	Debris Trail Showing Entrainment of MacLehose Trail (Photograph taken on 25 August 2005)	80
13	Old Landslide Debris adjacent to the Pre-1963 Landslide Scar (Photograph taken on 15 March 2006)	81

Plate No.		Page No.
14	Debris Trail below the Toe of Rupture of the August 2005 Landslide (Photograph taken on 24 August 2005)	81
15	Existing Ground Surface Exposed in the Base of the Debris Trail (Photograph taken on 25 May 2005)	82
16	Upper Debris Trail at Chainage CH136 (Photograph taken on 15 March 2006)	82
17	Lower Portion of the Upper Debris Trail (Photograph taken on 25 August 2005)	83
18	Debris Trail at Chainage CH220 Showing Deposition of Debris on the Inside Bend (Photograph taken on 25 May 2006)	83
19	Trees and Soil Adjacent to the Debris Trail Buried by Previous Landsliding (Photograph taken on 10 March 2006)	84
20	Boulder of Feldsparphyric Rhyolite at CH270 of the Debris Trail (Photograph taken on 28 April 2006)	84
21	View of the Upper Boulder Dam from Downstream (Photograph taken on 22 March 2006)	85
22	View of the Lower Boulder Dam from Downstream (Photograph taken on 22 March 2006)	85
23	View along Streamcourse Looking Uphill towards Boulder Dam (Photograph taken on 24 August 2005)	86
24	Washout Debris in Streamcourse below the Boulder Dams (Photograph taken on 24 August 2005)	86
25	One of a Series of Stepped Tension Cracks on the Western Flank of the Distressed Hillside (Photograph taken on 10 March 2006)	87
26	Discontinuous Tension Crack above Drillhole No. BH4 near the Western Flank of the Distressed Hillside (Photograph taken on 10 July 2006)	87
27	Collapse Feature Upslope of Main Scarp of the Distressed Hillside (Photograph taken on 22 March 2006)	88

Table of Contents
Table of Contents
Table of Contents
Table of Contents

Plate No.		Page No.
28	Boulder with Soil Movement within the Main Body of the Distressed Hillside (Photograph taken on 10 March 2006)	88
29	Leaning Trees near the Eastern Flank of the Distressed Hillside (Photograph taken on 28 April 2006)	89
30	Trees Disturbed by Boulder Movements and Subsurface Collapse (Photograph taken on 10 July 2006)	90
31	Tree Split across the Tension Crack on Western Flank of the Distressed Hillside (Photograph taken on 10 March 2006)	90
32	The Eastern and Western Gullies (Photograph taken on 14 June 2006)	91
33	Stone Line in Trial Pit No. TP10 Marking the Base of a Past Landslide (Photograph taken on 14 June 2006)	91
34	Old Colluvium Observed in Split Mazier Samples and Trial Pit	92
35	Boxwork Kaolin Veins in CDT in Trial Pit No. TP8	93
36	Offset Observed in Split Mazier Samples	94
37	Fault Gouge along Joint at 30.8 m Depth in Drillhole No. BH2	95
38	Clay Bands at 10 m Depth in Drillhole No. BH1	95
39	Clay Bands at 4.2 m Depth in Drillhole No. BH3	96
40	Clay Bands at 4.2 m Depth in Drillhole No. BH4	96
41	Clay Bands at 11.5 m Depth in Drillhole No. BH4	97
42	Clay Bands at 5.7 m Depth in Drillhole No. BH5	97
43	Clay Bands at 9 m Depth in Drillhole No. BH5	98
44	Clay Bands at 18.7 m Depth in Drillhole No. BH5	98
45	Layered Deposit in Soil Pipe Observed in Face B of Trial Pit No. TP2	99

Table of Contents
Table of Contents
Table of Contents
Table of Contents

Plate No.		Page No.
46	Accumulation of Clay on Top of Sandy Soil in Soil Pipe in Face C of Trial Pit No. TP8	99
47	Sandy Soil Pipe Deposit with Horizontal Clay Layer at 3 m Depth in Drillhole No. BH1	100
48	Sub-horizontal Clay Layer in Pipe Deposit at 3 m Depth in Drillhole No. BH1	100
49	Incipient Soil Pipe Development in Completely Decomposed Tuff	101

Table of Contents
Table of Contents
Table of Contents
Table of Contents

Plate 1 - Oblique Aerial View of the August 2005 Landslide
(Photograph taken on 28 August 2005)

Table of Contents
Table of Contents
Table of Contents
Table of Contents

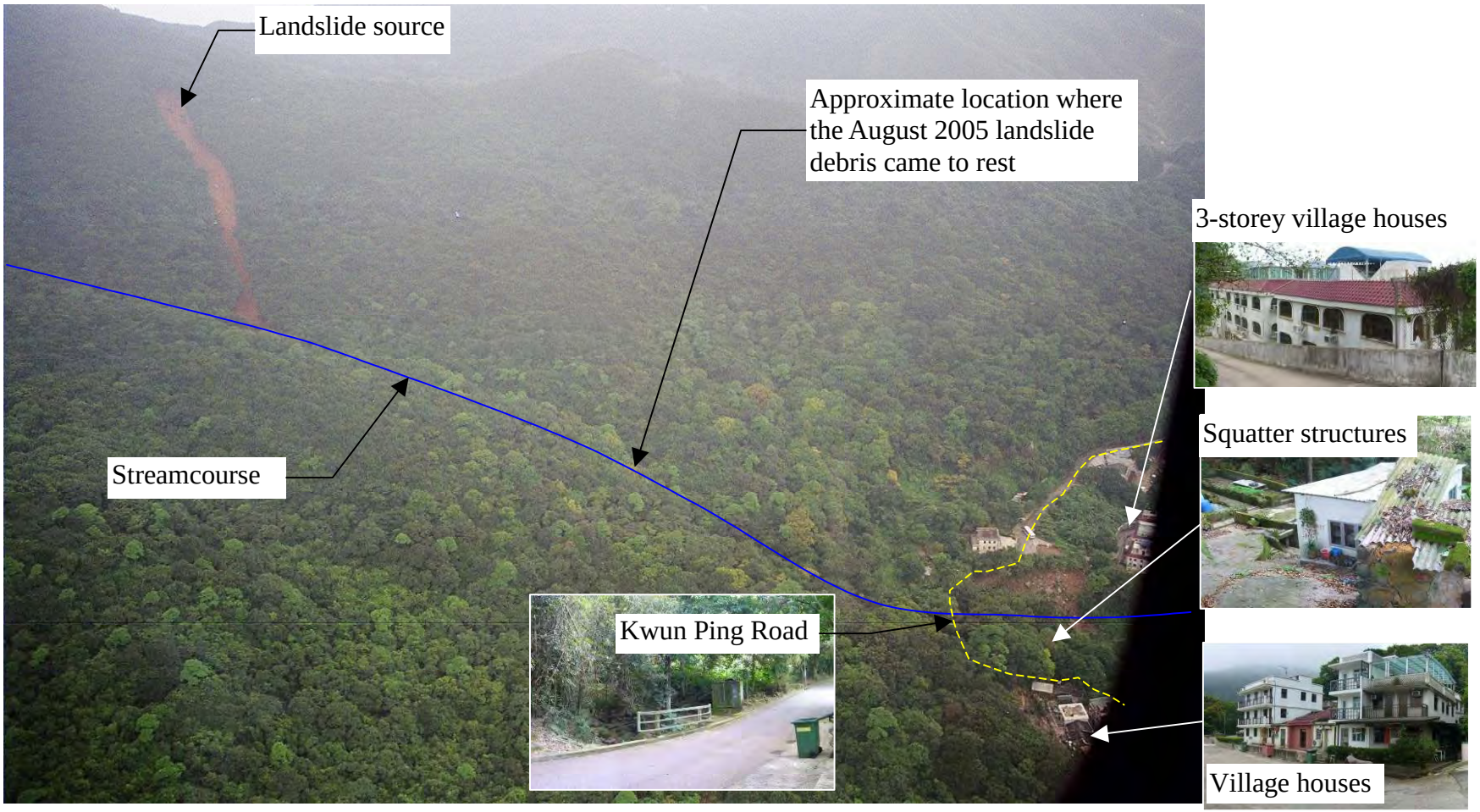

Plate 2 - Oblique Aerial View of the August 2005 Landslide and the Facilities at Kwun Ping Road
(Photograph taken on 28 August 2005)

Table of Contents
Table of Contents
Table of Contents
Table of Contents

Plate 3 - Central Part of the Eastern Flank of the Main Scarp within the Distressed Hillside (Photograph taken on 8 March 2006)

Note: See Figure 23 for locations and directions of photographs.

Table of Contents
Table of Contents
Table of Contents
Table of Contents

Plate 4 - Entrance to Wartime Tunnel
(Photograph taken on 10 March 2006)

Plate 5 - Wartime Trench above the Distressed Hillside
(Photograph taken on 29 May 2006)

Note: See Figure 23 for locations and directions of photographs.

Table of Contents
Table of Contents
Table of Contents
Table of Contents

Table of Contents
Table of Contents
Table of Contents

Plate 6 - General View of Main Scarp of the August 2005 Landslide
(Photograph taken on 24 August 2005)

Note: See Figure 23 for location and direction of photograph.

Plate 7 - Displaced Mass below Stepped Tension Cracks on Eastern Flank of the August 2005 Landslide Source (Photograph taken on 5 June 2006)

Plate 8 - Old Colluvium Exposed in the Western Flank of the August 2005 Landslide (Photograph taken on 14 March 2006)

Note: See Figure 23 for location and direction of photograph.

Table of Contents
Table of Contents
Table of Contents
Table of Contents

Table of Contents
Table of Contents
Table of Contents

Plate 9 - Lateral Tension Crack Immediately West of the August 2005 Landslide
(Photograph taken on 10 March 2006)

Plate 10 - Upslope Extension of the Lateral Tension Crack Immediately West of the August 2005 Landslide above the Main Scarp
(Photograph taken on 10 March 2006)

Note: See Figure 23 for location and direction of photograph.

Plate 11 - Completely Decomposed Tuff with Kaolin Veins Exposed in the Base of the August 2005 Landslide (Photograph taken on 14 March 2006)

Plate 12 - Debris Trail Showing Entrainment of MacLehose Trail (Photograph taken on 25 August 2005)

Note: See Figure 23 for location and direction of photograph.

Table of Contents
Table of Contents
Table of Contents
Table of Contents

Plate 13 - Old Landslide Debris adjacent to the Pre-1963 Landslide Scar (Photograph taken on 15 March 2006)

Plate 14 - Debris Trail below the Toe of Rupture of the August 2005 Landslide (Photograph taken on 24 August 2005)

Note: See Figure 23 for location and direction of photograph.

Table of Contents
Table of Contents
Table of Contents
Table of Contents

Plate 15 - Existing Ground Surface Exposed in the Base of the Debris Trail (Photograph taken on 25 May 2005)

Plate 16 - Upper Debris Trail at Chainage CH136 (Photograph taken on 15 March 2006)

Note: See Figure 23 for location and direction of photograph.

Table of Contents
Table of Contents
Table of Contents
Table of Contents

Plate 17 - Lower Portion of the Upper Debris Trail
(Photograph taken on 25 August 2005)

Plate 18 - Debris Trail at Chainage CH220 Showing Deposition of Debris on the Inside Bend (Photograph taken on 25 May 2006)

Note: See Figure 23 for location and direction of photograph.

Table of Contents
Table of Contents
Table of Contents
Table of Contents

Plate 19 - Trees and Soil Adjacent to the Debris Trail Buried by Previous Landsliding (Photograph taken on 10 March 2006)

Plate 20 - Boulder of Feldsparphyric Rhyolite at CH270 of the Debris Trail (Photograph taken on 28 April 2006)

Note: See Figure 23 for location and direction of photograph.

Table of Contents
Table of Contents
Table of Contents
Table of Contents

Plate 21 - View of the Upper Boulder Dam from Downstream
(Photograph taken on 22 March 2006)

Plate 22 - View of the Lower Boulder Dam from Downstream
(Photograph taken on 22 March 2006)

Note: See Figure 23 for location and direction of photograph.

Table of Contents
Table of Contents
Table of Contents
Table of Contents

Plate 23 - View along Streamcourse Looking Uphill towards Boulder Dam (Photograph taken on 24 August 2005)

Plate 24 - Washout Debris in Streamcourse below the Boulder Dams (Photograph taken on 24 August 2005)

Note: See Figure 23 for location and direction of photograph.

Table of Contents
Table of Contents
Table of Contents
Table of Contents

Plate 25 - One of a Series of Stepped Tension Cracks on the Western Flank of the Distressed Hillside (Photograph taken on 10 March 2006)

Plate 26 - Discontinuous Tension Crack above Drillhole No. BH4 near the Western Flank of the Distressed Hillside (Photograph taken on 10 July 2006)

Note: See Figure 23 for location and direction of photograph.

Table of Contents
Table of Contents
Table of Contents
Table of Contents

Plate 27 - Collapse Feature Upslope of Main Scarp of the Distressed Hillside (Photograph taken on 22 March 2006)

Plate 28 - Boulder with Soil Movement within the Main Body of the Distressed Hillside (Photograph taken on 10 March 2006)

Note: See Figure 23 for location and direction of photograph.

Table of Contents
Table of Contents
Table of Contents
Table of Contents

Plate 29 - Leaning Trees near the Eastern Flank of the Distressed Hillside (Photograph taken on 28 April 2006)

Note: See Figure 23 for location and direction of photograph.

Table of Contents
Table of Contents
Table of Contents
Table of Contents

Plate 30 - Trees Disturbed by Boulder Movements and Subsurface Collapse (Photograph taken on 10 July 2006)

Plate 31 - Tree Split across the Tension Crack on Western Flank of the Distressed Hillside (Photograph taken on 10 March 2006)

Note: See Figure 23 for location and direction of photograph.

Table of Contents
Table of Contents
Table of Contents
Table of Contents

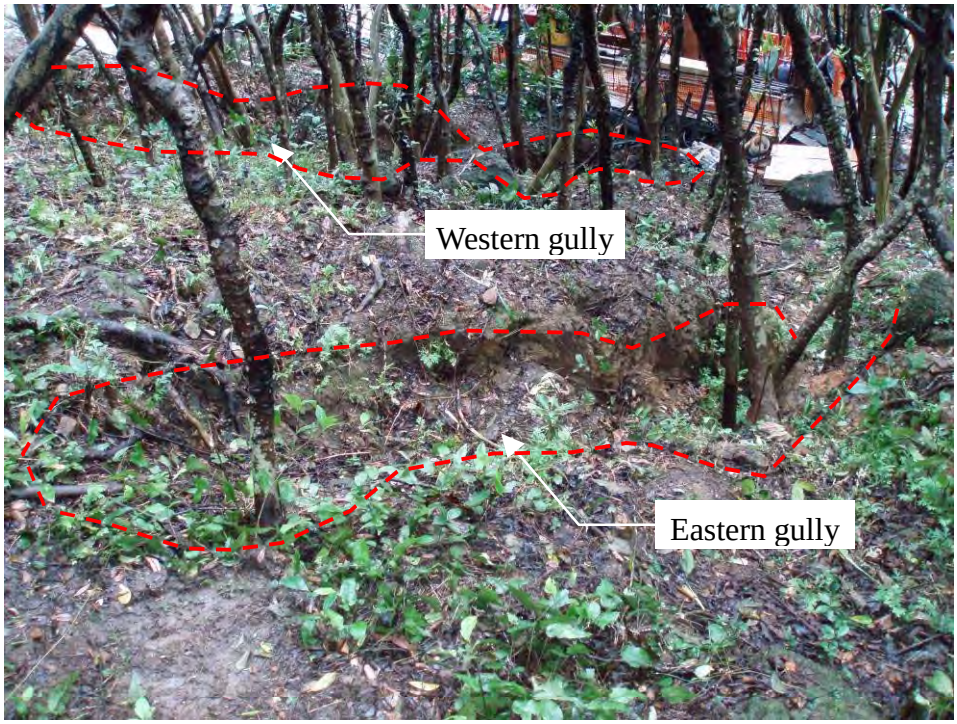

Plate 32 - The Eastern and Western Gullies
(Photograph taken on 14 June 2006)

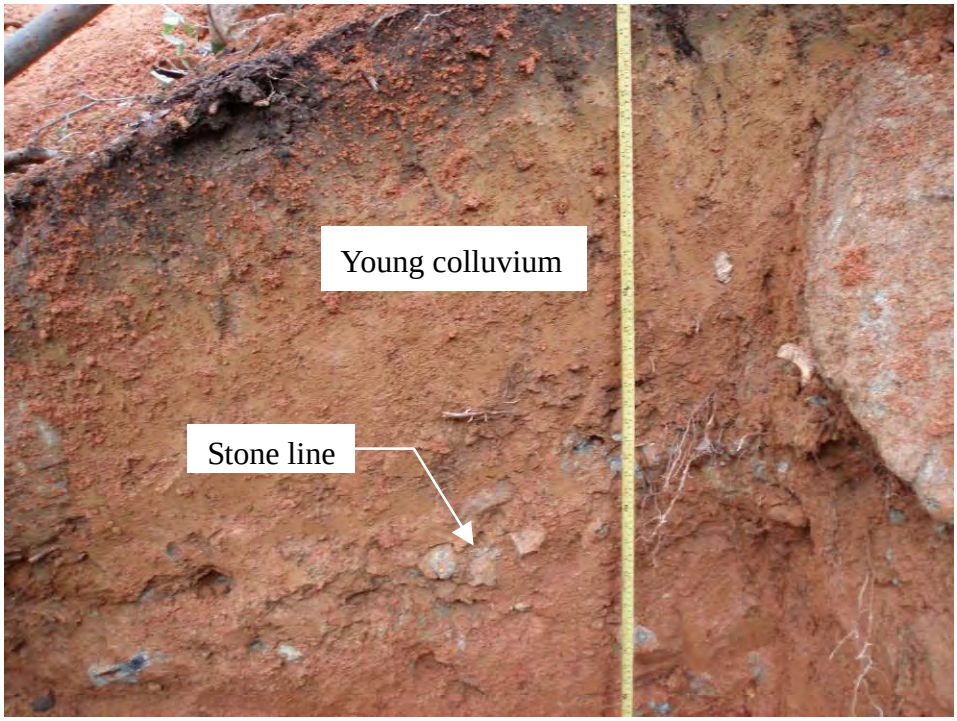

Plate 33 - Stone Line in Trial Pit No. TP10 Marking the Base of a Past Landslide
(Photograph taken on 14 June 2006)

Note: See Figure 23 for location and direction of photograph.

Table of Contents
Table of Contents
Table of Contents
Table of Contents

(a) Old Colluviumn BH1

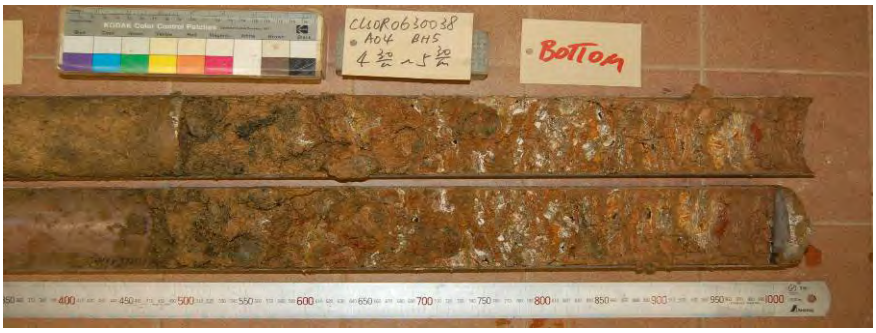

(b) Old Colluvium with Kaolin in BH5

(c) Old colluvium in BH3

(d) Old colluvium in TP10

Plate 34 - Old Colluvium Observed in Split Mazier Samples and Trial Pit

Note: See Figure 10 of GI station.

Table of Contents
Table of Contents
Table of Contents
Table of Contents

Plate 35 - Boxwork Kaolin Veins in CDT in Trial Pit No. TP8

Note: See Figure 10 for location of GI station.

Table of Contents
Table of Contents
Table of Contents
Table of Contents

(a) Offset observed at about 9 m Depth in drillhole No. BH4

(b) Offset observed at about 25 m Depth in drillhole No. BH5

Plate 36 - Offset Observed in Split Mazier Samples

Note: See Figure 10 for location of GI station.

Table of Contents
Table of Contents
Table of Contents
Table of Contents

Plate 37 - Fault Gouge along Joint at 30.8 m Depth in Drillhole No. BH2

Plate 38 - Clay Bands at 10 m Depth in Drillhole No. BH1

Note: See Figure 10 for location of GI station.

Table of Contents
Table of Contents
Table of Contents
Table of Contents

Plate 39 - Clay Bands at 4.2 m Depth in Drillhole No. BH3

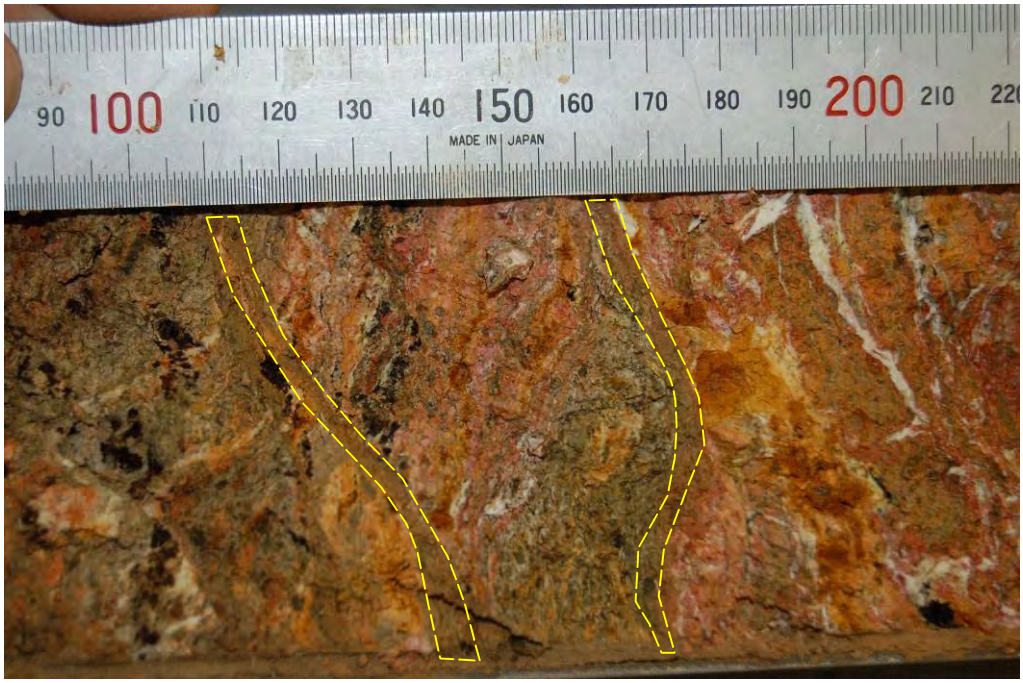

Plate 40 - Clay Bands at 4.2 m Depth in Drillhole No. BH4

Note: See Figure 10 for location of GI station.

Table of Contents
Table of Contents
Table of Contents
Table of Contents

Plate 41 - Clay Bands at 11.5 m Depth in Drillhole No. BH4

Plate 42 - Clay Bands at 5.7 m Depth in Drillhole No. BH5

Note: See Figure 10 for location of GI station.

Table of Contents
Table of Contents
Table of Contents
Table of Contents

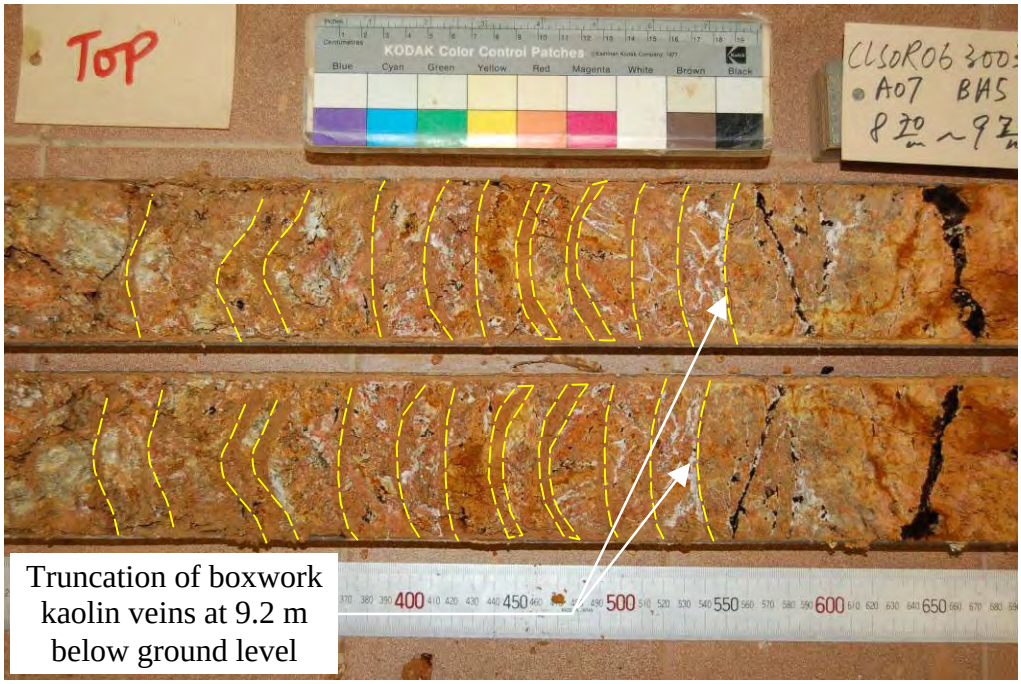

Plate 43 - Clay Bands at 9 m Depth in Drillhole No. BH5

Plate 44 - Clay Bands at 18.7 m Depth in Drillhole No. BH5

Note: See Figure 10 for location of GI station.

Table of Contents
Table of Contents
Table of Contents
Table of Contents

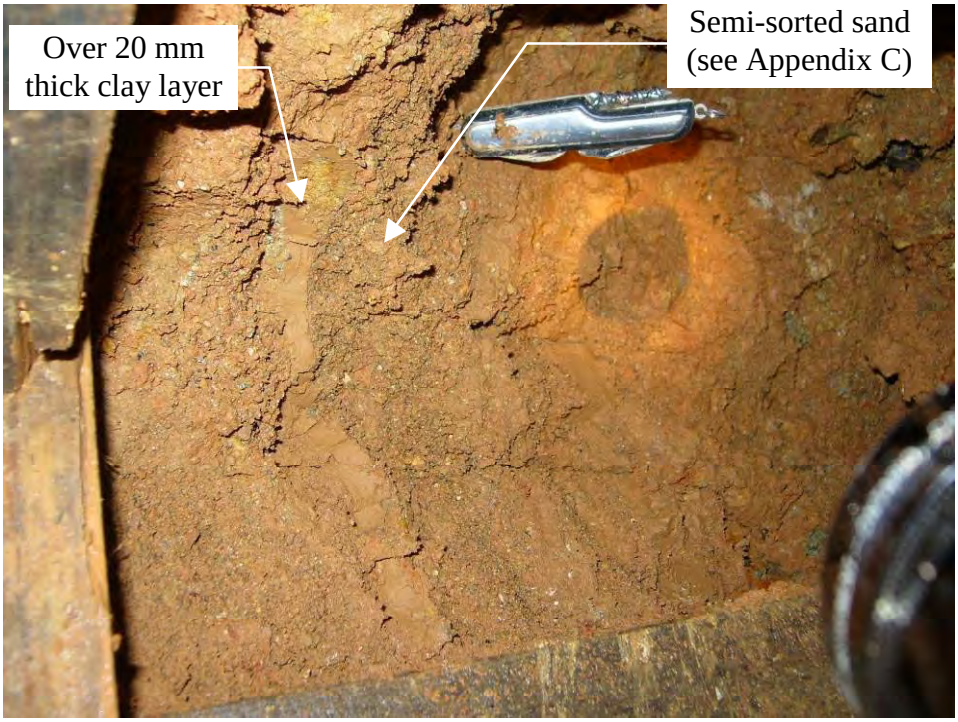

Plate 45 - Layered Deposit in Soil Pipe Observed
in Face B of Trial Pit No. TP2

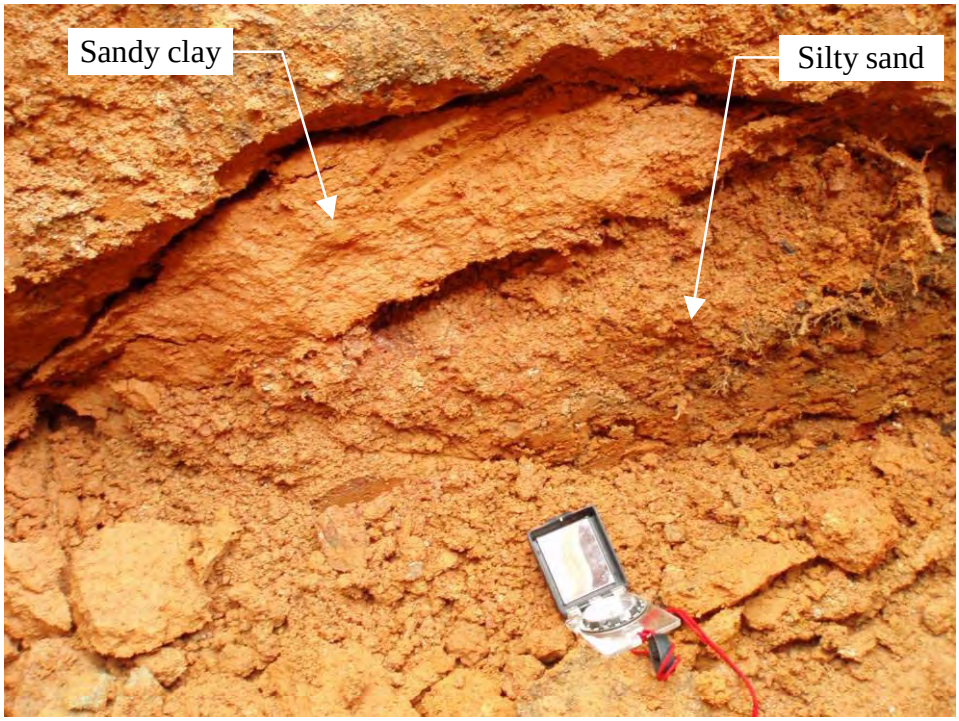

Plate 46 - Accumulation of Clay on Top of Sandy Soil in
Soil Pipe in Face C of Trial Pit No. TP8

Note: See Figure 10 for location of GI station.

Table of Contents
Table of Contents
Table of Contents
Table of Contents

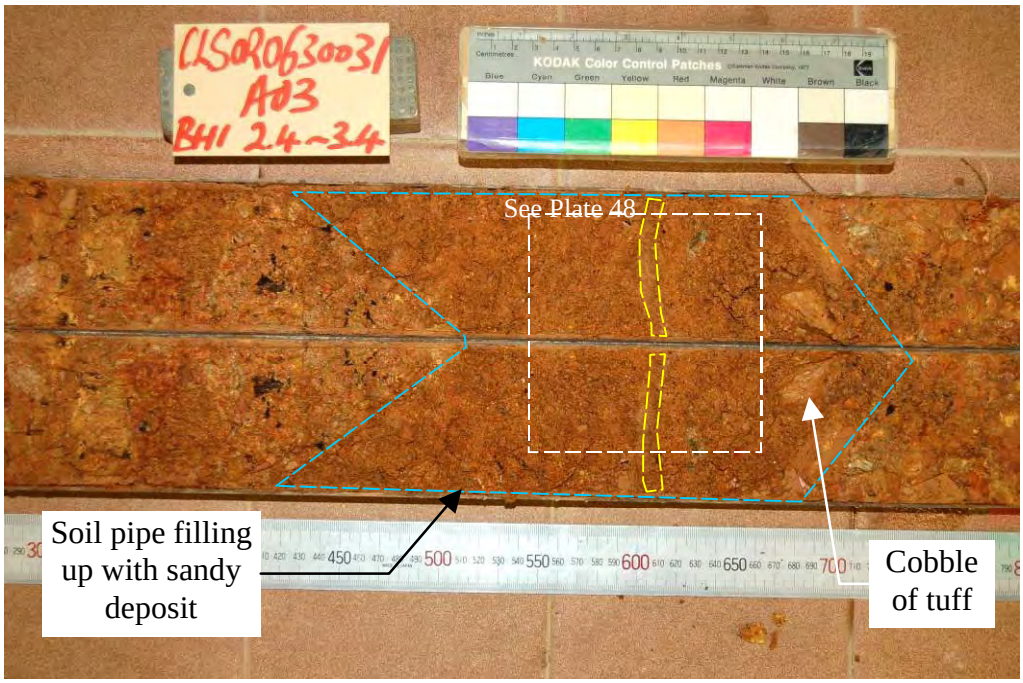

Plate 47 - Sandy Soil Pipe Deposit with Horizontal Clay Layer at 3 m Depth in Drillhole No. BH1

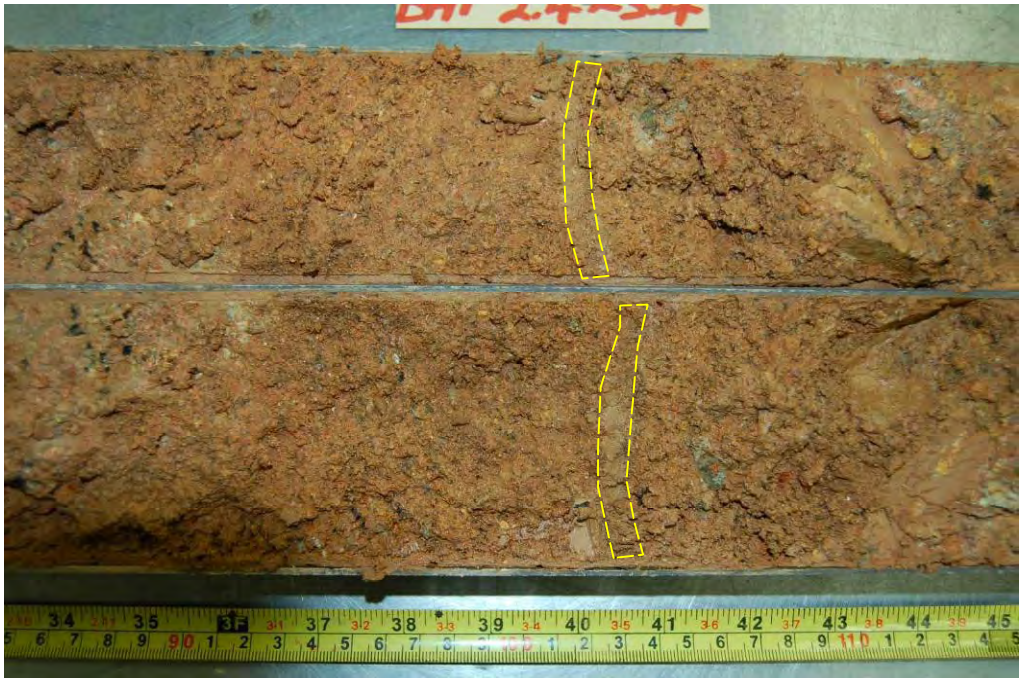

Plate 48 - Sub-horizontal Clay Layer in Pipe Deposit at 3 m Depth in Drillhole No. BH1

Note: See Figure 10 for location of GI station.

Table of Contents
Table of Contents
Table of Contents
Table of Contents

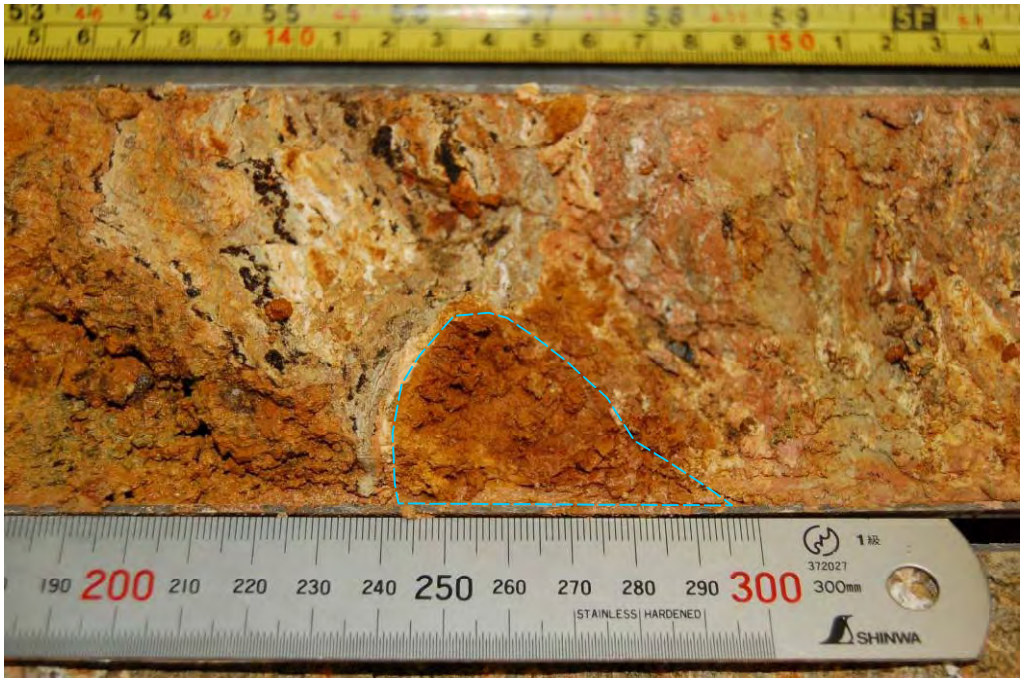

Plate 49 - Incipient Soil Pipe Development in Completely Decomposed Tuff

Note: See Figure 10 for location of GI station.

Table of Contents
Table of Contents
Table of Contents
Table of Contents

Table of Contents
Table of Contents
Table of Contents
Table of Contents

APPENDIX A

AERIAL PHOTOGRAPH INTERPRETATION

CONTENTS

		Page No.
	Cover Page	102
	CONTENT	103
A1.	INTRODUCTION	104
A2	SUMMARY	104
A3.	MORPHOLOGY, HYDROLOGY AND SUPERFICIAL MATERIALS	105
A4	DETAILED OBSERVATIONS	105
	LIST OF TABLES	109
	LIST OF FIGURES	111

Table of Contents
Table of Contents
Table of Contents
Table of Contents

A1. INTRODUCTION

The primary aims of the API were to access the geological and geomorphological conditions of the site and to identify any signs of instability in recent and historic aerial photographs. A review of available aerial photographs taken between 1956 and 2005 was undertaken (see list in Table A1). Based primarily on the 1963 aerial photographs, with some additional observations from the earlier 1956 aerial photographs, relevant observations relating to the site history are shown on Figure A1 with the morphology and hydrology shown in Figure A2. Pertinent observations from the 1956 and 1963 aerial photographs are highlighted in Figures A3, A4 and A5.

A2. SUMMARY

The study area comprises natural terrain. In the earliest aerial photographs reviewed (1956), the area of concern can be seen to occupy a linear topographical depression between rounded spurlines located below the northern side of Tate's Ridge (Figure A1 and Figure A3). The terrain along the western side of the linear topographical depression appears hummocky, which is indicative of disturbance most likely through landsliding. The eastern side, although partly covered in vegetation (1963), appears to have a more uniform morphology. Within the mid-portion of the linear depression, two rounded breaks-in-slope (Figure A3) may have been derived from much older landslide events, the scars of which have since degraded considerably. There is a series of parallel convex breaks-in-slope along the rounded spurline that bounds the eastern side of the topographical depression, which may be related to the underlying geological structure. Relict landslides R3 and R5 observed to the west of the spurline (Figure A1) bounding the west of the linear depression, appear to have a straight edge (which trends north-northwest to south-southeast) for at least part of the scar, suggesting possible structural control to the landslides.

There is much evidence of anthropogenic disturbance across the hillside. Military structures are present along the ridgeline, including chevron shaped wartime trenches. One such trench can be seen to extend into the upper eastern side of the depression (Figure A5), and other related excavations (possibly Japanese tunnels) are present on the natural terrain above the depression. Several footpaths cross the site, notably the MacLehose Trail, which crosses along to the north downslope of the study area, two footpaths, FP1 and FP2 (Figures A1 and A5) cross the central portion of the distressed, area and another footpath (FP3 in Figures A1 and A5) crosses above the linear depression. Footpaths FP1 to FP3 are no longer in use since late 1970's to early 1980's.

Two ephemeral drainage lines are observed along the western side of the topographical depression (Figures A2 and A3), and a third possible ephemeral drainage line runs approximately through the centre of the topographical depression. At the mouth and northern end of the topographical depression, a clear arcuate break-in-slope is discernible, possibly a relict landslide or two landslides, into which the ephemeral drainage lines can be seen to drain. In the 1963 aerial photographs, an incised gully can be seen at the western side of this break-in-lope (Figure A5). About 5 m to 10 m west of the mouth of the depression, two (approximately 4 m wide by 5 m long) clearly defined relict landslide scars R1 and R2 (Figure A1), are visible with a possible third small, degraded relict landslide immediately in front of the toe of these landslides. Landslides R1 and R2 are identified under the ENTLI as Tag Nos. 07SEC0135E and 07SEC0136E. The terrain in front of the

Table of Contents
Table of Contents
Table of Contents
Table of Contents

two relict landslides where the possible third landslide is identified, was affected by a landslide L1 before 1963 and possibly after 1956 (Figures A1 and A4), and the area encompassing that occupied by the two 1956 relict landslides, was affected by the 2005 landslide.

There is no observable change to the terrain between the pre-1963 landslide and the present day, other than a general increase in vegetation density.

A3. MORPHOLOGY, HYDROLOGY AND SUPERFICIAL MATERIALS

The study area is located on north-facing natural terrain. Rock exposure and possible boulders are scattered across the mid-slope of the hillside, with a number of possible colluvial boulders (for example B1, B2 and B3) present on the terrain to the east of the linear depression. The general morphology and hydrology of the area is shown on Figure A2.

Three photolineaments are apparent within the vicinity of the study area (Figure A2). Photolineaments P1s and P3s are strong features while P2w is a relatively ill-defined weak lineament. Both P1s and P3s correspond to the main natural drainage line draining towards north-northwest and west-northwest respectively. P1s and P2w strike north-northwest to south-southeast, while P3w strikes east-northeast to west-southwest.

A north trending perennial streamcourse (S1) with some ill-defined ephemeral branches drains the central portion of the study area, and a west-trending streamcourse (S2) drains the west of the study catchment (Figure A2).

The terrain units within the study area consist of localised interfluves along the main ridgelines, with convex, gentle gradient terrain (approximately 22°) located immediately downslope. The terrain units become steeper transportational mid-slopes (approximately 28°) before reducing in gradient within their mid-slope sections.

A4. DETAILED OBSERVATIONS

Detailed observations from an examination of the aerial photographs for the period between 1956 and 2005 are presented below. Key observations are shown in Figures A1 to A5. A list of the aerial photographs examined is presented in Table A1.

YEAR	OBSERVATIONS
1956	High flight, poor resolution, aerial photographs. The study area comprises a linear topographical depression and drainage line below (Figures A1 and A3) located north of a prominent ridgeline. The area appears lightly vegetated with shrubs and grasses and few trees. Two relict landslides (R1 and R2) are apparent at the mouth of the linear depression and above the MacLehose Trail, which crosses the mid-slope of the terrain. These relict landslide scars are laterally defined by rounded convex

Table of Contents
Table of Contents
Table of Contents
Table of Contents

YEAR	OBSERVATIONS

1956 (cond't) breaks in slope. The lack of apparent downslope debris suggests that the landslides occurred a long time ago. Within the central portion of the linear depression, there appears to be a concave break-in-slope with a second convex break-in-slope at the mouth of the depression (Figure A3).

A cave-like structure (M1) is apparent at the mid-slope area, and may be an entrance to a wartime military tunnel. A second similar feature (M2) is apparent to the north of M1, which may be another military tunnel entrance. Some seemingly former military structures (M3) are located on Tate's Ridge upslope of the study area. Five areas of high reflectivity (M4 to M8) are evident near the crest of the study area and are also likely to be military related excavation works.

Two high reflectivity areas (G1 and G2) are visible adjacent to the MacLehose Trail and appear to be graves.

1963 Low flight, excellent resolution, aerial photographs.

A recent landslide (L1) is observed to have affected the area in front of relict landslides R1 and R2, with high reflectivity on the western flank of R1 suggesting that it has been partly reactivated. Landslide (L1) appears to comprise a debris slide failure emanating from an area of locally over-steepened terrain below a break-in-slope, with the debris travelling into a drainage line below (Figures A1, A4 and A5).

A parallel series of convex breaks-in-slope are visible along the eastern spurline (Figure A5).

The former military structures (M3) located on the ridgeline above the study area have been demolished.

Two cave-like features (M9 and M10), possible military structures, are visible to the northwest of M3. Three military related trenches (M11 to M13) are evident to the west of the study catchment.

Possible rock exposures and boulders are visible and scattered across the mid-slope of the terrain. Boulder field (B1), locally with some probably exposed corestones are visible near the crest of the study area while boulder fields (B2 and B3) are apparent adjacent to the MacLehose Trail.

Seventeen additional relict landslides (R3 to R21) are apparent in the vicinity of the study area. These relict landslide scars are laterally defined by rounded convex breaks-in-slope, although there is little evidence of associated downslope debris.

Another grave (G3) is evident adjacent to the MacLehose Trail.

Table of Contents
Table of Contents
Table of Contents
Table of Contents

YEAR	OBSERVATIONS
1964	High flight, good resolution, aerial photographs. No observable changes.
1974	The location of landslide (L1) appears to have re-vegetated. Seven recent landslides (L2 to L8) are visible above the perennial streamcourse (S2). Some of the recent landslides may be recurring landslides as the positions of recent landslides L2, L3, L4, L5 and L7, L8 are coincident with the relict landslide scars R12, R14, R15, R16, R3 and R11 respectively.
1976	High flight, good resolution, single aerial photograph. No significant changes to the study area are observed except the density of vegetation has increased. The military trenches are obscured by dense vegetation. Recent landslides L2 to L8, identified in 1974, appear to have re-vegetated with grass and shrubs.
1978	High flight, good resolution, single aerial photograph. A high reflectivity area is visible at the location of relict landslide scar (R21), which is possibly an area of erosion.
1979	High flight, good resolution, single aerial photograph. The erosion area in the location of relict landslide scar (R21) appears to have re-vegetated with grass and shrubs.
1981	No significant changes to the study area are observed.
1982	No significant changes to the study area are observed.
1983	Excavation works have taken place at the crest of the study area apparently for the purposes of installing an electricity pole.
1985	A new zig-zagging footpath along the spurline to the west of the linear depression has been formed to connect to the MacLehose Trail.
1988 to 1989	High flight, good resolution, single aerial photograph. No significant changes to the study area are observed.

Table of Contents
Table of Contents
Table of Contents
Table of Contents

YEAR	OBSERVATIONS
1990	High flight, good resolution, single aerial photograph. No significant changes to the study area, except the density of vegetation has increased.
1991 to 1992	High flight, good resolution, single aerial photograph. No significant changes to the study area are observed.
1995 to 1998	No significant changes to the study area are observed.
1999	No significant changes to the study area, except that the density of vegetation has increased.
2000 to 2002	No significant changes to the study area are observed.
2003	No significant changes to the study area, except that the density of vegetation has increased.
2004	A large area around the ridgeline above the study area appears to have been affected by hillfire (HF1), which has removed all the vegetation to reveal military trenches. M12 and M13 are visible again as the dense vegetation was removed by the hillfire.
2005	Low flight, excellent resolution, single aerial photograph. The scar of the 2005 landslide is clearly visible, and green erosion control mat can be seen to have been placed over the scar and a high reflective brown soil defines the extent of the debris trail. A brown area visible through the trees some distance down the drainage line represents the limit of the debris trail. The area affected by the 2003/2004 hillfire (HF1) has already re-vegetated with grasses and shrubs.

Table of Contents
Table of Contents
Table of Contents
Table of Contents

LIST OF TABLES

Table No.		Page No.
A1	List of Aerial Photographs Examined	110

Table of Contents
Table of Contents
Table of Contents
Table of Contents

Table A1 - List of Aerial Photographs Examined

Date taken	Altitude (ft)	Photograph Number
27 December 1956	16700	Y3441-42
5 October 1959	40000	Y4622-23
17 January 1961	30000	Y4914-15
26 January 1963	4100	Y8650-53
13 December 1964	12500	Y12975-76
21 November 1974	12500	9785-86
28 January 1976	12500	12906
10 January 1978	12500	20726
28 November 1979	10000	28100
10 February 1981	5500	36581-82
10 October 1982	10000	44565-66
13 December 1983	5000	51964-65
4 October 1985	15000	A2685-86
16 January 1988	10000	A12076-77
4 June 1988	10000	A13745
20 November 1989	10000	A19364
3 December 1990	10000	A24375
29 October 1991	10000	A28820
4 October 1993	20000	CN4435
12 February 1995	10000	CN9560
23 November 1995	10000	CN12313
21 November 1996	10000	CN16190
1 November 1997	10000	CN19022-23
10 November 1998	8000	CN21873-74
3 September 1999	5500	A49441-43
27 October 1999	4000	A50525-27
9 December 1999	8000	CN25468-70
16 February 2000	20000	CN25993, CN26071
21 November 2001	8000	CW36416-17
21 January 2002	16000	RW851-852
9 October 2002	8000	CW45038-39
12 November 2003	8000	RW3270-71
25 September 2003	8000	CW49827-28
4 March 2004	4000	CW55664-65
26 October 2005	4000	CW66966

Note: All aerial photographs are in black and white apart from those with prefix CN and CW. RW refers to infrared.

Table of Contents
Table of Contents
Table of Contents
Table of Contents

LIST OF FIGURES

Figure No.		Page No.
A1	Site History	112
A2	General Geomorphology and Hydrology	113
A3	Interpretation of 1956 Aerial Photograph	114
A4	Interpretation of 1963 Aerial Photograph	115
A5	Close-up of Distressed Area Extracted from the 1963 Aerial Photograph	116

Table of Contents
Table of Contents
Table of Contents
Table of Contents

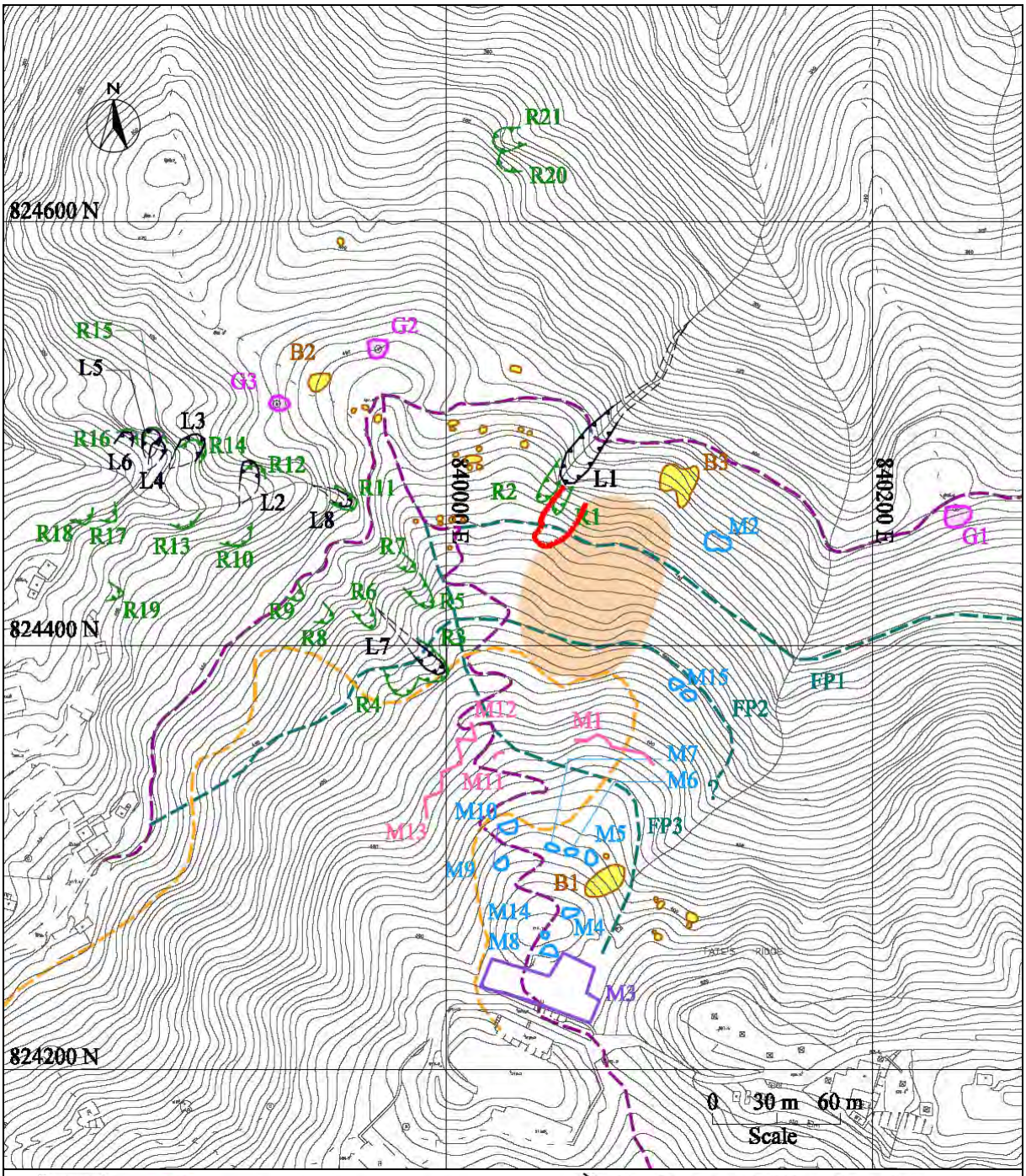

Notes: (1) Base plan is extracted from 1:1000 survey sheets Nos. 7SE-22B and 7SE-22D dated March 2004.
(2) Site history based on review of aerial photographs taken between 1945 and 2005.

Figure A1 - Site History

Table of Contents
Table of Contents
Table of Contents
Table of Contents

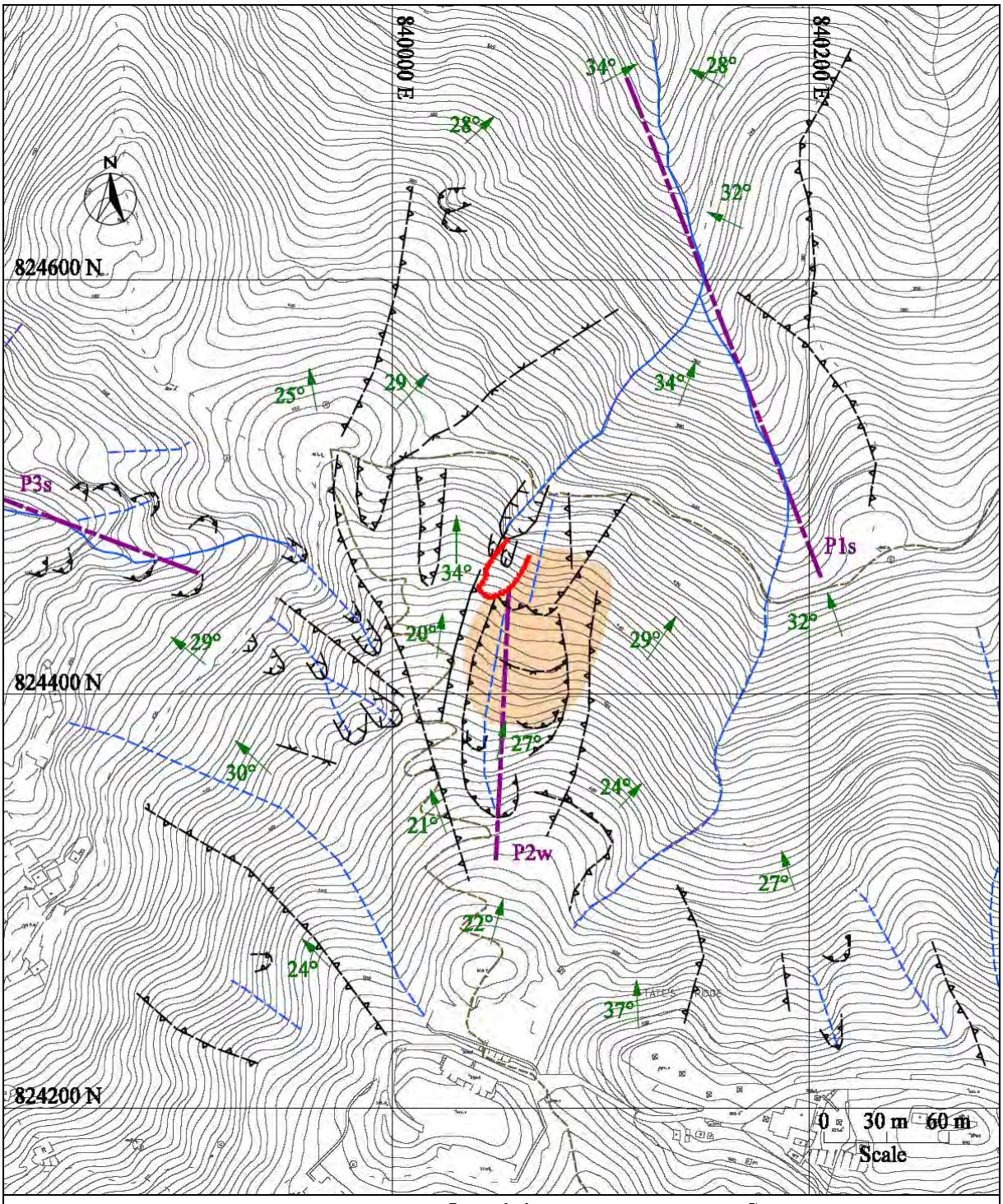

Notes: (1) Base plan is extracted from 1:1000 survey sheets Nos. 7SE-22B and 7SE-22D dated March 2004.
(2) General morphology and hydrology based on 1963 aerial photograph Nos. Y8650-51.

Figure A2 - Geineral Geomorphology and Hydrology

Table of Contents
Table of Contents
Table of Contents
Table of Contents

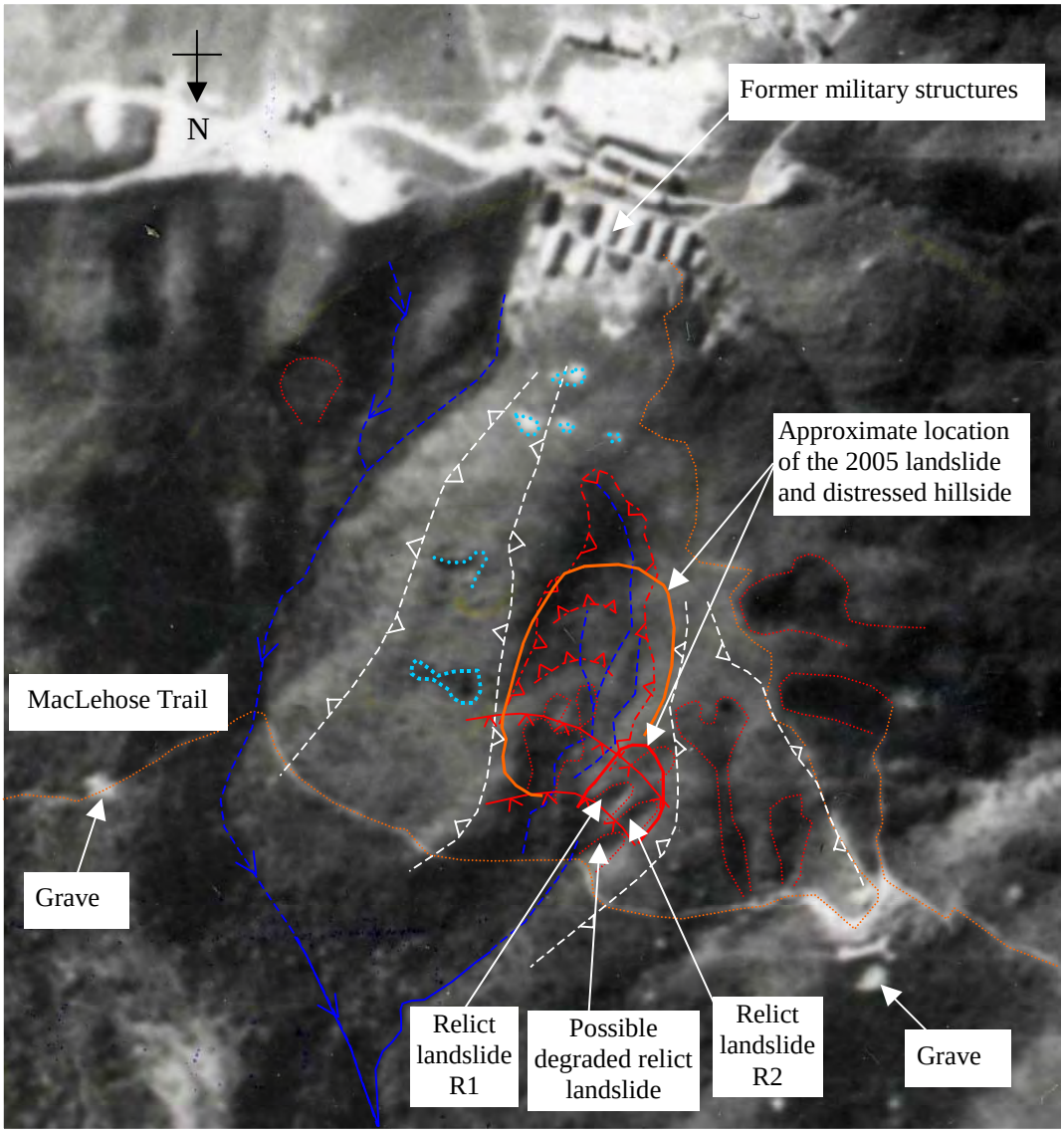

(Photograph Y03441 taken on 27 December 1956)

Legend:

Anthropogenic disturbance	Rounded spurline
Convex break in slope	Landslide scar
Convex break in slope	Footpath
Concave break in slope	Ephemeral drainage line

Figure A3 - Interpretation of 1956 Aerial Photograph

Table of Contents
Table of Contents
Table of Contents
Table of Contents

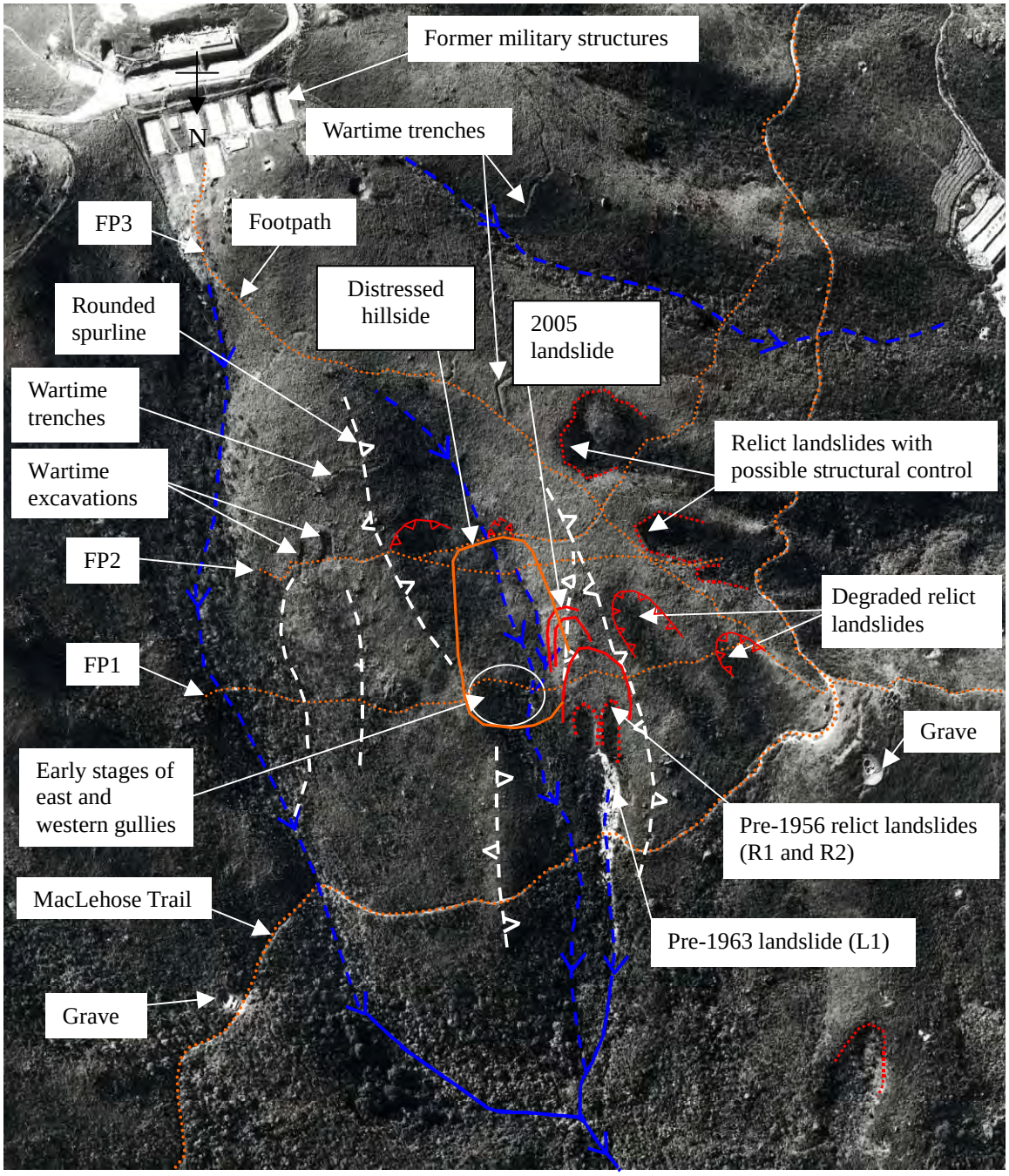

(Photograph Y08651 (4100 ft) taken on 26 January 1963)

Legend:

- Ephemeral drainage line
- Stream course
- Rounded spurline
- Hollow
- Rounded spurline
- FP1 Footpath and number
- Convex break in slope

Figure A4 - Interpretation of 1963 Aerial Photograph

Table of Contents
Table of Contents
Table of Contents
Table of Contents

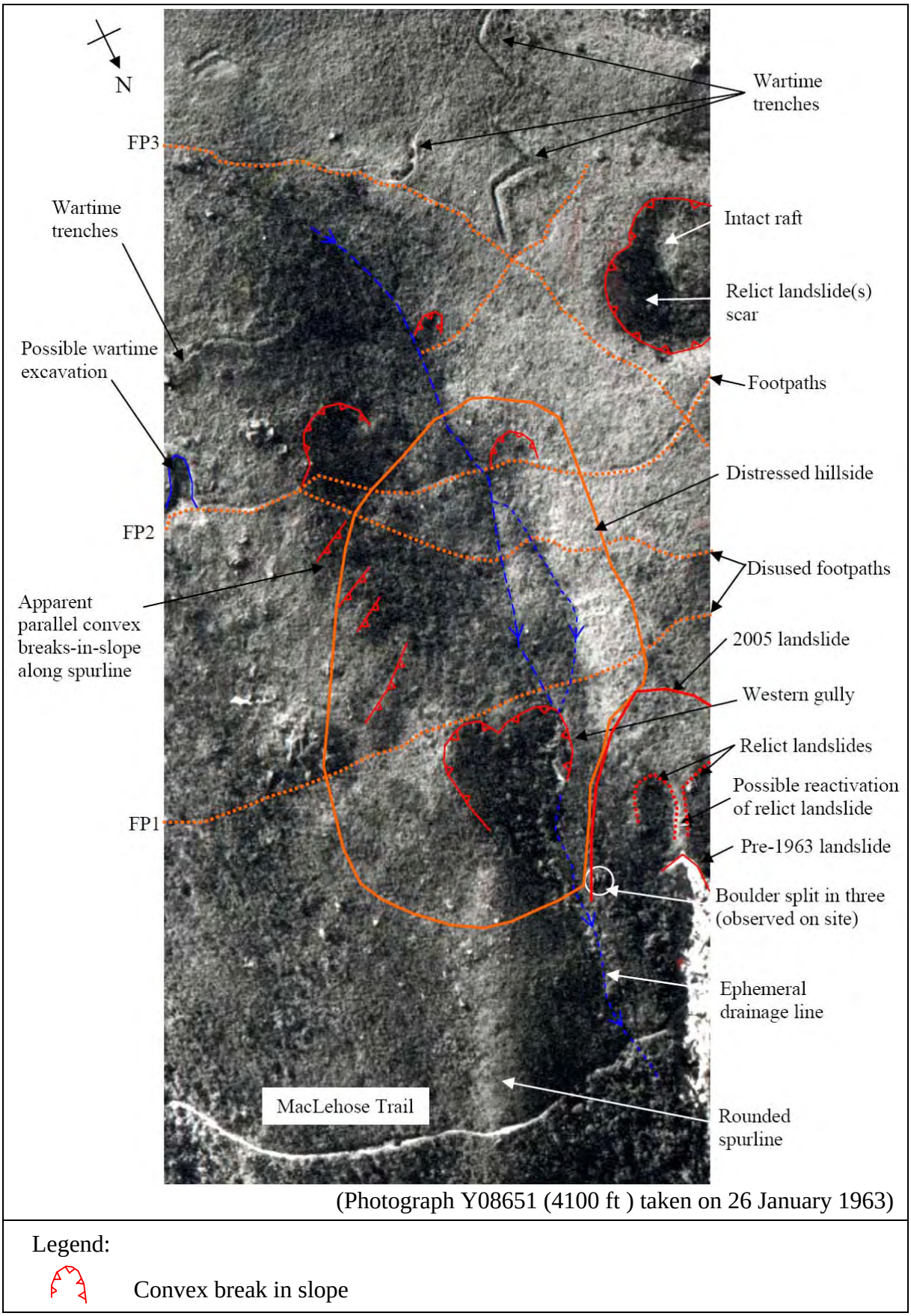

Figure A5 - Close-up of Distressed Area Extracted from the 1963 Aerial Photograph

Table of Contents
Table of Contents
Table of Contents
Table of Contents

Table of Contents
Table of Contents
Table of Contents
Table of Contents

APPENDIX B

CROSS-SECTIONS ALONG DEBRIS TRAIL

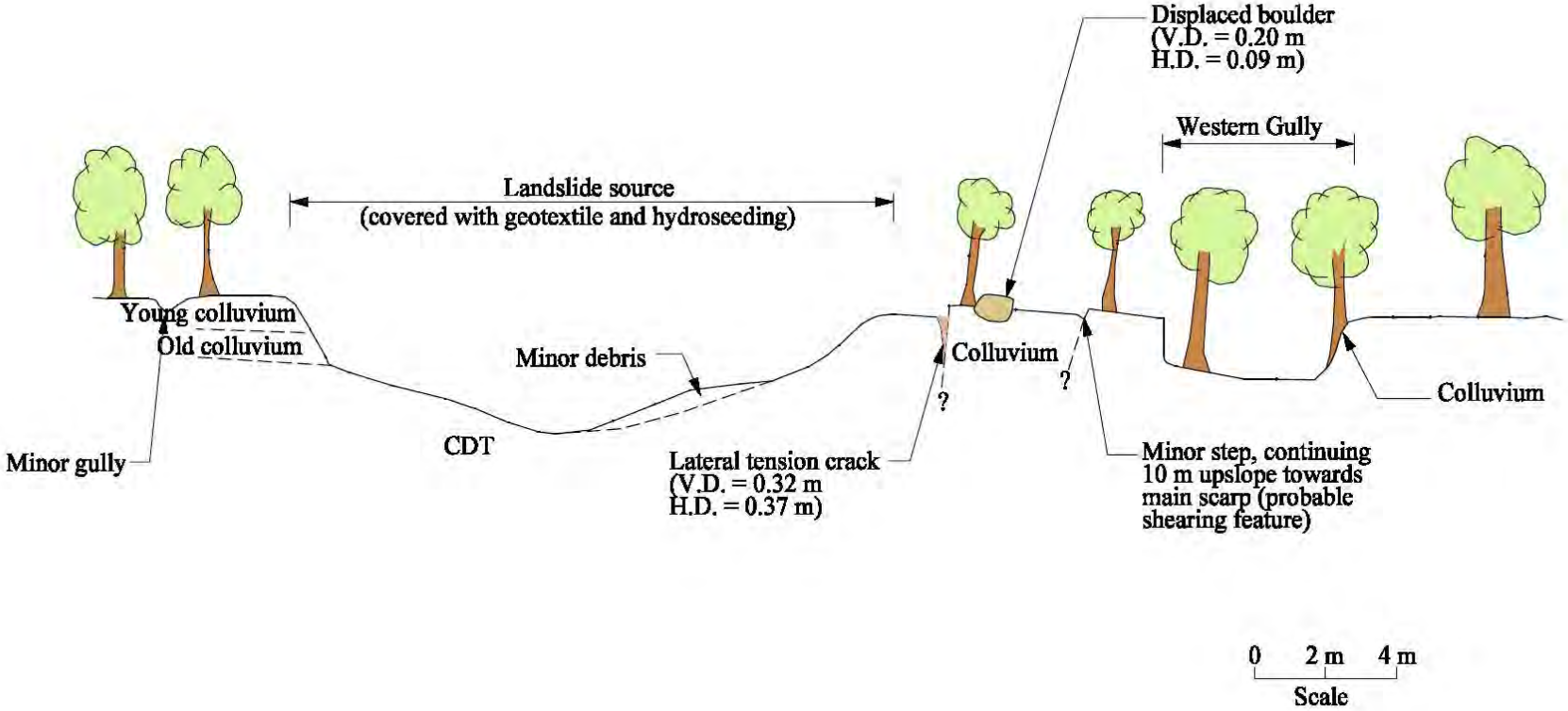

Notes: (1) V.D. denotes vertical displacement and H.D. denotes horizontal displacement.
(2) See Drawing No. 1 for location of cross section.

Figure B1 - Section 1-1 at Chainage 19 of August 2005 Lanslide Source

Table of Contents
Table of Contents
Table of Contents
Table of Contents

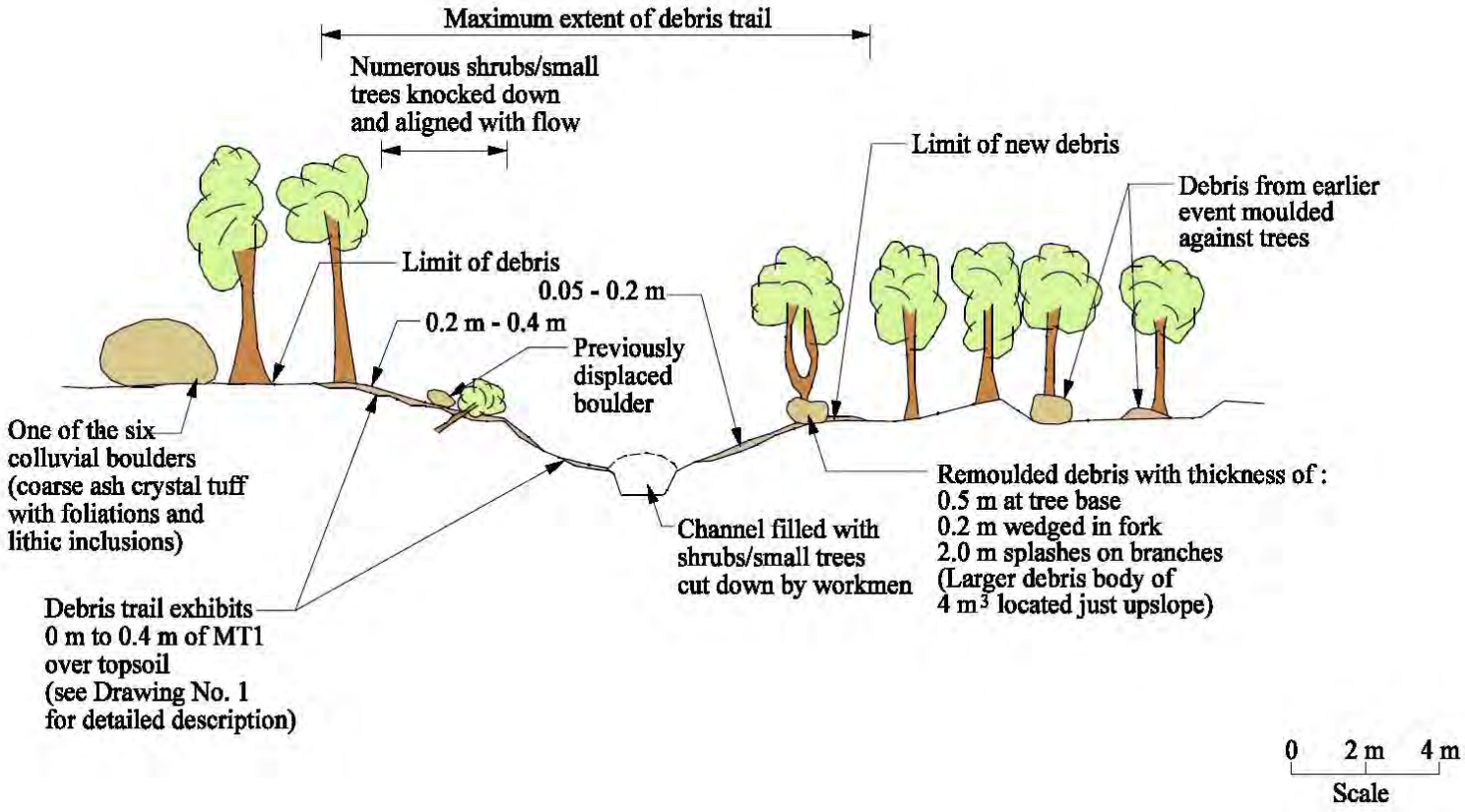

Note: See Drawing No. 1 for location of cross section.

Figure B2 - Section 2-2 at Chainage 88 of Debris Trail

Table of Contents
Table of Contents
Table of Contents
Table of Contents

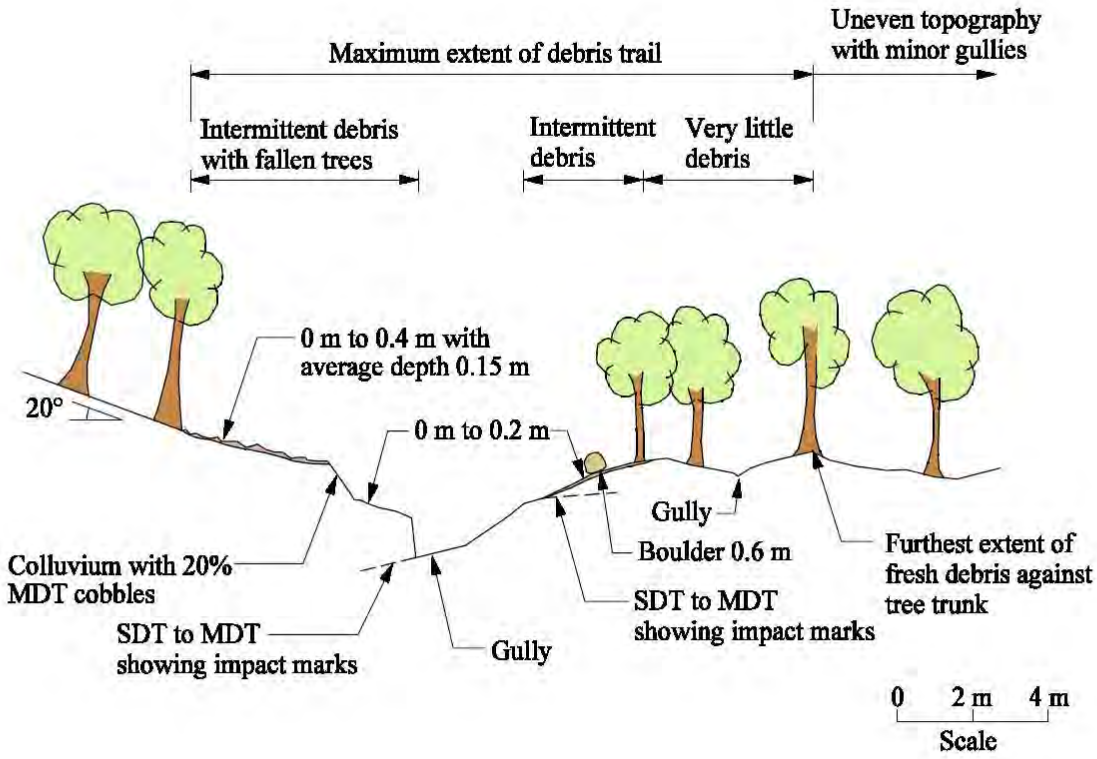

Note: See Drawing No. 1 for location of cross section.

Figure B3 - Section 3-3 at Chainage 108 of Debris Trail

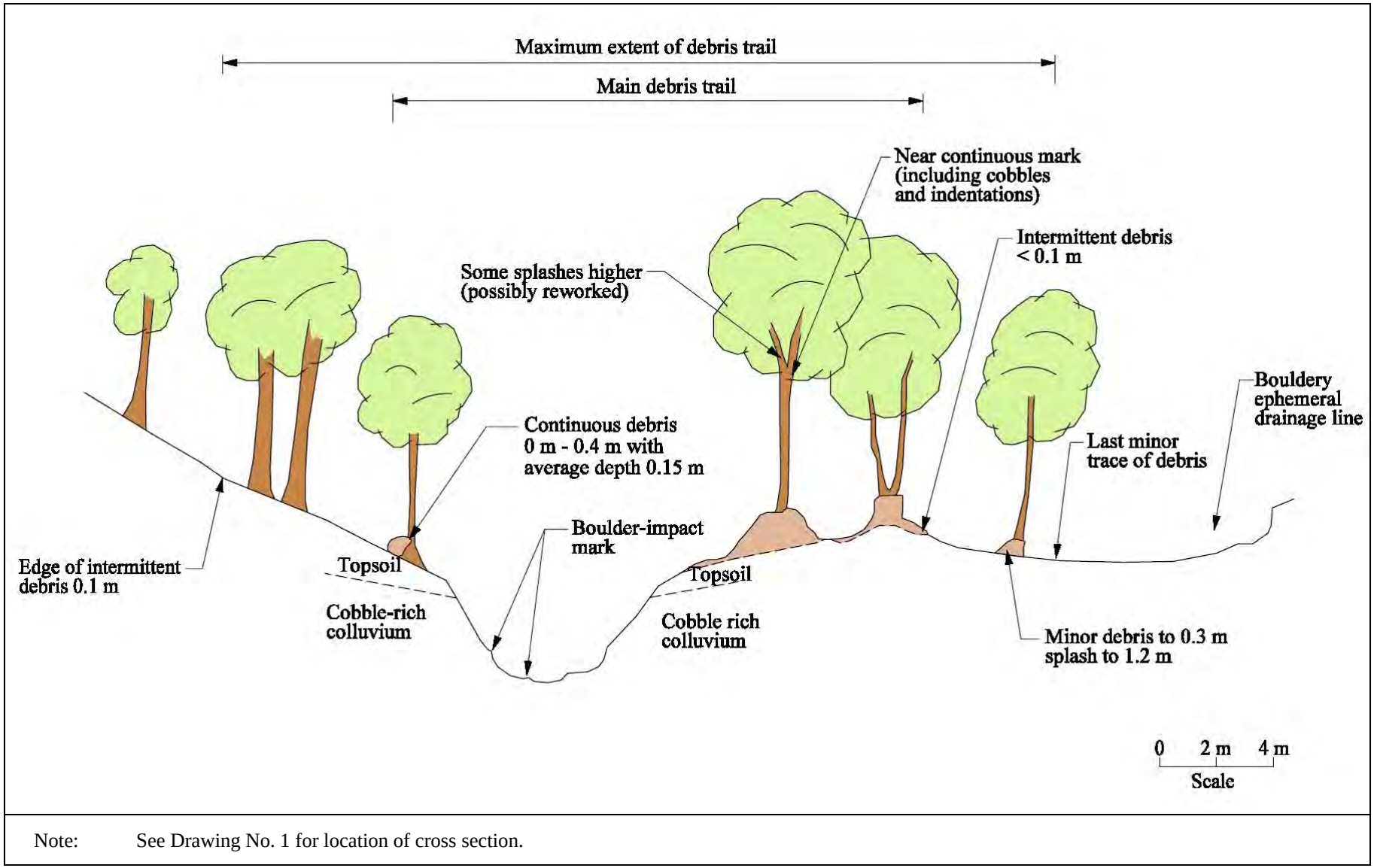

Note: See Drawing No. 1 for location of cross section.

Figure B4 - Section 4-4 at Chainage 140 of Debris Trail

Table of Contents
Table of Contents
Table of Contents
Table of Contents

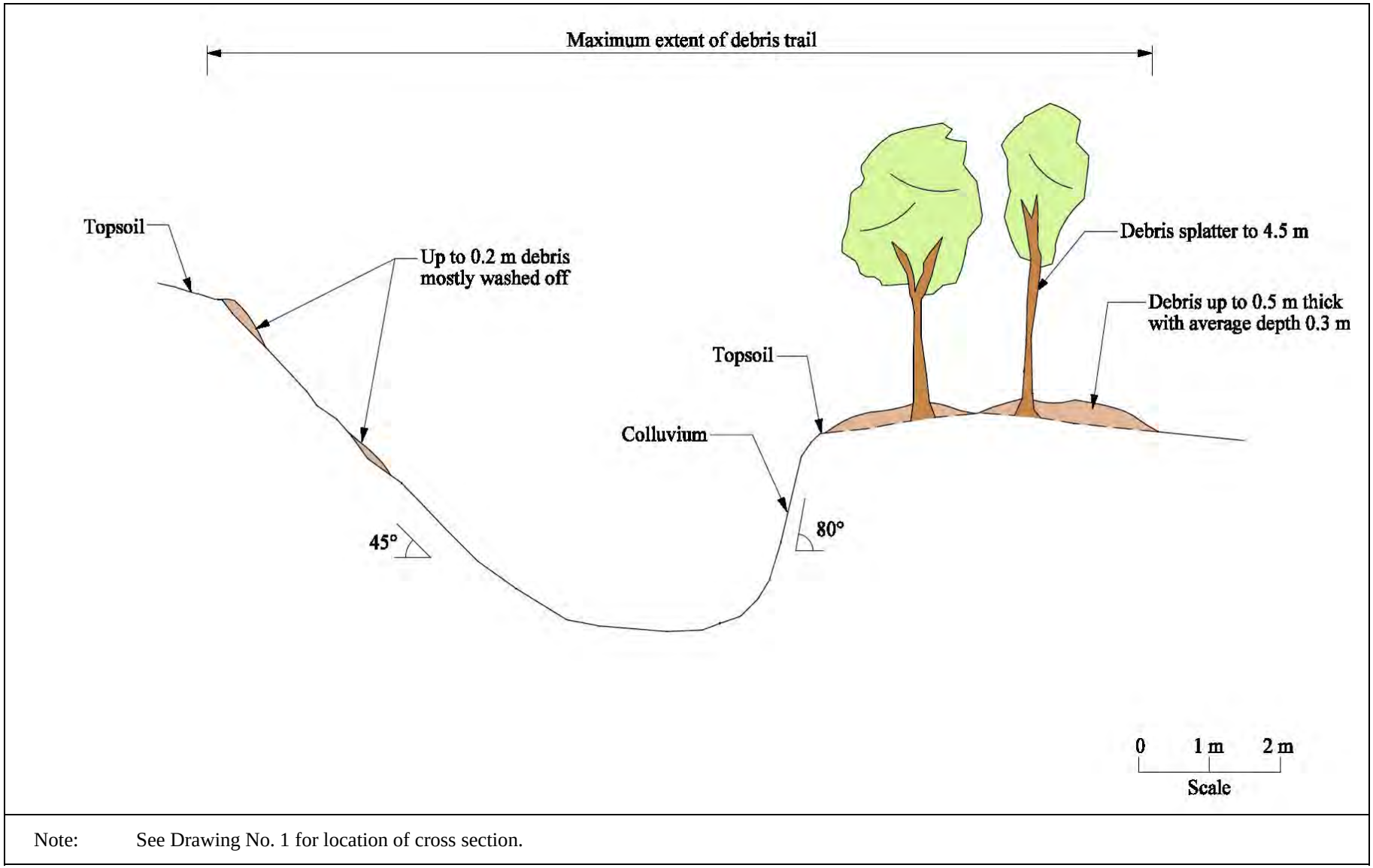

Note: See Drawing No. 1 for location of cross section.

Figure B5 - Section 5-5 at Chainage 160 of Debris Trail

Table of Contents
Table of Contents
Table of Contents
Table of Contents

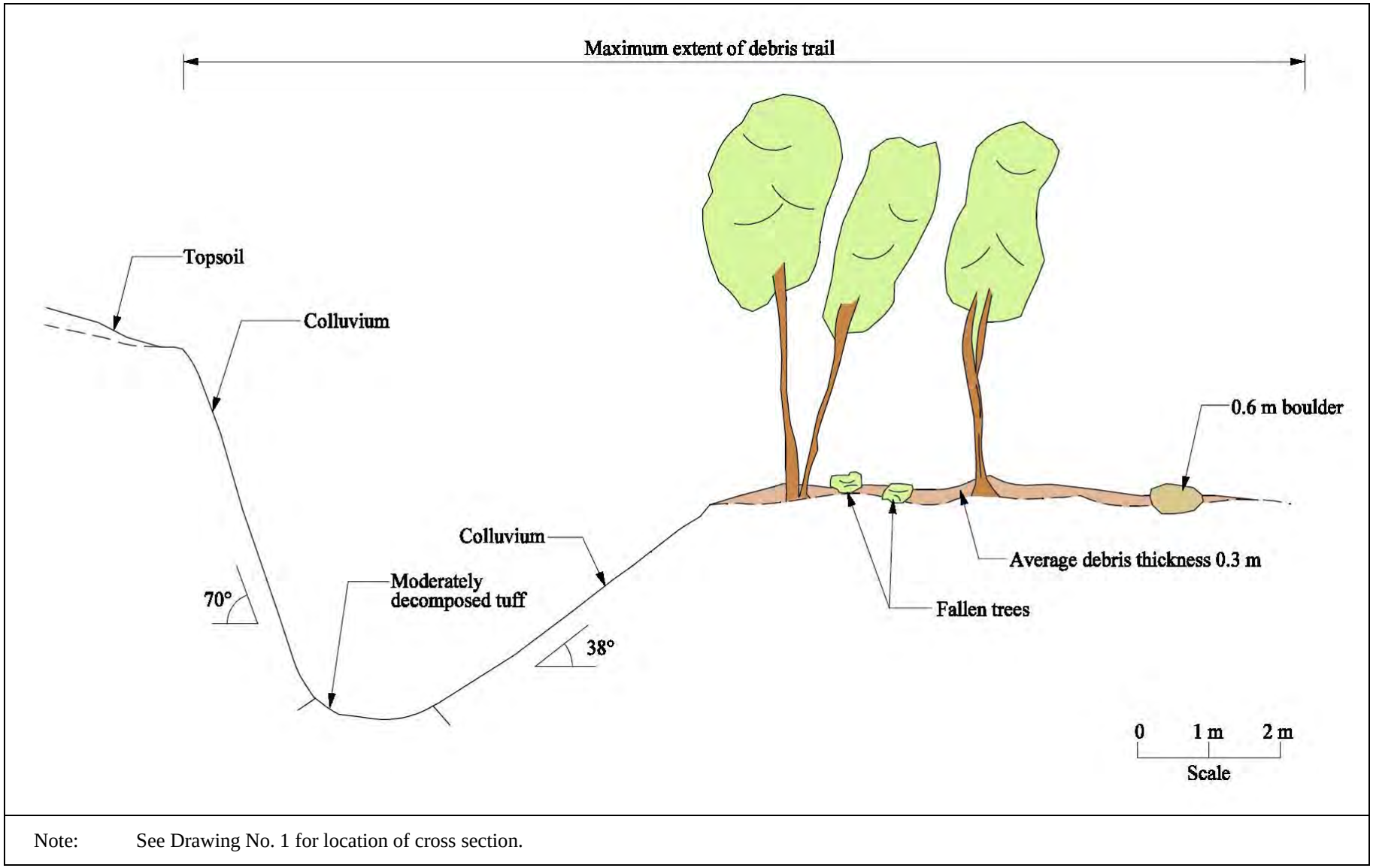

Note: See Drawing No. 1 for location of cross section.

Figure B6 - Section 6-6 at Chainage 173 of Debris Trail

Table of Contents
Table of Contents
Table of Contents
Table of Contents

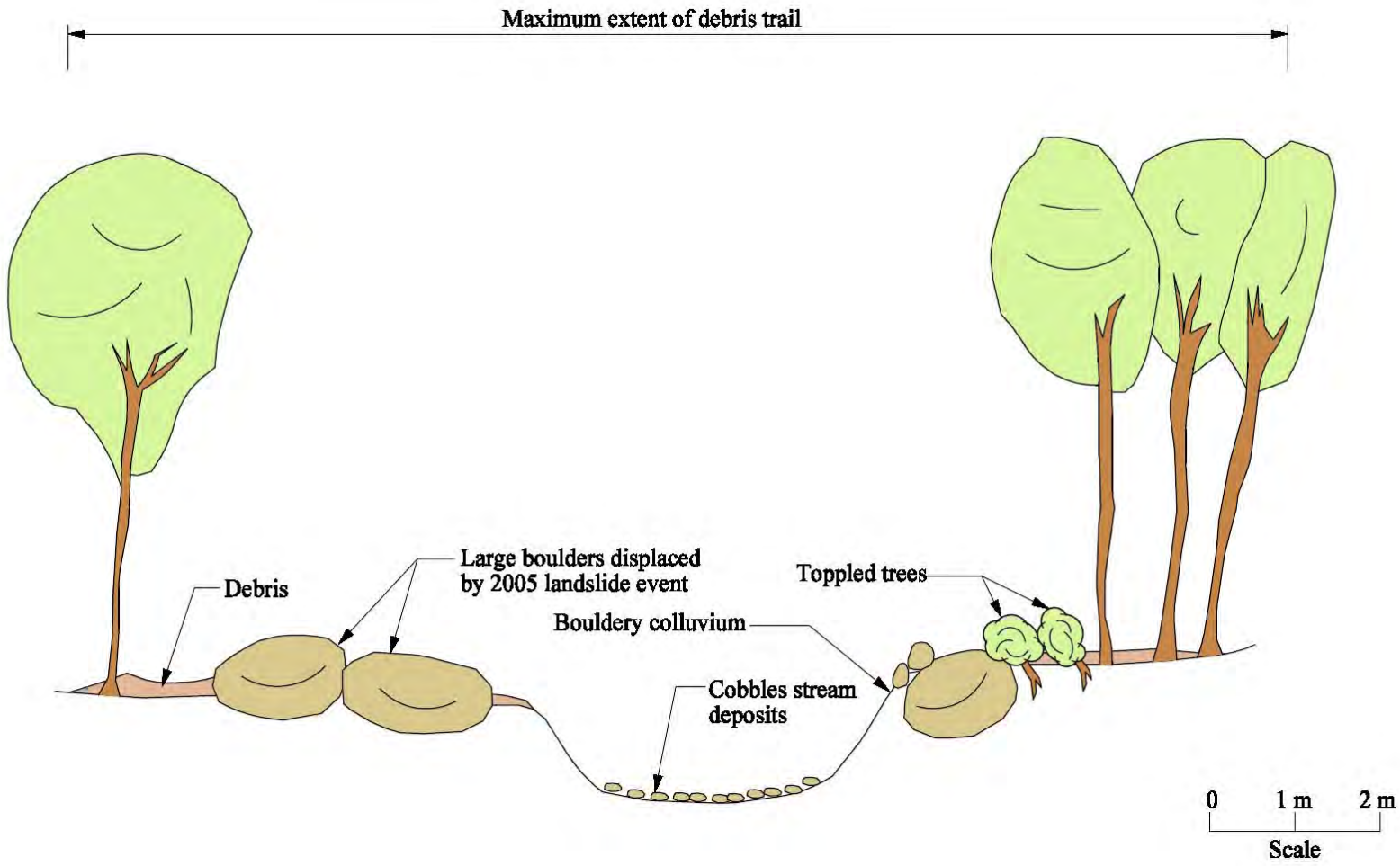

Note: See Drawing No. 1 for location of cross section.

Figure B7 - Section 7-7 at Chainage 185 of Debris Trail

Table of Contents
Table of Contents
Table of Contents
Table of Contents

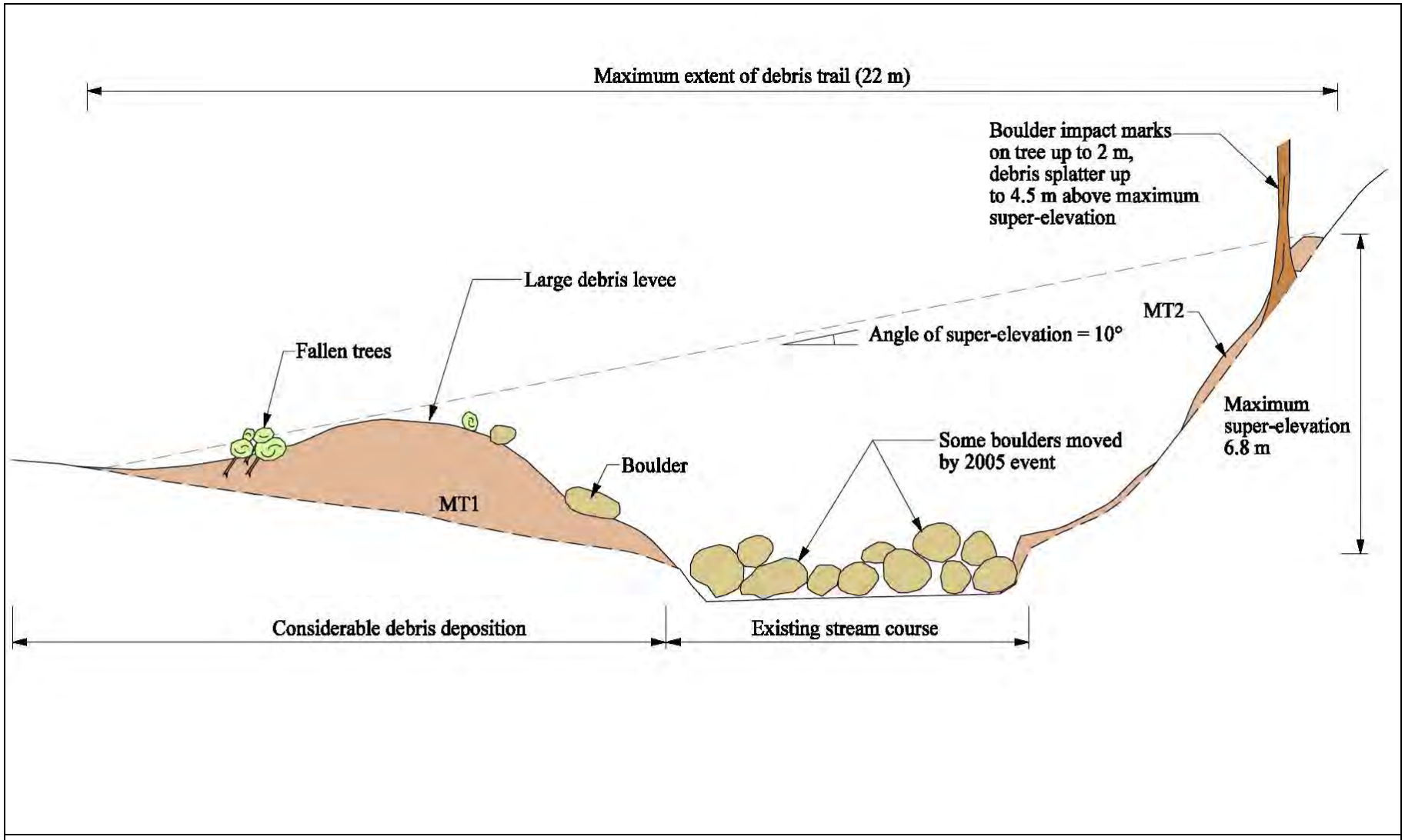

Note: See Drawing No. 1 for location of cross section and detailed description of MT1 and MT2.

Figure B8 - Section 8-8 at Chainage 220 of Debris Trail

Table of Contents
Table of Contents
Table of Contents
Table of Contents

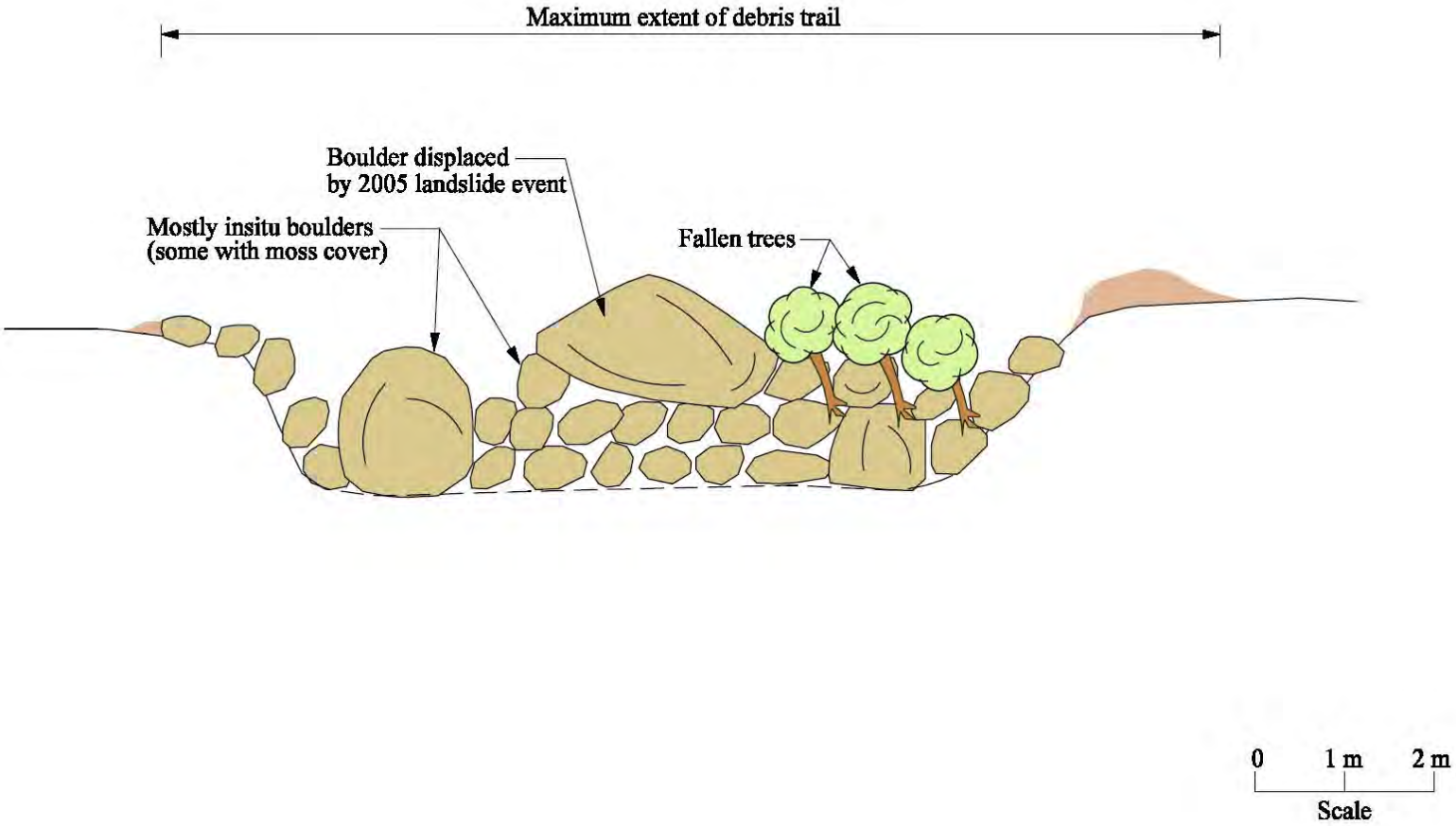

Note: See Drawing No. 1 for location of cross section.

Figure B9 - Section 9-9 at Chainage 252 of Debris Trail

Table of Contents
Table of Contents
Table of Contents
Table of Contents

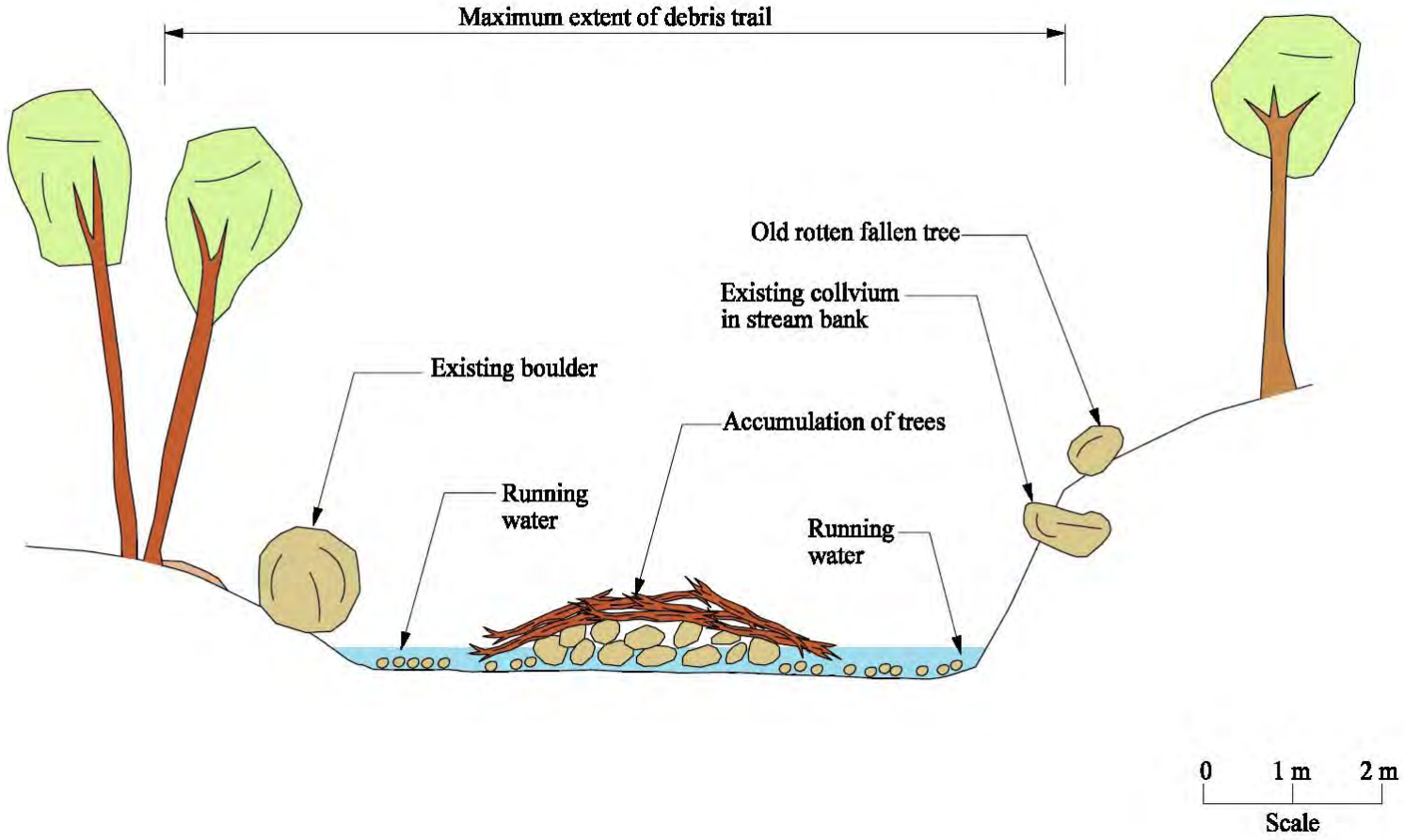

Note: See Drawing No. 1 for location of cross section.

Figure B10 - Section 10-10 at Chainage 270 of Debris Trail

Table of Contents
Table of Contents
Table of Contents
Table of Contents

APPENDIX C

GROUND INVESTIGATION INFORMATION

Table C1 - Summary of Subsurface Stratum in Drillholes

Borehole No.	Ground level (mPD)	Depth to base of material (m)					Rockhead Level (mPD)	Instrument	Depth to tip (m)
		Superficial soils			Saprolite				
		Top Soil	Young Colluvium	Old Colluvium	Grade V (CD Tuff)	Grade IV (HD Tuff)			
BH1	444.050	0.20	2.90	5.62	31.80	48.25	395.80	Double Piezometer	5.9/48.1
BH2	429.880	0.20	1.90	-	19.80	28.36	401.52	Piezometer and Standpipe	3.0/31.0
BH3	440.36	0.20	2.20	5.50	22.10	32.52	407.84	Inclinometer	37.83
BH4	454.29	0.20	2.90	4.45	30.50	33.65	420.64	Inclinometer	38.95
BH5	452.73	0.20	2.60	5.40	32.75	40.35	412.38	Double Piezometer	2.6/40.0
IBH1	459.13	0.50	4.00	-	9.55	25.10	-	None	-

Note: The base of the saprolite stratum were determined with the majority of the material fall within the grading which excluding localised corestones and small bands of more weather materials.

Table of Contents Table of Contents Table of Contents Table of Contents

Table C2 - Results of GCO Probes

GCO Probe No	GC1	GC2	GC3	GC4	GC5	GC6	GC7	GC8	GC9	GC10	GC11	GC12	GC13	GC14
Approx. ground level (mPD)	436.12	424.26	426.97	440.4	441.86	439.86	443.51	442.55	453.12	448.06	452.07	451.83	453.74	451.52
Blow Count	Depth of blow count (m)													
0 to 5 Blows	4.2	0.9	2.5	2	mixed to 4.2	0.9	1.8	-	0.9	1.8	2.4	4	1.9	2
6 to 10 Blows	4.3	2.9	3.3	4.8		4.9	4.9	5.7	4.3	5.9	mixed to 7.3	4.9	Mixed to 3.9	4.3
11 to 20 Blows	6.3	3.1	-	5.1	-	7.5	6.3	6.1	4.9	6.7		5.2		5.1
21 to 40 Blows	6.5	-	3.4	5.2	-	7.6	-	-	-	-	7.4	-	-	-
>41 Blows	-	-	-	-	-	7.7	-	6.2.	-	-	-	-	-	-
Refusal	6.74	3.19	3.42	5.24	4.29	7.77	6.39	6.35	4.97	6.8	7.44	5.22	3.98	5.18

GCO Probe No	GC15	GC16	GC17	GC18	GC19	GC20	GC21	GC22	GC23	GC24	GC25	GC26	GC27	GC28
Approx. ground level (mPD)	450.16	454.83	455.37	454.52	454.41	457.55	458.61	457.53	461.8	460.57	462.42	460.77	464.19	463.86
Blow Count	Depth of blow count (m)													
0 to 5 Blows	1.5	2.7	2	1	1.1	1.8	2.7	2.9	1.8	2.3	1.5	0.1	1.7	1
6 to 10 Blows	1.9	4.9	3.3	3.5	1.9	2.9	3.3	3.3	3.9	2.4	1.8	5.4	5.4	2.3
11 to 20 Blows	Mixed to 7.6	6.3	-	7.9	2	4	3.8	4.2	4.3	-	2.5	5.5	6.2	2.4
21 to 40 Blows		-	-	-	2.1	4.6	-	-	4.6	-	-	6	6.3	-
>41 Blows	-	-	-	-	-	-	3.9	-	-	-	-	-	-	-
Refusal	7.65	6.39	3.34	7.99	2.18	4.67	3.91	4.25	4.62	2.47	2.57	6.02	6.36	2.44

GCO Probe No	GC29	GC30	GC31	GC32	GC33	GC34	GC35	GC36	GC37	GC38	GC39	GC40	GC41	GC41
Approx. ground level (mPD)	463.12	446.38	468.46	464.85	463.21	442.37	441.86	456.27	445.88	452.17	442.21	454.26	466.28	443.61
Blow Count	Depth of blow count (m)													
0 to 5 Blows	0.9	0.5	0.8	2.3	2.7	2.2	0.1	0.5	2	1.6	2.1	2.8	1.1	3.5
6 to 10 Blows	2	0.6	1.7	4.5	Mixed to 5.7	4.8	3.9	3.2	4.6	4.7	3	3.4	3.9	4.6
11 to 20 Blows	-	1	2.3	4.6		5.5	4.1	3.5	4.7	5.8	4.2	3.6	4.1	4.7
21 to 40 Blows	-	1.1	2.4	4.8	5.8	-	-	-	-	-	4.4	3.8	-	-
>41 Blows	-	1.3	-	-	-	-	-	-	-	-	-	-	-	-
Refusal	2.07	1.35	2.48	4.86	5.97	5.78	4.18	3.59	4.75	5.95	4.45	3.82	4.18	4.72

Note: The depth of blow count was selected with the majority of the reading fall within the range and exclude localised abrupt changes

Table of Contents
Table of Contents
Table of Contents

Trail Pit No. TP1 Logged by : MD Date : 26 & 19 May 2006

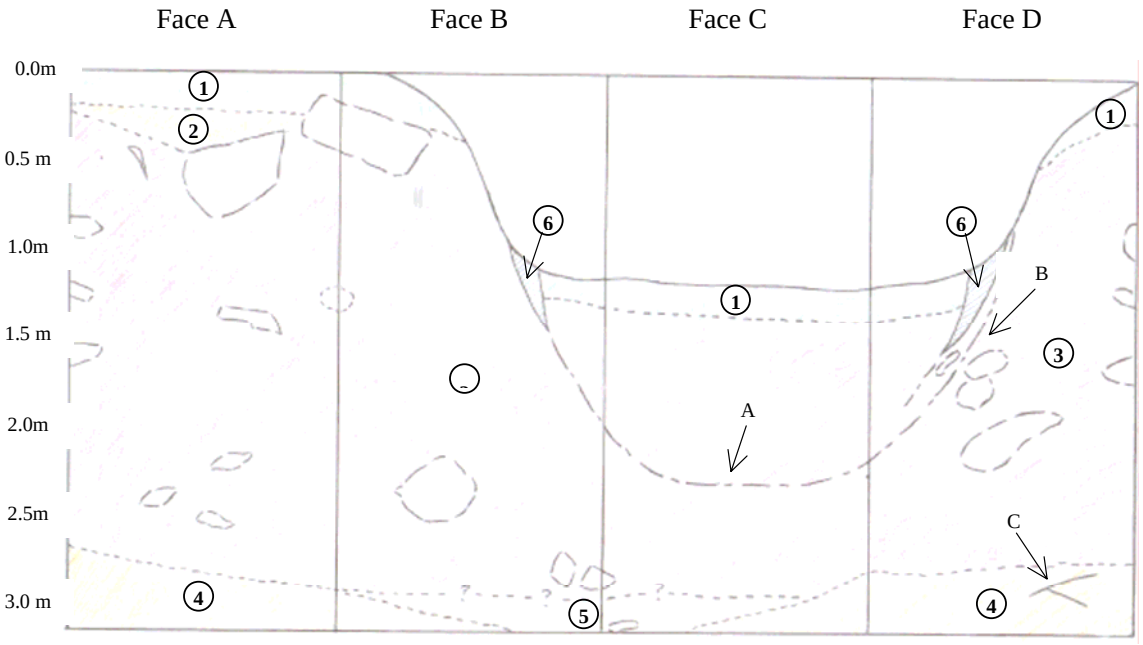

Notes:
A - becoming very soft
B - tension crack opened up to 8 mm between angular cobbles of tuff, roots along opening
C - sheared surface 12°/005° with up to 4 mm of brown clay infill

Descriptions

1. Soft to firm, dark brown to dark greenish brown sandy SILT/CLAY, with occasional angular to sub rounded cobbles and occasional sub angular boulders of moderately decomposed coarse ash crystal tuff and abundant roots [Top Soil]
2. Firm, light brown to greenish brown sandy SILT/CLAY with some coarse gravel to occasional angular cobbles of moderately decomposed tuff [Young Colluvium
3. Firm, reddish brown, moist slightly sandy silty CLAY with occasional to some angular cobbles and boulders of tuff up to 0.5 m × 0.3 m × 1 m in size [Young Colluvium]
4. Firm to stiff, grey and greyish brown mottled reddish brown sandy SILT/CLAY [Extremely weak, completely decomposed Coarse Ash Tuff] with closely spaced relict joints infilled with white clay (kaolin) up to 5 mm wide and coated with manganese (manganese slickensided) [CDT]
5. Firm to stiff, greyish brown mottled reddish brown coarse sandy SILT/CLAY with occasional angular cobbles of light grey moderately decomposed tuff [Old Colluvium/Disturbed CDT]
6. Loose dark brown clayey/silty sand to soft to firm dark brown sandy silty CLAY with abundant roots and fallen leaves [Tension Crack Infill] - placed April 2006.

Figure C1 - Trail Pit Record for TP 1

Table of Contents
Table of Contents
Table of Contents
Table of Contents
Table of Contents

Trail Pit No. TP2 Logged by : MD Date : 29 May 2006

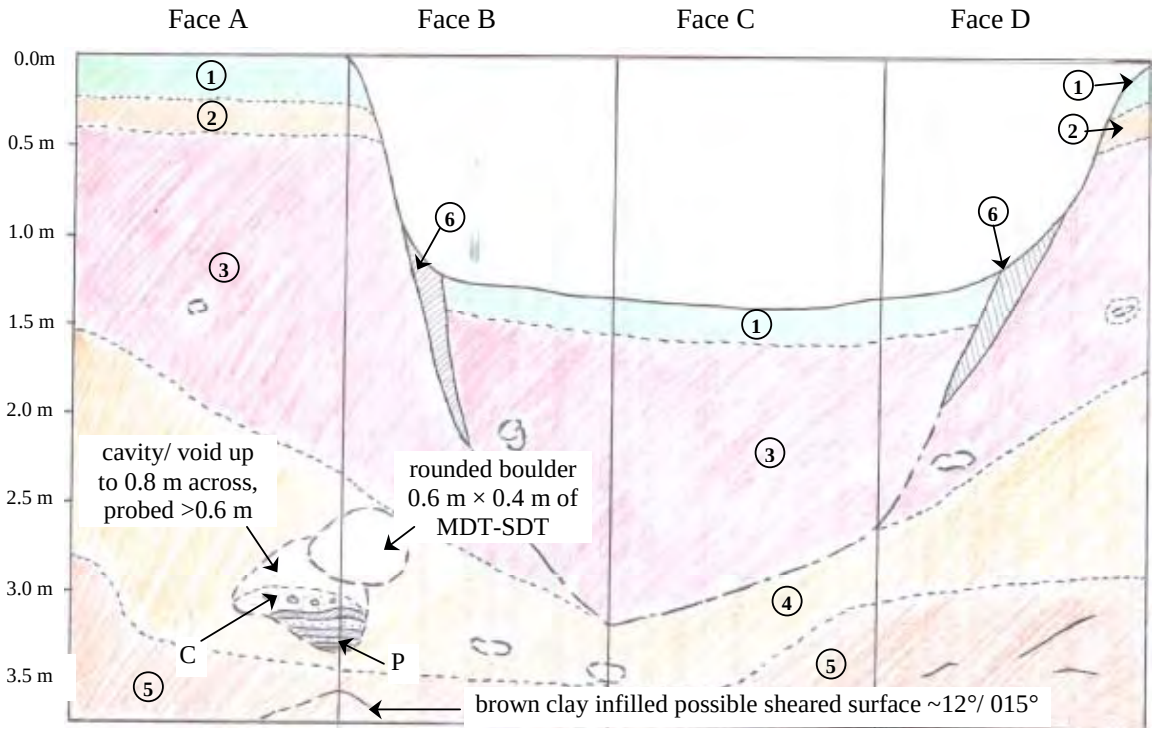

Notes: P - Alternate sand and clay bands [Pipe Deposit]
(loose, moist, grey to greyish brown fine to medium SAND with much subrounded to rounded gravel of quartz and occasional angular medium gravel size moderately decomposed tuff)
(very soft to soft, moist reddish brown CLAY up to 30 mm thick)
C - Soft reddish brown sandy CLAY with occasional angular cobbles of black stained moderately decomposed tuff.

Descriptions

(1) Soft to firm, dark brown to dark greenish brown sandy SILT/CLAY, with occasional angular to sub-rounded cobbles and occasional sub angular boulders of moderately decomposed coarse ash crystal tuff and abundant roots [Top Soil]

(2) Firm, light brown to light greenish brown sandy SILT/CLAY with occasional angular cobbles of moderately decomposed tuff [Young Colluvium]

(3) Soft to firm, reddish brown, slightly sandy silty CLAY with occasional subangular to subrounded gravel to boulder [up to 0.6 m x 0.4 m] moderately decomposed coarse ash crystal tuff. (some cobbles notably have a purple outer weathered band/ halo) occasional roots [Young Colluvium]

(4) As (3) above but appears lighter reddish brown to brown possible disturbed completely decomposed tuff/ Old Colluvium

(5) Firm to stiff, greyish brown to occasionally grey mottled reddish brown, sandy silty Clay with occasional angular gravel of quartz [completely decomposed Coarse Ash Crystal Tuff with relict joints infilled up to 6mm wide with white kaolin and coated with manganese (slickensided) [Possibly disturbed CDT]

(6) Loose dark brown clayey/silty SAND with abundant roots and fallen leaves [Tension Crack Infill] - placed April 2006

Figure C2 - Trail Pit Record for TP 2

Table of Contents Table of Contents Table of Contents Table of Contents Table of Contents

Trail Pit No. TP8 Logged by : MD Date : 7 June 2006

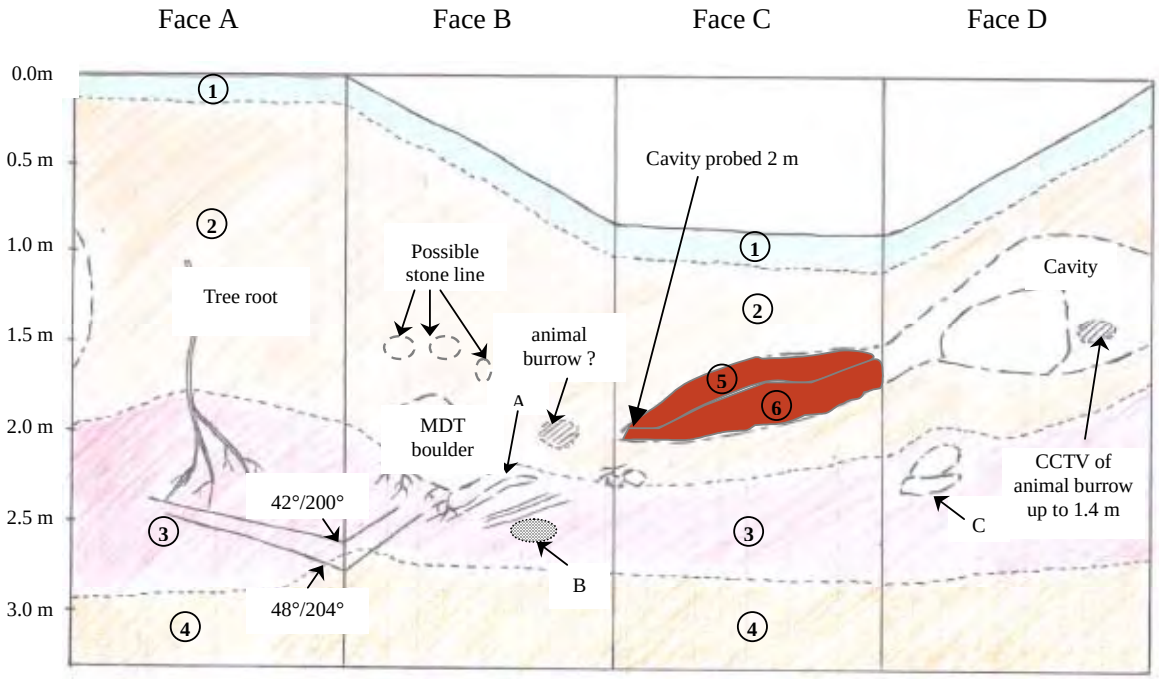

Notes:
A - veins appear to bend towards boundary with Young Colluvium
B - box work of kaolin veins
C - joint surface with orientation 50°/258°, slickenside on joint surface at 40°/305°

Descriptions

1. Soft to firm, dark brown to dark greenish brown sandy SILT/CLAY, with occasional angular to sub rounded cobbles and occasional sub angular boulders of moderately decomposed coarse ash crystal tuff and abundant roots [Top Soil].

2. Firm, reddish brown, moist slightly sandy clayey SILT with occasional to some angular cobbles and boulders of tuff up to 0.5 m × 0.3 m × 1 m in size [Young Colluvium]

3. Firm to stiff, greyish brown mottled reddish brown coarse sandy SILT/CLAY with occasional angular cobbles of light grey moderately decomposed tuff with several discontinuities kaolin infilled and manganese coated relict joints some localized 'box work' veining of kaolin [Old Colluvium]

4. Firm to stiff, grey and greyish brown mottled reddish brown, sandy SILT/ CLAY [Extremely weak, completely decomposed Coarse Ash Crystal Tuff] with closely spaced relict joints infilled with white kaolin up to 5mm wide and coated with manganese (slickensided) [CDT]

5. Soft to firm, reddish brown slightly sandy silty CLAY

6. Loose, light reddish brown clayey silty medium to coarse SAND

Figure C3 - Trail Pit Record for TP 8

Table of Contents
Table of Contents
Table of Contents
Table of Contents
Table of Contents

Trail Pit No. TP10 Logged by : MD Date : 20 June 2006

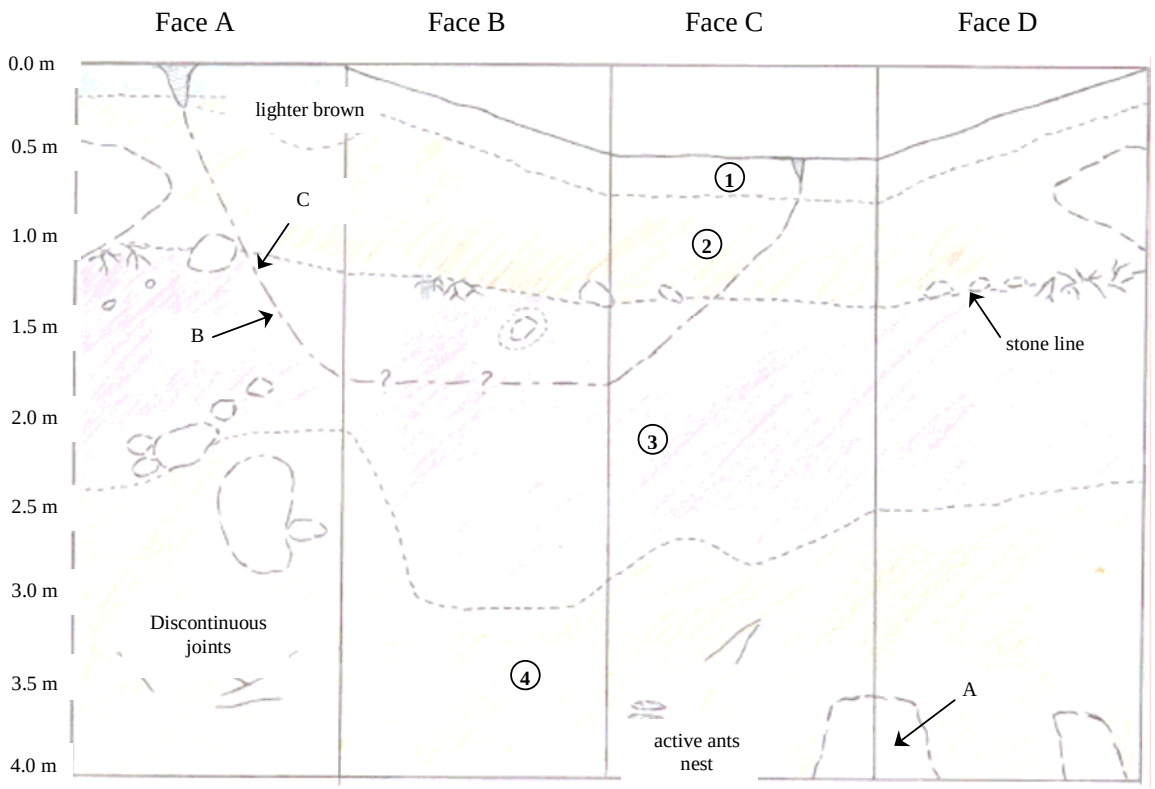

Notes:
A - boulders of MDT/ disturbed corestone
B - 30 mm to 40 mm across brown sandy SILT/CLAY infill
C - 3 mm wide light brown clay

Descriptions

(1) Top Soil with roots and occasional cobbles and boulders.

(2) Soft to very soft, light reddish brown to light brown gravelly silty CLAY with some cobbles and occasional boulders up to 0.7 m × 0.6 m × 0.4 m of coarse ash crystal tuff and many roots near base of material [Landslide Debris]

(3) Soft to firm, reddish brown sandy silty CLAY to SILT/ CLAY with occasional cobbles, boulders of tuff and occasional roots [Young Colluvium/ Older Landslide Debris]

(4) Firm to stiff, light reddish brown to occasionally dark reddish brown with light brown patches sandy gravelly clayey SILT with occasional subangular cobbles and angular boulders of highly to moderately decomposed coarse ash tuff [Disturbed CDT/ Residual Colluvium ?] several kaolin and manganese infilled discontinuities with low persistence (i.e. none are continuous) may be relict joints from boulders in colluvium or truncated due to disturbance of CDT, very few roots

Figure C4 - Trail Pit Record for TP 10

Table of Contents
Table of Contents
Table of Contents
Table of Contents

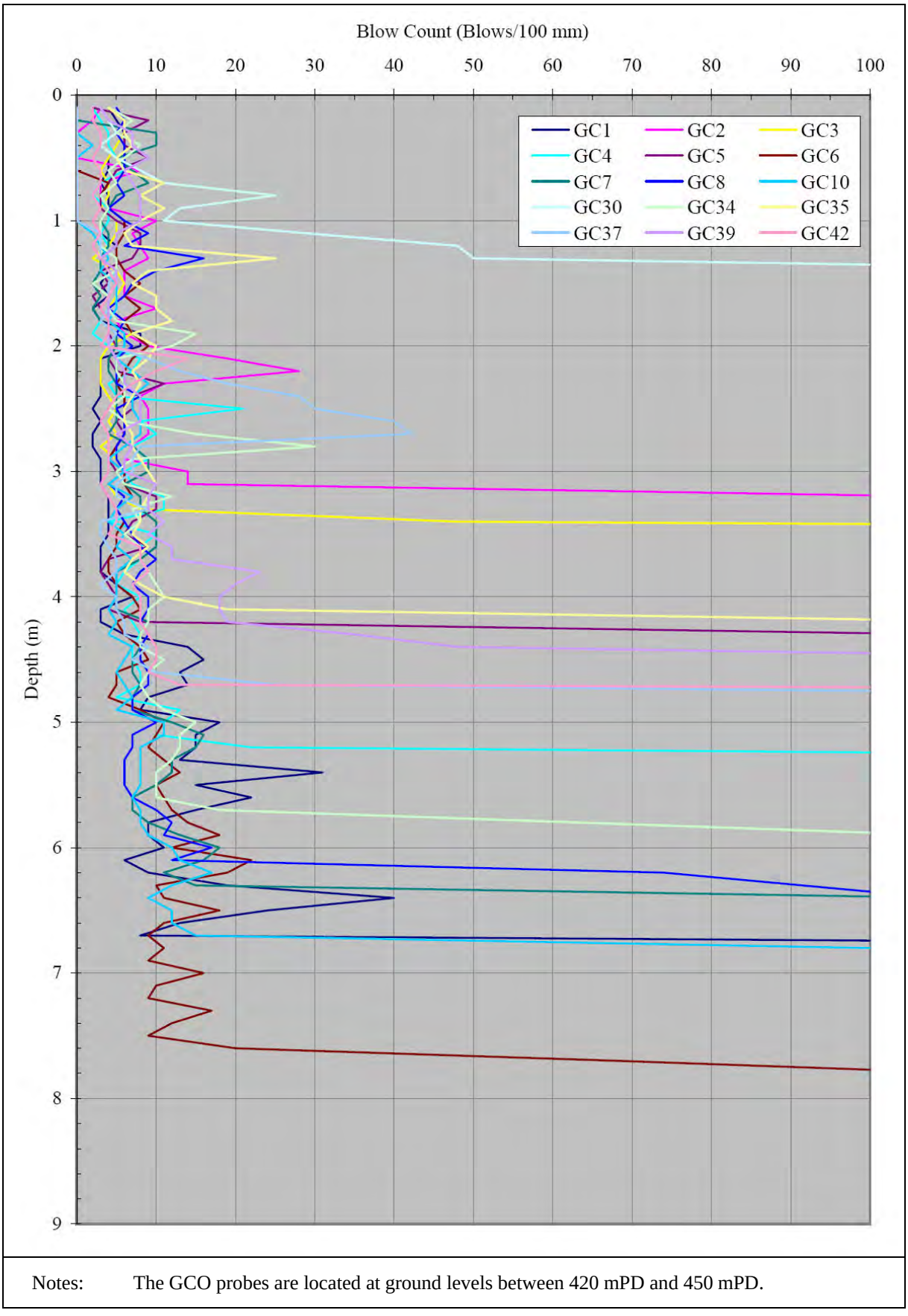

Notes: The GCO probes are located at ground levels between 420 mPD and 450 mPD.

Figure C5 - GCO Probe vs Depth at Lower Portion of Distressed Hillside

Table of Contents
Table of Contents
Table of Contents
Table of Contents

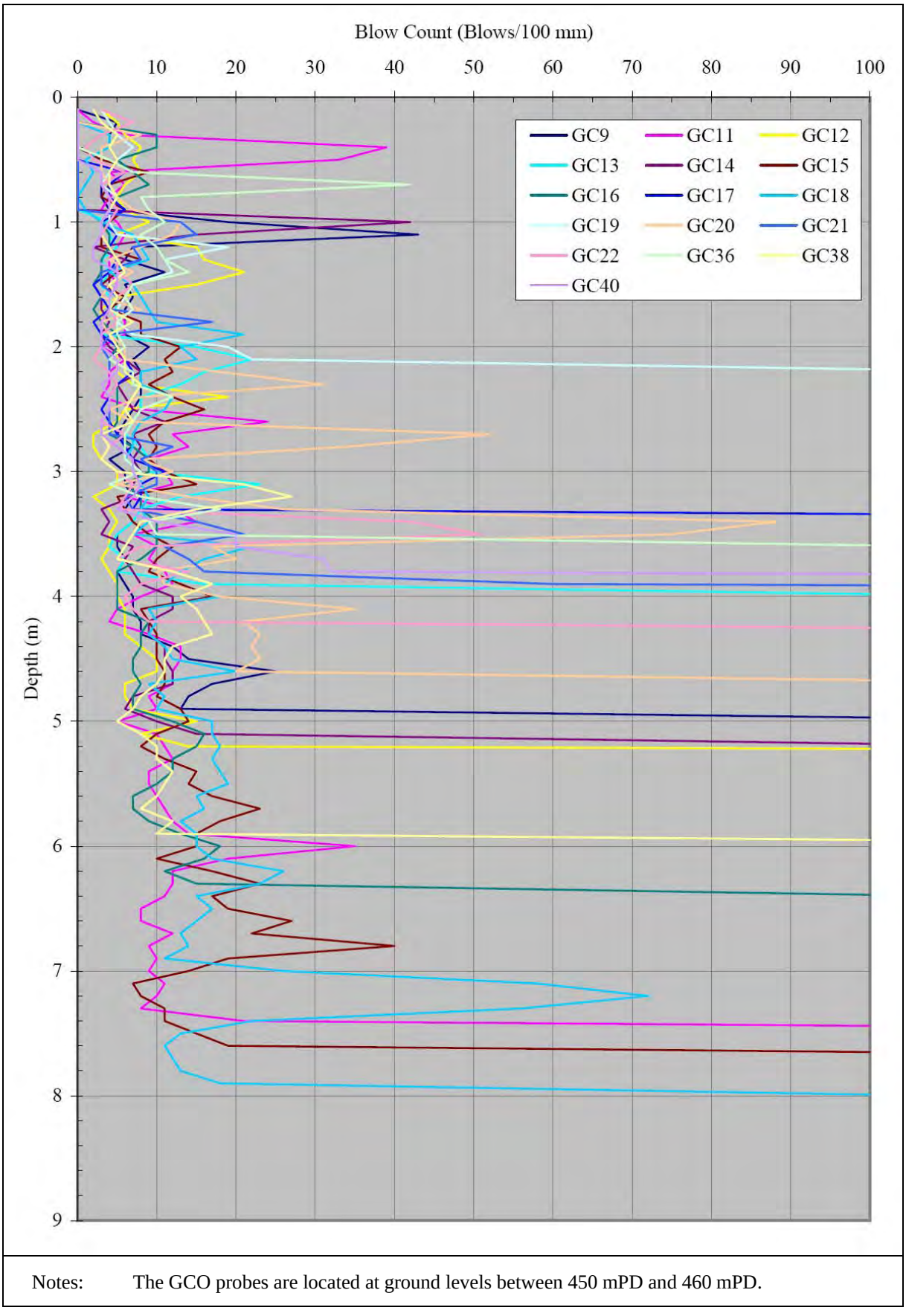

Notes: The GCO probes are located at ground levels between 450 mPD and 460 mPD.

Figure C6 - GCO Probe vs Depth at Middle Portion of Distressed Hillside

Table of Contents
Table of Contents
Table of Contents
Table of Contents

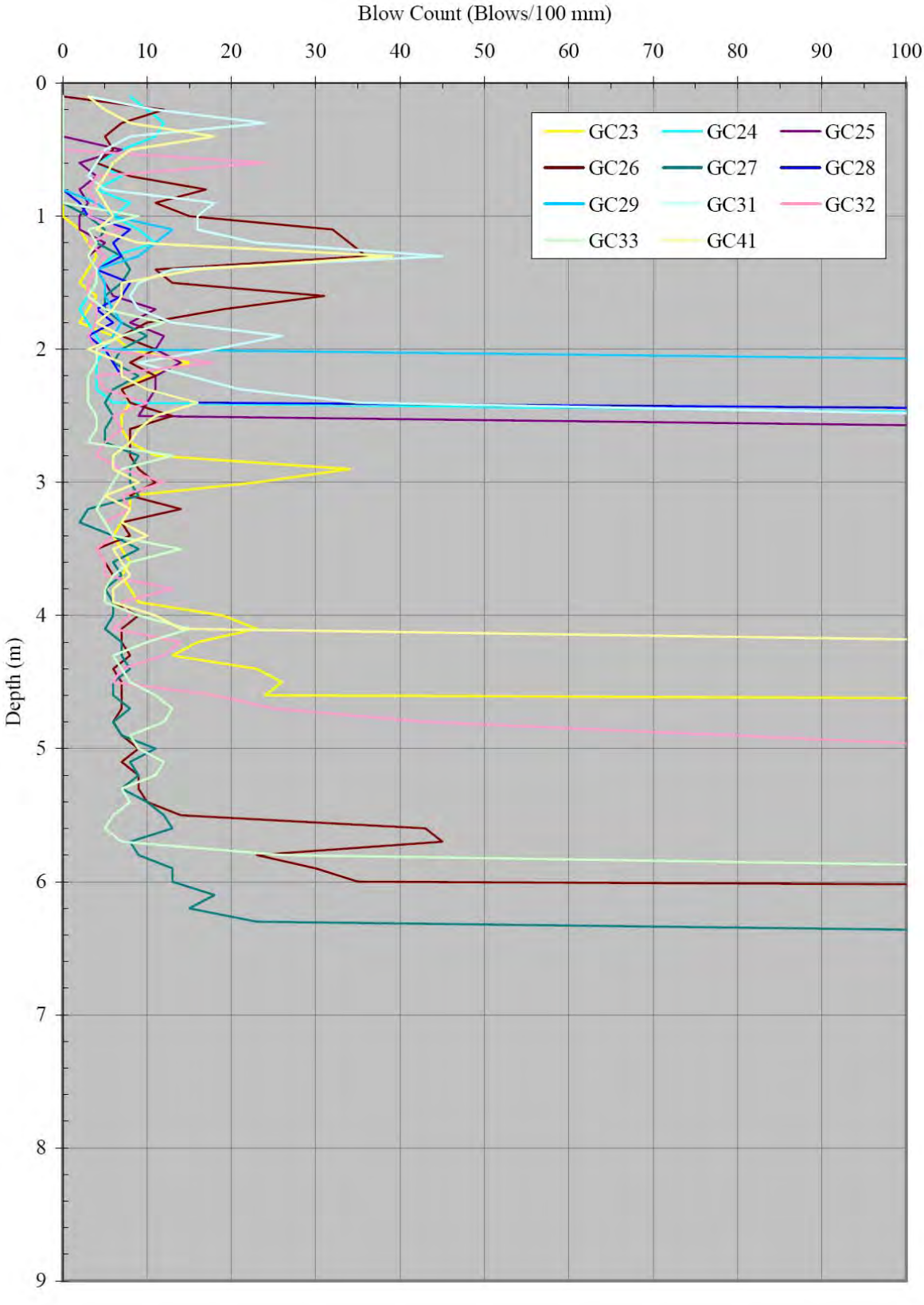

Notes: The GCO probes are located at ground levels between 460 mPD and 470 mPD.

Figure C7 - GCO Probe vs Depth at Upper Portion of Distressed Hillside

Table of Contents
Table of Contents
Table of Contents
Table of Contents

LIST OF DRAWINGS

Drawing No.	
1	Detailed Field Mapping of the August 2005 Landslide
2	Detailed Field Mapping of the Distressed Hillside

Table of Contents
Table of Contents
Table of Contents
Table of Contents

N

824100 E

824700 N

824600 N

824500 N

Boulder filled streamcourse

Lower boulder dam

Several boulders appear not to have been displaced by 2005 event

Upper boulder dam

Ephemeral streamcourse

Dense woodland

Approx. 280 m^3 debris between CH 188 and CH 230 mostly deposited in up to 1.5 thick debris levee

Approx. 100 m^3 debris deposited between CH 118 and CH 188

~ 5 m^3 sandy SILT/CLAY

Many trees mostly over 100 mm trunk diameter

Deposition of many trees in streamcourse

Boulders of feldsparphyric rhyolite

Old rotten fallen tree possibly from earlier event

Older buried trees (possibly from earlier debris flow event)

Debris thickness 0.3 m to 0.4 m

Boulders displaced by 2005 landslide

2 m high boulder choke

250 mm diameter 25 m long fallen tree

Levee of debris up to 1.5 m thick predominantly fines 50 % - 60 % with up to 40 % cobbles and boulders, some boulders up to 2 m across

Maximum super-elevation of 6.8 m

Boulders moved by 2005 landslide

Two insitu large trees 300 mm to 400 mm diameter. Debris splatter to 4.5 m, bark scraped off for lower 2m

Entrained material up to 20 m^3 (may be post-2005 landslide collaspe)

Existing boulder up to 4 m across

A very thin (< 0.1 m thick) drape of debris

Bouldery deposit with many trees

Minor entrainment ~ 1 m^3 of highly decomposed tuff

Rock exposed in stream bed

Accumulation of fallen trees over 1 m thick with trees up to 100 mm trunk diameter

Start of sinuous streamcourse

Large fallen tree (approx. 300 mm diameter)

2.5 m diameter circular hole with 2 -3 m^3 debris

Average debris thickness 0.3 m

Rock (coarse ash crystal tuff) exposed in base of drainage line

Debris splatter on trees up to 4.5 m above ground

Abraded existing soil surface

Average debris thickness 0.2 m

Trees cut as part of 2005 emergency works by AFCD dumped in gully

Gully washed through debris

Debris splatter marks on tree up to 1.5 m above ground

Sharp convex break-in-slope

Existing MacLehose Trail

Debris levee up to 0.5 m thick

Rock joint (60°/314)

Reconstructed MacLehose Trail

Boulders moved by 2005 landslide

Ephemeral drainage line

Average debris thickness 0.4 m

Bouldery colluvium exposed in 1963 landslide scar

The source area of the August 2005 landslide was covered with erosion control mat as part of the urgent repair works by AFCD and only part of the source area was exposed and mapped

Water pipe (30 mm to 50 mm diameter plastic pipe)

Intact rafts

Limits of 2005 scar

MT1a MT1b MT2 MT4 MT5 MT6 MT7 MT8 MT9

340 360 380 400 420 440

Legend :

- Erosion / Depletion erosion > 0.1 m
- Transportation abraded original ground with removal of vegetation, minor erosion
- Deposition of landslide debris (boulders, cobbles, silt, sand and trees)
- Existing streamcourse
- Existing streamcourse with constant flow of water
- Ephemeral drainage line
- Streamcourse
- —30 Chainage from erosion of landslide
- 34° Slope angle
- Fallen tree
- Convex break-in-slope
- Concave break-in-slope
- Boulder
- Boundary of landslide scar / debris trail
- Erosion scarp
- 7_1 survey marker

no.	date	description	chk.	appr.
REVISION				

	name	date
surveyed		
designed	MD	8/2006
drawn	ATCL	8/2006
traced		
checked		
examined		
contract no.		
file no.		
job no.		

project

Detailed Study of the 22 August 2005 Landslide and Distress on the Natural Hillside at Kwun Yam Shan, below Tate's Ridge

drawing title

Detailed Field Mapping of the August 2005 Landslide

drawing no.

DRAWING NO. 1

scale

1 : 400

office

LANDSLIP PREVENTATIVE MEASURES DIVISION 1
GEOTECHNICAL ENGINEERING OFFICE

CIVIL ENGINEERING AND DEVELOPMENT DEPARTMENT
HONG KONG

Material Types (MT)

Material Eroded

MT1a 'YOUNG COLLUVIUM'
Soft reddish brown and orangish brown slightly sandy SILT/CLAY with some to many subangular to subrounded cobbles and boulders of highly to moderately decomposed coarse ash crystal tuff with abundant roots

MT1b 'OLD COLLUVIUM'
Soft to firm light olive locally mottled reddish brown slightly sandy SILT/CLAY with few cobbles and boulders of weak to extremely weak completely decomposed tuff

MT2 'COMPLETELY DECOMPOSED TUFF'
Extremely weak, moist light yellowish brown to reddish brown completely decomposed tuff (sandy clayey SILT) with very closely spaced rough undulating occasionally planar white clay (Kaolin) infilled and black manganese coated up to 20 mm thick

MT3 'HIGHLY DECOMPOSED TUFF'
Weak to moderately weak, reddish brown to light greenish grey highly decomposed coarse ash crystal tuff (stiff, clayey sandy SILT)

MT4 'TUFF BEDROCK'
Moderately strong to strong, dark greenish grey (often with light brown weathered patina), moderately decomposed to slightly decomposed, coarse ash crystal tuff, with medium to widely spaced steeply dipping joints

MT5 'STREAM DEPOSITS (FINE)'
Medium dense to dense, greenish grey to occassionally reddish brown silty, sandy GRAVEL with many rounded cobbles and some boulders (occassional cobbles and boulders)

MT6 'STREAM DEPOSITS (COARSE)'
Loose BOULDERS with much gravel and many cobbles of coarse ash crystal tuff (occassional to some cobbles and boulders from 2005 event)

Material Deposited

MT7 'FINE DEBRIS' (less than 0.1 m thick in areas of mostly transport)
Soft, light reddish brown, sandy SILT/CLAY with occassional cobbles. Existing surface exposed in several planes showing brown TOPSOIL stripped of vegetation although many roots remain

MT8 'REMOULDED' (Matrix supported) DEBRIS
Soft to firm, reddish brown, sandy clayey SILT with much gravel and many sub-angular cobbles and boulders of coarse ash crystal tuff

MT9 ' CLASTIC DEBRIS' (Clast supported debris)
Greenish grey occasionally reddish brown BOULDERS with many cobbles and much sandy gravel occassionally silty sand

840050 E

840100 E

824450 N

824400 N

MacLehose Trail

Recent landslide 1963

Water pipe (30 mm to 50 mm plastic pipe)

Scar from mobilised material

28°

One very large boulder split in three (5 m x 3 m)

Eastern gully

Recent fallen boulder

Surface soil movement

Soakaway

Fallen tree

Step

Boulder showing movement

30°

2005 landslide source area (See Drawing No. 1 for detail)

20°

Seepage

Soakaway

38° - 40°

Cluster of boulders

Boulders rest against tree

Soil pushed towards gulley

15°

18°

Concave break

60°

42°

54°

Large boulders 2.5 - 3 m across

30°

Boulder showing movement with 80 mm wide gap on downslope side

Toppled tree

Cavity

Boulders appear to have moved (2005 ?)

Boulder fallen into cavity

Tension crack soil movement towards gully

Fallen tree (may indicate headward erosion)

Boulders showing movement

Generally less boulders on surface

Detached masses remaining in source

40°

32°

Western gully

Soil movement towards gullies

Boulders at end of gully

A 1.1 m long portion of tension crack opened up with 150 mm aperture

Soil movement towards gully

Boulder showing movement

Boulders showing movement

Tree growth around boulder

Large cavity collapse feature

Generally less boulders

Larger tree split by tension crack

8°

Boulder showing movement

Flat lying hollow

Several leaning trees

Cavity (0.4 m x 0.4 m)

12°

Boulders up to 1.5 m diameter strewn along toe of concave break-in-slope

Boulder filled soakaway with collapse

Small tree split by tension crack

34°

Crack Scarp

Tension crack with 50 mm dia. root broken across crack

35°

20°

Step

Step

Step

Cavity (probed 2 m)

Animal burrow probed 1.4 m

0.5 m size cavity/collapse feature

200 mm step (possible wartime track)

Portion of main scarp with weathered patina indicating open for some time

0.75 m size cavity/collapse feature

Animal burrow probed 1.0 m (observed in Trial pit No. TP8)

Concave break-in-slope

Possible wartime tunnel (CCTV in tunnel revealed larger cavity below)

Possible wartime tunnel

Collasped feature

M1

Wartime military trench

1 : 100

2 : 1 Vertical exaggeration

1 : 200

(m)

0.2 m dia. boulder

1.2 m dia boulder of coarse ash crystal tuff with "onion layer" weathering (exfoliation)

MT1

MT2

GC

Void below boulder

Soil surface has a green algal cover and appears to have a weathered patina (possibly open for for some time)

Ephemeral drainage line

Less cobbles

1.5 m dia .boulder of moderately decomposed crystal tuff with lithics

0 2 4 6 8 10 12 14 16 18 20 22 24 26 28 30 32 (m)

Main Tension Crack - Southern Scarp

(m)

Tree 150 mm dia.

Tree 80 - 100mm dia.

200 mm dia. hole behind (probed > 1 m)

Trial pit TP2

Tree 500 mm dia.

200 mm dia. hole (depth > 1m)

Boulders (approx. 0.5 m across)

42°/341

Northern end of open tension crack

Light greenish brown

Boulder 0.5 m x 0.5 m

12°

MT1

MT2

MT3

GC13

GC17

Slip surface

Tree roots

200 mm dia. former insect nest

Slip surface 53°/331

Less cobbles in this portion

60 mm dia. hole (probed 100 mm)

30 mm dia. hole (probed 400 mm)

GC9

Soft to firm, grey to greenish grey spotted black completely decomposed tuff

Moderately decomposed tuff with dark reddish brown weathered band

Hole 60 mm x 50 mm (probed 150 mm) sandy deposit at base may indicate water flow

1 : 100

2 : 1 Vertical exaggeration

1 : 200

0 2 4 6 8 10 12 14 16 18 20 22 24 26 28 30 32 (m)

Main Scarp - East Flank

Legend :

- The August 2005 landslide source area
- Continuous open tension crack
- Tension crack with intermittent surface opening
- Erosion gullies
- 12° Inclination
- Boulder
- 1_1 Survey marker
- Ephemeral drainage line
- Ephemeral drainage line (with width of channel shown)
- Open tension crack with observed vertical displacement
- Convex break-in-slope
- Concave break-in-slope

MT1	Soft to firm, brown to dark greenish brown, slightly sandy SILT/CLAY with many rootlets and occassional angular cobbles and boulders of tuff [TOP SOIL]
MT2	Firm to stiff, light reddish brown to predominantly reddish brown slightly sandy SILT/CLAY with occassional angular cobbles of moderately decomposed tuff [COLLUVIUM]
MT3	Firm, light brown to greenish brown sandy SILT/CLAY with some coarse gravel to angular cobbles of moderately deccmposed tuff [COLLUVIUM]

no.	date	description	chk.	appr.
REVISION				

	name	date
surveyed		
designed	MD	8/2006
drawn	ATCL	8/2006
traced		
checked		

examined

contract no.

file no.

job no.

project

Detailed Study of the 22 August 2005 Landslide and Distress on the Natural Hillside at Kwun Yam Shan, below Tate's Ridge

drawing title

Detailed Field Mapping of the Distressed Hillside

drawing no.

DRAWING NO. 2

scale

1 : 200

office

LANDSLIP PREVENTATIVE MEASURES DIVISION 1
GEOTECHNICAL ENGINEERING OFFICE

CIVIL ENGINEERING AND DEVELOPMENT DEPARTMENT

HONG KONG

GEO PUBLICATIONS AND ORDERING INFORMATION
土力工程處刊物及訂購資料

A selected list of major GEO publications is given in the next page. An up-to-date full list of GEO publications can be found at the CEDD Website http://www.cedd.gov.hk on the Internet under "Publications". Abstracts for the documents can also be found at the same website. Technical Guidance Notes are published on the CEDD Website from time to time to provide updates to GEO publications prior to their next revision.

部份土力工程處的主要刊物目錄刊載於下頁。而詳盡及最新的土力工程處刊物目錄，則登載於土木工程拓展署的互聯網網頁 http://www.cedd.gov.hk 的"刊物"版面之內。刊物的摘要及更新刊物內容的工程技術指引，亦可在這個網址找到。

Copies of GEO publications (except maps and other publications which are free of charge) can be purchased either by:

writing to
Publications Sales Section,
Information Services Department,
Room 402, 4th Floor, Murray Building,
Garden Road, Central, Hong Kong.
Fax: (852) 2598 7482

or

- Calling the Publications Sales Section of Information Services Department (ISD) at (852) 2537 1910
- Visiting the online Government Bookstore at http:// www.bookstore.gov.hk
- Downloading the order form from the ISD website at http://www.isd.gov.hk and submit the order online or by fax to (852) 2523 7195
- Placing order with ISD by e-mail at puborder@isd.gov.hk

讀者可採用以下方法購買土力工程處刊物(地質圖及免費刊物除外):

書面訂購
香港中環花園道
美利大廈4樓402室
政府新聞處
刊物銷售組
傳真: (852) 2598 7482

或

- 致電政府新聞處刊物銷售小組訂購 (電話：(852) 2537 1910)
- 進入網上「政府書店」選購，網址爲 http://www.bookstore.gov.hk
- 透過政府新聞處的網站 (http://www.isd.gov.hk) 於網上遞交訂購表格，或將表格傳真至刊物銷售小組 (傳真：(852) 2523 7195)
- 以電郵方式訂購 (電郵地址：puborder@isd.gov.hk)

1:100 000, 1:20 000 and 1:5 000 maps can be purchased from:

Map Publications Centre/HK,
Survey & Mapping Office, Lands Department,
23th Floor, North Point Government Offices,
333 Java Road, North Point, Hong Kong.
Tel: 2231 3187
Fax: (852) 2116 0774

讀者可於下列地點購買1:100 000，1:20 000及1:5 000地質圖：

香港北角渣華道333號
北角政府合署23樓
地政總署測繪處
電話: 2231 3187
傳真: (852) 2116 0774

Requests for copies of Geological Survey Sheet Reports, publications and maps which are free of charge should be sent to:

For Geological Survey Sheet Reports and maps which are free of charge:
Chief Geotechnical Engineer/Planning,
(Attn: Hong Kong Geological Survey Section)
Geotechnical Engineering Office,
Civil Engineering and Development Department,
Civil Engineering and Development Building,
101 Princess Margaret Road,
Homantin, Kowloon, Hong Kong.
Tel: (852) 2762 5380
Fax: (852) 2714 0247
E-mail: jsewell@cedd.gov.hk

For other publications which are free of charge:
Chief Geotechnical Engineer/Standards and Testing,
Geotechnical Engineering Office,
Civil Engineering and Development Department,
Civil Engineering and Development Building,
101 Princess Margaret Road,
Homantin, Kowloon, Hong Kong.
Tel: (852) 2762 5346
Fax: (852) 2714 0275
E-mail: wmcheung@cedd.gov.hk

如欲索取地質調查報告、其他免費刊物及地質圖，請致函：

地質調查報告及地質圖:
香港九龍何文田公主道101號
土木工程拓展署大樓
土木工程拓展署
土力工程處
規劃部總土力工程師
(請交:香港地質調查組)
電話: (852) 2762 5380
傳真: (852) 2714 0247
電子郵件: jsewell@cedd.gov.hk

其他免費刊物:
香港九龍何文田公主道101號
土木工程拓展署大樓
土木工程拓展署
土力工程處
標準及測試部總土力工程師
電話: (852) 2762 5346
傳真: (852) 2714 0275
電子郵件: wmcheung@cedd.gov.hk

Table of Contents
Table of Contents
Table of Contents

MAJOR GEOTECHNICAL ENGINEERING OFFICE PUBLICATIONS
土力工程處之主要刊物

GEOTECHNICAL MANUALS

Geotechnical Manual for Slopes, 2nd Edition (1984), 300 p. (English Version), (Reprinted, 2000).

斜坡岩土工程手冊(1998)，308頁(1984年英文版的中文譯本)。

Highway Slope Manual (2000), 114 p.

GEOGUIDES

Geoguide 1	Guide to Retaining Wall Design, 2nd Edition (1993), 258 p. (Reprinted, 2007).
Geoguide 2	Guide to Site Investigation (1987), 359 p. (Reprinted, 2000).
Geoguide 3	Guide to Rock and Soil Descriptions (1988), 186 p. (Reprinted, 2000).
Geoguide 4	Guide to Cavern Engineering (1992), 148 p. (Reprinted, 1998).
Geoguide 5	Guide to Slope Maintenance, 3rd Edition (2003), 132 p. (English Version).
岩土指南第五冊	斜坡維修指南，第三版(2003)，120頁(中文版)。
Geoguide 6	Guide to Reinforced Fill Structure and Slope Design (2002), 236 p.
Geoguide 7	Guide to Soil Nail Design and Construction (2008), 97 p.

GEOSPECS

Geospec 1	Model Specification for Prestressed Ground Anchors, 2nd Edition (1989), 164 p. (Reprinted, 1997).
Geospec 3	Model Specification for Soil Testing (2001), 340 p.

GEO PUBLICATIONS

GCO Publication No. 1/90	Review of Design Methods for Excavations (1990), 187 p. (Reprinted, 2002).
GEO Publication No. 1/93	Review of Granular and Geotextile Filters (1993), 141 p.
GEO Publication No. 1/2000	Technical Guidelines on Landscape Treatment and Bio-engineering for Man-made Slopes and Retaining Walls (2000), 146 p.
GEO Publication No. 1/2006	Foundation Design and Construction (2006), 376 p.
GEO Publication No. 1/2007	Engineering Geological Practice in Hong Kong (2007), 278 p.

GEOLOGICAL PUBLICATIONS

The Quaternary Geology of Hong Kong, by J.A. Fyfe, R. Shaw, S.D.G. Campbell, K.W. Lai & P.A. Kirk (2000), 210 p. plus 6 maps.

The Pre-Quaternary Geology of Hong Kong, by R.J. Sewell, S.D.G. Campbell, C.J.N. Fletcher, K.W. Lai & P.A. Kirk (2000), 181 p. plus 4 maps.

TECHNICAL GUIDANCE NOTES

TGN 1	Technical Guidance Documents